GEOMETRY OF THE STABILITY SCATTERING DIAGRAM FOR \mathbb{P}^2 AND APPLICATIONS

MARK GROSS AND FATEMEH REZAEE

ABSTRACT. We give a detailed analysis of the stability scattering diagram for \mathbb{P}^2 introduced by Bousseau in [7]. This scattering diagram lives in a subset of \mathbb{R}^2 , and we decompose this subset into three regions, R_{Δ} , R_{\Diamond} and R_{unbdd} . The region R_{Δ} has a chamber structure whose chambers are in one-to-one correspondence with strong exceptional triples. No ray of the stability scattering diagram enters the interior of such a triangle, replicating a result of Prince [34] and generalizing a result of Bousseau. The region R_{\Diamond} is decomposed into *diamonds*, which are in one-to-one correspondence with exceptional bundles. Each diamond has a vertical diagonal corresponding to a rank zero object and is traversed by a dense set of rays. Crucially, however, there are no collisions of rays inside diamonds, making it still possible to control the scattering diagram in R_{\Diamond} . Finally, the behaviour of R_{unbdd} is chaotic, in that every rational point inside it is a collision of an infinite number of rays. We show that the bounded region $R_{\text{bdd}} = R_{\Delta} \cup R_{\Diamond}$ has as upper boundary the Le Potier curve, thus showing that this curve arises naturally through the algorithmic scattering process. We give an application of these results by describing the first wall-crossing for the moduli space of one-dimensional rank zero objects on \mathbb{P}^2 . In the sequel [22], we apply these results to describe the full Bridgeland wall-crossing for $\operatorname{Hilb}^n(\mathbb{P}^2)$ for any n.

CONTENTS

0.	Introduction	1
1.	Background: Stability conditions and scattering diagram for \mathbb{P}^2	7
2.	Structure of the scattering diagram: the discrete region	16
3.	Diamonds	35
4.	Vertical diagonals and vertex-freeness of the outer diamonds	40
5.	Characterization of R_{unbdd} and moduli non-emptiness	51
6.	An application: First wall-crossing for the moduli spaces of one-dimensional	
	rank-zero objects	58
7.	An application: Connection to [29] and the Le Potier curve	68
Ref	References	

0. Introduction

Moduli spaces of sheaves on projective varieties X have been studied for decades and play a crucial role in algebraic and enumerative geometry. From a modern viewpoint, it has proved to be very fruitful to study these moduli spaces by examining how they change under variation of stability conditions. More specifically, fix a non-singular projective variety X. If γ is a fixed Chern character, and σ is a Bridgeland stability condition [10] on $D^b(X)$, denote by $\mathcal{M}^{\sigma}_{\gamma}$ the moduli space of S-equivalence classes of σ -semistable objects with Chern character γ on X. Then as σ varies, this moduli space may undergo changes as σ passes through a "wall" in the space of Bridgeland stability conditions. These changes typically preserve the

1

birational equivalence class of the moduli space, but perform some interesting non-trivial birational operation, such as a flop. Wall-crossing of this nature for three-folds has been studied in [39, 38, 44, 17, 35, 36], where the authors use complicated methods to even list the walls. An initial motivation for the current article was to introduce a correspondence between the space of stability conditions on \mathbb{P}^3 and a "stability scattering diagram for \mathbb{P}^3 ", to handle the traditional wall-crossing more systematically. This motivation led us to study the stability scattering diagram for \mathbb{P}^2 more closely and discover several interesting facts which should eventually be applicable to the higher dimensional case as well.

There is an even longer history of study of moduli spaces of sheaves specifically on \mathbb{P}^2 . The pioneering work of Drezet and Le Potier [15] initiated a systematic study of these moduli spaces. They explored the structure of exceptional bundles, whose moduli spaces consist of reduced points, and determined when a moduli space of semi-stable sheaves of fixed Chern character is non-empty. More recently, the wall-crossing point of view has been explored extensively for \mathbb{P}^2 in many works, including [1, 30, 31, 5, 32, 42, 41, 12, 4, 6]. In particular, the wall-crossing point of view underpins the program of study of the birational geometry of Hilbert schemes of points in \mathbb{P}^2 initiated in [1].

The moduli space of Bridgeland stability conditions is a complex manifold of dimension 3, and thus it is rather difficult to visualize walls and think about them. However, Bridgeland [10] constructed an action of the universal cover of $GL_2(\mathbb{R})^+$ on the moduli space of stability conditions; this action preserves moduli spaces, and in particular all walls are pulled back from the quotient, which is now of real dimension 2.

Work of Bousseau [7] then was able to give a much cleaner picture of the structure of wall-crossing on \mathbb{P}^2 . He chose a particular two-dimensional slice of the above-mentioned group action, and made a clever choice of coordinates on this two-dimensional slice. He showed that in this two-dimensional slice, one could build an object called a *scattering diagram* which encodes the topology of moduli spaces of semi-stable objects. Scattering diagrams are a notion arising in the study of mirror symmetry, initially introduced by Kontsevich and Soibelman in [28] and then given a vast generalization by Gross and Siebert in [23]. Since then scattering diagram technology has found widespread applications. In particular, Bousseau showed [8] that the scattering diagram constructed from moduli spaces of semi-stable objects on \mathbb{P}^2 was directly related to the scattering diagram which arises in constructing the mirror to \mathbb{P}^2 . This latter scattering diagram, in the case of the mirror to \mathbb{P}^2 , was first studied by Carl, Pumperla and Siebert in [11], and further analyzed by Prince in [34]. Further applications of the \mathbb{P}^2 scattering diagram for enumerative purposes were explored by Gräfnitz in [24], [25] and by Gräfnitz, Ruddat and Zaslow in [27].

We now turn to the specifics of this paper. Fix a lattice $M = \mathbb{Z}^2$ and $M_{\mathbb{R}} = M \otimes_{\mathbb{Z}} \mathbb{R}$, and consider the open subset

$$U := \{(x, y) | y > -x^2/2\}$$

where x, y are coordinates on $M_{\mathbb{R}}$. For the purpose of this introduction, one can view a scattering diagram \mathfrak{D} as a collection of $rays(\mathfrak{d}, H_{\mathfrak{d}})$, where $\mathfrak{d} \subseteq \mathbb{R}^2$ is a ray of the form $(a_0, b_0) - \mathbb{R}_{\geq 0}(a, b) \subseteq \overline{U}$ with $a, b \in \mathbb{Z}$ relatively prime, and $H_{\mathfrak{d}}$ is a formal power series in the monomial $z^{(a,b)} \in \mathbb{Q}[M]$ with no constant term. Associated to crossing a ray from one side to the other is an automorphism of a certain algebra. A consistent scattering diagram is one for which a composition of automorphisms associated to wall-crossings around a closed loop in U is always the identity. [28] showed that one could construct a consistent scattering diagram given

an initial set of rays via an algorithmic procedure. Even though this procedure is quite simple (to the extent that it can easily be put on a computer), the resulting scattering diagram can be exceedingly complicated and it can be very difficult to control.

Bousseau's main result [7] says that there is a scattering diagram $\mathfrak{D}^{\mathrm{stab}}$, constructed via the Kontsevich-Soibelman algorithm from an initial choice of rays, such that the functions attached to rays are generating functions for Euler characteristics of moduli spaces of coherent sheaves on \mathbb{P}^2 with respect to various Bridgeland stability conditions. For a review of the precise statements, see §1.2 and in particular Theorem 1.15. However, roughly, if $\sigma \in U$ is contained in some ray $(\mathfrak{d}, H_{\mathfrak{d}})$, then the function $H_{\mathfrak{d}}$ will encode the Euler characteristic of the moduli space of Bridgeland stable objects $\mathcal{M}^{\sigma}_{\gamma}$ for those Chern characters γ such that $Z^{\sigma}(\gamma) \in i\mathbb{R}_{>0}$, where Z^{σ} is the central charge associated to the stability condition σ .

The fact that \mathfrak{D}^{stab} essentially coincides with the scattering diagram arising from mirror symmetry as studied in [11] and [34] is a surprising observation. See [8, §7] for a heuristic explanation for why these two scattering diagrams should agree. This proved to be a powerful tool in [8], where Bousseau used sheaf theory to solve a long-standing problem about enumeration of certain kinds of curves on \mathbb{P}^2 . Going backwards, one may use results obtained about the mirror symmetry scattering diagram to understand \mathfrak{D}^{stab} . For example, Prince in [34] proved some structure results for the scattering diagram arising from mirror symmetry. Let us still write \mathfrak{D}^{stab} for the diagram that Prince studied, even though it arose in a completely different way. Prince showed that there was a region of \mathbb{R}^2 split into a countable number of triangles, such that the interior of each triangle is disjoint from any ray in \mathfrak{D}^{stab} .

From our point of view, $\mathfrak{D}^{\text{stab}}$ gives us a powerful way of visualizing wall-crossing for moduli spaces of sheaves. The basic idea is as follows. Fix a possible Chern character γ for a sheaf of interest (excluding the Chern character of skyscraper sheaves). Define

$$L_{\gamma} := \{ \sigma \in M_{\mathbb{R}} \, | \, Z^{\sigma}(\gamma) \in i \, \mathbb{R} \};$$

this is in fact a line in $M_{\mathbb{R}}$. Then $L_{\gamma} \cap U$ has two connected components provided $\mathcal{M}_{\gamma}^{\sigma}$ is non-empty for some σ (this follows from the Bogomolov-Gieseker inequality). If $\sigma \in L_{\gamma}$ and the moduli space $\mathcal{M}_{\gamma}^{\sigma}$ is non-empty (and with non-zero Euler characteristic), then there will be a ray $(\mathfrak{d}, H_{\mathfrak{d}}) \in \mathfrak{D}^{\mathrm{stab}}$ with $\sigma \in \mathfrak{d}$ and $\mathfrak{d} \subseteq L_{\gamma}$. Typically, for σ near the endpoint of one of the two connected components of $L_{\gamma} \cap U$, the moduli space $\mathcal{M}_{\gamma}^{\sigma}$ is empty, but for σ very far from the endpoint, the moduli space stabilizes and remains unchanged as σ goes off to infinity in the plane. As σ moves from one extreme to the other, the moduli space $\mathcal{M}_{\gamma}^{\sigma}$ is expected to undergo a number of birational changes. This may or may not result in a change of Euler characteristic, so may or may not be reflected in a change of the functions $H_{\mathfrak{d}}$. Regardless, this gives us a strong hint as to where to look for wall-crossing.

With this motivation in mind, in this paper we prove some finer points of the structure of $\mathfrak{D}^{\text{stab}}$. To state the results, we introduce some notation. We define

$$R := \{(x, y) \in \mathbb{R}^2 | y \ge nx - 3n^2/2 \text{ for some } n \in \mathbb{Z}\}.$$

This set has the feature that all rays of $\mathfrak{D}^{\text{stab}}$ are contained in R, and the initial rays needed to construct $\mathfrak{D}^{\text{stab}}$ inductively are contained in the lines $y = nx - 3n^2/2$ for various n, so that the boundary of R is contained in the union of these rays. We then have a decomposition of R into three regions,

$$R = R_{\Delta} \cup R_{\Diamond} \cup R_{\text{unbdd}}$$
.

Here, R_{Δ} decomposes as a countable union of triangles, indexed by strong exceptional triples containing at most two line bundles, with the property that the interior of each triangle is disjoint from any ray of $\mathfrak{D}^{\text{stab}}$. This is Prince's chamber structure.

The region R_{\Diamond} , on the other hand, consists of a countable union of diamond shapes. There is a one-to-one correspondence between these diamonds and exceptional bundles. Further, each diamond \Diamond_v has a vertex v we call the *base* of the diamond, and this vertex determines the diamond \Diamond_v , hence the notation. Most crucially, the only rays of $\mathfrak{D}^{\mathrm{stab}}$ which meet the interior of \Diamond_v have end point at v, and if $\mathfrak{d} := v - \mathbb{R}_{\geq 0}(a,b)$ with $a,b \in \mathbb{Z}$ intersects the interior of \Diamond_v , then there is a ray of $\mathfrak{D}^{\mathrm{stab}}$ with support \mathfrak{d} . Hence, $\mathfrak{D}^{\mathrm{stab}}$ is in fact very complicated inside \Diamond_v in the sense that it is dense, but nevertheless it is quite controlled.

Finally, $R_{\rm unbdd}$ is truly chaotic. We show that *every* rational point of $R_{\rm unbdd}$ is contained in an infinite number of distinct rays of $\mathfrak{D}^{\rm stab}$, and hence we expect that it will be impossible to make any general statements in $R_{\rm unbdd}$. Nevertheless, as we shall see in the sequel paper [22], where we apply the results in this paper to study wall-crossing for Hilb $^n(\mathbb{P}^2)$, it is still possible to get useful information in $R_{\rm unbdd}$. Here, in §6, we apply our results to describe the first walls for moduli spaces of sheaves of rank 0 but non-zero first Chern class. To the best of our knowledge, this is the first description of such moduli spaces, thanks to the powerful machinery of the scattering diagram.

Another lovely aspect of the scattering diagram technology is that many classical aspects of the theory of coherent sheaves on \mathbb{P}^2 appear algorithmically. As already mentioned, the triangles of R_{Δ} are indexed by strong exceptional triples. The rays which make up the boundaries of the triangles are indexed by exceptional bundles. The *Le Potier curve* C_{LP} [15], [31, Def. 1.6] is visible as the union over all diamonds of the upper two edges of the diamond (what we call the *roof* of the diamond). We explain this last point in §7.

We now turn to more precise statements of our main results.

0.1. **Main results.** As mentioned above, the scattering diagram $\mathfrak{D}^{\text{stab}}$ is generated by a set $\mathfrak{D}^{\text{stab}}_{\text{in}}$ of initial rays, this set being in one-to-one correspondence with $\{\mathcal{O}(d),\mathcal{O}(-d)[1]|d\in\mathbb{Z}\}$. We construct an additional set of rays, which we call the *discrete rays*, $\mathfrak{D}_{\text{discrete}}$, which are in one-to-one correspondence with the set

```
\{\mathcal{E}, \mathcal{E}[1] | \mathcal{E} \text{ is an exceptional vector bundle of rank} > 1\}.
```

We also define a set \mathfrak{D}_{dense} of rays which are the rays with endpoints being bases of diamonds. Then one helpful way of describing our analysis is:

Theorem A (See Corollaries 2.13 and 4.15). The two scattering diagrams $\mathfrak{D}^{\text{stab}}$ and $\mathfrak{D}^{\text{stab}}_{\text{in}} \cup \mathfrak{D}_{\text{discrete}} \cup \mathfrak{D}_{\text{dense}}$ are equivalent (see Definition 1.10) in $R_{\text{bdd}} := R_{\Delta} \cup R_{\Diamond}$.

Theorem B (See Corollary 5.4). Every point in R_{unbdd} with rational coordinates is contained in the interior of a countably infinite number of non-trivial rays of $\mathfrak{D}^{\text{stab}}$.

These statements are really statements at the numerical level, in the sense that the scattering diagram only records the Euler characteristic of moduli spaces and may not see non-empty moduli spaces of Euler characteristic zero. For applications to wall-crossing, we need stronger results, and show the following:

Theorem C (See Theorems 2.7 and 4.8). We have the following additional information for moduli spaces for $\sigma \in R_{bdd}$:

- (i) For σ in the interior of a triangle chamber of R_{Δ} and γ a Chern character with $Z^{\sigma}(\gamma) \in i\mathbb{R}_{>0}$, the moduli space $\mathcal{M}_{\gamma}^{\sigma}$ is empty.
- (ii) If σ is in the interior of a diamond chamber \Diamond_{v} of R_{\Diamond} and γ a Chern character with $Z^{\sigma}(\gamma) \in i\mathbb{R}_{>0}$, then $\mathcal{M}_{\tau}^{\sigma}$ is non-empty only if L_{γ} passes through v.

In particular, the first item yields Prince's chamber structure as a consequence of the properties of exceptional triples. The second item is more involved and requires a careful combinatorial analysis. In general, the non-empty moduli spaces for σ in the interior of a diamond are generalizations of Steiner bundles.

Here, we state several new interesting consequences for wall-crossing for rank zero sheaves. We note that the line L_{γ} is vertical if and only if γ is the Chern character of a rank zero sheaves with non-zero first Chern class. Furthermore, we show in Theorem 4.1 that the line segments connecting the base of a diamond to its apex are also vertical. We call this line segment the *vertical diagonal* of a diamond.

Theorem D (See Theorem 6.11). Writing a Chern character γ as the triple $(\operatorname{ch}_0, \operatorname{ch}_1, \operatorname{ch}_2)$, let $\gamma = (0, u, v)$ or (0, -u, -v), for $u \in \mathbb{Z}^{>0}$, $v \in \frac{\mathbb{Z}}{2}$. Suppose γ is a primitive Chern character and L_{γ} contains a vertical diagonal of a diamond. Then the value of $\sigma \in L_{\gamma}$ with the smallest y-coordinate such that $\mathcal{M}_{n\gamma}^{\sigma} \neq \emptyset$ for some n > 0 is given by the the base of the diamond, with value $\sigma = (\frac{v}{u}, \frac{5}{8} - \frac{1+v^2}{2u^2})$.

Theorem E (See Theorem 6.19). Let \mathcal{E} be an exceptional bundle, and consider the diamond \Diamond_v whose base v corresponds to the exceptional bundle \mathcal{E} . We call the upper right edge of \Diamond_v the right roof of \Diamond_v . Then the image of the projection of the right roof onto the x-axis is the closed interval

$$\left[\frac{d}{r} - \frac{3}{2}, \frac{d}{r} - \frac{\sqrt{9r^2 - 4}}{2r}\right].$$

If $\gamma = (0, u, v)$ is a Chern character of a rank zero sheaf such that v/u lies in the interior of this interval, then the value of $\sigma \in L_{\gamma}$ with the smallest y-coordinate such that $\mathcal{M}_{n\gamma}^{\sigma} \neq \emptyset$ for some n > 0 is given by the intersection of L_{γ} with the right roof of \Diamond_v .

See §6 for more results, which give a complete description of first walls for (multiples of) Chern characters of rank zero sheaves. The above result is also used in §7 to show how the Le Potier curve arise as the union of roofs of all diamonds. In particular, the following theorem follows immediately from [15] and our own results, but is a good summation of these results:

Theorem F (See Corollary 7.2). Let $(x_0, y_0) \in U$ be a point with rational coordinates. Then (x_0, y_0) is the intersection of two rays of $\mathfrak{D}^{\text{stab}}$ with distinct tangent lines if and only if $(x_0, y_0) = \left(\frac{\operatorname{ch}_1(\mathcal{E})}{\operatorname{ch}_0(\mathcal{E})} - \frac{3}{2}, \frac{3d - \chi(\mathcal{E})}{\operatorname{ch}_0(\mathcal{E})}\right)$ for some slope-stable coherent sheaf of positive rank \mathcal{E} .

Remark 0.1. Since our main motivation for this work is to understand wall-crossing for moduli spaces, we point out that [13] described the first wall, and [31, Thm. 0.1] gives a different description of this first wall. Meanwhile, [31, Thm. 0.4] yields an algorithm for determining all other walls. For certain moduli spaces, such as the Hilbert scheme of points in \mathbb{P}^2 , we will be able to read off similar information, see the forthcoming [22]. However, the slice of the stability moduli space used by Bousseau, and hence in this paper, is quite different than that of [31], and as a result the statements take a quite different form.

The stability scattering diagram has also been studied further from different points of view in [9].

0.2. **Outline.** §1 recalls basics about coherent sheaves on \mathbb{P}^2 , Bridgeland stability conditions, and finally recalls the main results of [7]. In §2, we recall basic facts about exceptional collections of bundles on \mathbb{P}^2 , and then use this to provide an analysis of the region R_{Δ} and $\mathfrak{D}_{\text{discrete}}$. In particular, these results reproduce Prince's results of [34] about the chamber structure on R_{Δ} , but we prove a stronger result of moduli emptiness of the interior of each triangle, modelled after a result and proof of Bousseau in [7]. Finally we make use of results of [26] to analyze the structure of $\mathfrak{D}_{\text{stab}}$ at each vertex of a triangle and introduce $\mathfrak{D}_{\text{dense}}$.

In §3, we introduce diamonds. On the other hand, §4 shows that we have now accounted for all rays intersecting each diamond. We call this "vertex freeness", as this means that in the interior of a diamond, there are no rays meeting transversally. This is what allows us to have good control inside the diamonds.

In §5, we move on to prove our results about $R_{\rm unbdd}$. In §6, we give an application to studying wall-crossing for moduli of sheaves of rank 0 and non-zero first Chern class. Finally, in §7, we show how classical aspects of the theory of sheaves on \mathbb{P}^2 , such as the Le Potier curve, show up naturally in the structure of $\mathfrak{D}^{\rm stab}$.

Conventions. If $r = \operatorname{ch}_0 = \operatorname{ch}_0(\mathcal{E})$, $d = \operatorname{ch}_1 = \operatorname{ch}_1(\mathcal{E})$, $e = \operatorname{ch}_2 = \operatorname{ch}_2(\mathcal{E})$ and $\chi = \operatorname{ch}_2(\mathcal{E}) + 3/2\operatorname{ch}_1(\mathcal{E}) + \operatorname{ch}_0(\mathcal{E})$, for some $\mathcal{E} \in D^b(\mathbb{P}^2)$, then we denote $L_{\operatorname{ch}(\mathcal{E})}$ by $L_{\mathcal{E}}$. Also, we alternatively use $(\operatorname{ch}_0, \operatorname{ch}_1, \operatorname{ch}_2)$, (r, d, e) or (r, d, χ) , for the corresponding information of an object in the derived category. Sometimes, we use (0, u, v) for the Chern character of one-dimensional rank-0 objects. We call an object with primitive Chern character a *primitive object*. We call a rational number s/t so that $s, t \in \mathbb{Z}$ are coprime a *reduced rational number*.

Acknowledgments. Both authors were supported by the ERC Advanced Grant MSAG. FR was also supported by UKRI grant No. EP/X032779/1. In addition, MG was supported by the Research Institute for Mathematical Sciences, an International Joint Usage/Research Center located in Kyoto University, and FR was hosted by ETH Zürich, when some of this research was carried out. The authors thank Arend Bayer, Pierrick Bousseau and Tim Gräfnitz for helpful correspondence and discussions.

Notation.

```
\mathfrak{D}^{\mathrm{stab}}: Stability scattering diagram (Definition 1.7). \mathfrak{D}^{\mathrm{stab}}_{\mathrm{in}}: Initial rays in \mathfrak{D}^{\mathrm{stab}} (Definition 1.12). \mathfrak{D}_{\mathrm{discrete}}: Discrete rays in \mathfrak{D}^{\mathrm{stab}} (Section 2.1). \mathfrak{D}_{\mathrm{dense}}: Dense rays in \mathfrak{D}^{\mathrm{stab}} (Definition 2.26). (\mathfrak{d}, H_{\mathfrak{d}}): Stability ray (Definition 1.2). L_{\gamma} or L_{E}: The line associated to an object E with \mathrm{ch}(E) = \gamma (see (1.11)). \mathcal{T}: The infinite binary tree (Construction 2.1). \Delta_{w}: The associated triangle to a vertex w of \mathcal{T} (Construction 2.1). \mathcal{T}_{M}: The Markov tree (Construction 2.1). \Diamond_{v} or \Diamond: Dense diamond based at the vertex v. For simplicity, we omit v, when there is no confusion (Definition 3.4)
```

 \Diamond_v^{out} or \Diamond^{out} : Outer diamond based at the vertex v. For simplicity, we omit v, when there

is no confusion (Definition 3.4).

 \Diamond_v^{init} or \Diamond^{init} : Initial diamond generated by initial objects based at the vertex v.

For simplicity, we omit v, when there is no confusion (Definition 3.5).

 \Diamond_{v}^{\sup} or \Diamond^{\sup} : Supper-diamond based at the vertex ν . For simplicity, we omit ν , when there is no confusion. Note that a super-diamond contains infinitely

many diamonds, and it is not a diamond itself (Definition 3.10).

 R_{Λ} : Triangle structure of the scattering diagram (Corollary 2.12).

 R_{\Diamond} : Diamond structure of the scattering diagram (Definition 3.7).

The bounded region which is define to be $R_{\Delta} \cup R_{\Diamond}$ (Definition 3.7).

The unbounded region, which is the complement of R_{bdd} in $\mathfrak{D}^{\text{stab}}$ $R_{\rm unbdd}$: (Definition 3.7).

The fractal upper boundary of the bounded region R_{bdd} in the scattering diagram (Corollary 4.13).

1. Background: Stability conditions and scattering diagram for \mathbb{P}^2

1.1. Preliminaries and stability conditions on \mathbb{P}^2 . We set

(1.1)
$$\Gamma := K_0(D^b(\mathbb{P}^2)).$$

We identify the latter with a rank 3 lattice in two different ways. First, the map

$$\Gamma \to \mathbb{Z}^3$$
, $\mathcal{E} \mapsto (r(\mathcal{E}), d(\mathcal{E}), \chi(\mathcal{E}))$

is an isomorphism, where r, d, χ denote rank, degree and Euler characteristic respectively. Second, we use

$$\operatorname{ch}: \Gamma \to \mathbb{Z}^2 \oplus (1/2)\mathbb{Z}, \quad \mathcal{E} \mapsto (\operatorname{ch}_0(\mathcal{E}), \operatorname{ch}_1(\mathcal{E}), \operatorname{ch}_2(\mathcal{E})),$$

where ch_i denotes the *i*th Chern character. Note that $\operatorname{ch}_0(\mathcal{E}) = r(\mathcal{E})$ and $\operatorname{ch}_1(\mathcal{E}) = d(\mathcal{E})$, but by Riemann-Roch,

(1.2)
$$\chi(\mathcal{E}) = \operatorname{ch}_2(\mathcal{E}) + \frac{3}{2}\operatorname{ch}_1(\mathcal{E}) + \operatorname{ch}_0(\mathcal{E}) = \operatorname{ch}_2(\mathcal{E}) + \frac{3}{2}d(\mathcal{E}) + r(\mathcal{E}).$$

In particular, ch induces an isomorphism with its image

$$\{(r,d,e) \in \mathbb{Z}^{\oplus 2} \oplus (1/2)\mathbb{Z}\} | d/2 + e \in \mathbb{Z}\}.$$

We often write (r, d, e) instead of (ch_0, ch_1, ch_2) .

The lattice Γ has a pairing (\cdot, \cdot) given by

$$(1.4) \qquad ((r,d,\chi),(r',d',\chi')) = -3dr' - rr' - dd' + r\chi' + \chi r'.$$

This arises from Riemann-Roch (see [7, Lemma 2.2]): if $\mathcal{E}, \mathcal{E}'$ are sheaves on \mathbb{P}^2 , then

(1.5)
$$\chi(\mathcal{E}, \mathcal{E}') = \sum_{i=0}^{2} (-1)^{i} \dim \operatorname{Ext}^{i}(\mathcal{E}, \mathcal{E}') = \left((r(\mathcal{E}), d(\mathcal{E}), \chi(\mathcal{E})), (r(\mathcal{E}'), d(\mathcal{E}'), \chi(\mathcal{E}')) \right).$$

Denote by $\operatorname{Stab}(\mathbb{P}^2)$ the space of all Bridgeland stability conditions on $D^b(\mathbb{P}^2)$. We recall from [2] a two-dimensional subfamily of Stab(\mathbb{P}^2) parameterized by two real parameters $\alpha \in$ $\mathbb{R}^+, \beta \in \mathbb{R}$.

First define the twisted Chern characters

$$\mathrm{ch}^{\beta}(\mathcal{E}) = (\mathrm{ch}^{\beta}_{0}(\mathcal{E}), \mathrm{ch}^{\beta}_{1}(\mathcal{E}), \mathrm{ch}^{\beta}_{2}(\mathcal{E})) = e^{-\beta H}.\mathrm{ch}(\mathcal{E}),$$

where H denotes the hyperplane class. Define a torsion pair of subcategories of $Coh(\mathbb{P}^2)$ by

$$\mathcal{T}_{\beta} := \{ \mathcal{E} \in \operatorname{Coh}(\mathbb{P}^2) \colon \mu_{\beta}(\mathcal{G}) > 0 \text{ for all } \mathcal{E} \twoheadrightarrow \mathcal{G} \},$$
$$\mathcal{F}_{\beta} := \{ \mathcal{E} \in \operatorname{Coh}(\mathbb{P}^2) \colon \mu_{\beta}(\mathcal{F}) \le 0 \text{ for all } \mathcal{F} \hookrightarrow \mathcal{E} \},$$

where $\mu_{\beta}(\mathcal{E}) := \frac{\mathrm{ch}_{1}^{\beta}(\mathcal{E})}{\mathrm{ch}_{0}(\mathcal{E})}$ if $\mathrm{ch}_{0}(\mathcal{E}) \neq 0$, and $\mu_{\beta}(\mathcal{E}) = +\infty$ otherwise. Note that $\mu_{\beta}(\mathcal{E}) = \mu(\mathcal{E}) - \beta$, where $\mu(\mathcal{E}) = \mathrm{ch}_{1}(\mathcal{E})/\mathrm{ch}_{0}(\mathcal{E})$ is the standard slope. These produce via tilting a *heart of a bounded t-structure* on $D^{b}(\mathbb{P}^{2})$ given as

$$\operatorname{Coh}^{\beta}(\mathbb{P}^2) := \langle \mathcal{F}_{\beta}[1], \mathcal{T}_{\beta} \rangle.$$

We recall this is the subcategory of $D^b(\mathbb{P}^2)$ consisting of objects \mathcal{E} with $\mathcal{H}^i(\mathcal{E}) = 0$ for $i \neq -1, 0$, $\mathcal{H}^{-1}(\mathcal{E}) \in \mathcal{F}_\beta$ and $\mathcal{H}^0(\mathcal{E}) \in \mathcal{T}_\beta$.

The central charge of the stability condition parameterized by α, β is defined to be

(1.6)
$$Z_{\alpha,\beta} := -(\cosh_2^{\beta}) + (\alpha^2/2) \cosh_0^{\beta} + i(\cosh_1^{\beta}) \alpha.$$

The relevant slope function is defined as usual as

$$v_{\alpha,\beta} := -\frac{\operatorname{Re}(Z_{\alpha,\beta})}{\operatorname{Im}(Z_{\alpha,\beta})} = \frac{\operatorname{ch}_2^{\beta} - (\alpha^2/2)\operatorname{ch}_0^{\beta}}{\operatorname{ch}_1^{\beta}\alpha}$$

if $\operatorname{ch}_1^{\beta}(E) \neq 0$, and $\nu_{\alpha,\beta}(E) = +\infty$ if $\operatorname{ch}_1^{\beta}(E) = 0$.

Then the pair $(\operatorname{Coh}^{\beta}(\mathbb{P}^2), Z_{\alpha,\beta})$ form a Bridgeland stability condition on $D^b(\mathbb{P}^2)$, see [2].

Theorem 1.1 (Bogomolov-Gieseker inequality [3, Corollary 7.3.2]). Any $v_{\alpha,\beta}$ -semistable object $\mathcal{E} \in \mathsf{Coh}^{\beta}(\mathbb{P}^2)$ satisfies

$$2\operatorname{ch}_0(E)\operatorname{ch}_2(E) \le \operatorname{ch}_1^2(E).$$

Following Bousseau [7], we make a change of coordinates from α, β to x, y with

$$\alpha = \sqrt{x^2 + 2y}, \quad \beta = x.$$

Now (x, y) takes values in

(1.7)
$$U := \left\{ (x, y) \middle| y > -\frac{x^2}{2} \right\}.$$

For the remainder of the paper, we only work with stability conditions parameterized by $\sigma = (x, y) \in U$.

From this, the central charge (1.6) becomes

(1.8)
$$Z^{\sigma} = Z^{(x,y)} := -\operatorname{ch}_{2} + \beta \operatorname{ch}_{1} - \frac{\beta^{2}}{2} \operatorname{ch}_{0} + \frac{\alpha^{2}}{2} \operatorname{ch}_{0} + i(\operatorname{ch}_{1} - \beta \operatorname{ch}_{0})\alpha$$
$$= ry + dx - e + i(d - rx)\sqrt{x^{2} + 2y}.$$

We then obtain a stability condition

$$(\mathcal{A}^{\sigma}, Z^{\sigma}) := (\operatorname{Coh}^{x}(\mathbb{P}^{2}), Z^{\sigma}).$$

1.2. Bousseau's scattering diagram for stability conditions in \mathbb{P}^2 . We fix $M = \mathbb{Z}^2$ and write $M_{\mathbb{R}} = M \otimes_{\mathbb{Z}} \mathbb{R}$, with basis e_1, e_2 , and set $N = \text{Hom}_{\mathbb{Z}}(M, \mathbb{Z})$ with dual basis e_1^*, e_2^* . We define a skew-symmetric bilinear form on M given by

$$\langle e_1, e_2 \rangle = -3.$$

For discussions of the stability scattering diagram, we first fix a graded Lie algebra

$$\mathfrak{g}=\bigoplus_{m\in M}\mathfrak{g}_m,$$

so that $[\mathfrak{g}_m,\mathfrak{g}_{m'}]\subseteq \mathfrak{g}_{m+m'}$. For $m\in M\setminus\{0\}$ primitive, k a positive integer, define

$$\mathfrak{g}_{m,k} := \bigoplus_{j=1}^k \mathfrak{g}_{jm}$$

with obvious surjections $\mathfrak{g}_{m,k+1} \to \mathfrak{g}_{m,k}$, and set

$$\hat{\mathfrak{g}}_m = \lim_{\stackrel{\longleftarrow}{k}} \mathfrak{g}_{m,k}.$$

Write

$$\pi_{m,k}:\hat{\mathfrak{g}}_m\to\mathfrak{g}_{m,k}$$

for the projection.

Definition 1.2. A *ray or line* is a pair $(\mathfrak{d}, H_{\mathfrak{d}})$ where

- (1) There exists an $m_0 \in M_{\mathbb{R}}$ and $m_0 \in M$ primitive such that $\mathfrak{d} = m_0 \mathbb{R}_{\geq 0} m_0$ in the case of a ray, and $\mathfrak{d} = m_0 \mathbb{R} m_0$ in the case of a line. We view m_0 as part of the data of a ray or line although it is not made explicit. We refer to $-m_0$ as the *direction vector* of the ray and m_0 as the *opposite vector* of the ray.
- (2) $H_{\mathfrak{d}} \in \hat{\mathfrak{g}}_{m_{\mathfrak{d}}}$.

The *support* of a ray or line $(\mathfrak{d}, H_{\mathfrak{d}})$ is the set \mathfrak{d} . A ray or line $(\mathfrak{d}, H_{\mathfrak{d}})$ is *non-trivial* if $H_{\mathfrak{d}} \neq 0$.

Let $\mathbb{Q}[t^{\mathbb{R}_{\geq 0}}]$ denote a polynomial ring with coefficients in \mathbb{Q} and arbitrary non-negative real exponents. For any positive integer k, let \mathfrak{m}_k be the ideal generated by t^r for r > k, so that $\mathfrak{m} = \mathfrak{m}_0$ is a maximal ideal. Set

$$R_k := \mathbb{Q}[t^{\mathbb{R}_{\geq 0}}]/\mathfrak{m}_k$$

and

$$\widehat{R} := \lim_{\stackrel{\longleftarrow}{k}} R_k$$

We write the completed tensor products

$$\mathfrak{g}\widehat{\otimes}\widehat{R}:=\lim_{\stackrel{\longleftarrow}{k}}\mathfrak{g}\otimes R_k,\quad \mathfrak{g}\widehat{\otimes}\mathfrak{m}:=\lim_{\stackrel{\longleftarrow}{k}}\mathfrak{g}\otimes\mathfrak{m}/\mathfrak{m}^{k+1}.$$

Definition 1.3. Given $H \in \mathfrak{g} \widehat{\otimes} \mathfrak{m}$, we obtain an automorphism

$$\theta_H := \exp([H, \cdot]) : \mathfrak{g} \widehat{\otimes} \widehat{R} \to \mathfrak{g} \widehat{\otimes} \widehat{R}$$

given by

$$\theta_H(f) := \sum_{k=0}^{\infty} \frac{[H, [H, \dots [H, f] \dots]]}{k!},$$

where the k^{th} term involves k Lie brackets. This infinite sum makes sense in $\mathfrak{g} \widehat{\otimes} \widehat{R}$ as $H \in \mathfrak{g} \widehat{\otimes} \mathfrak{m}$.

For the most part, we will work with $\mathfrak{g} = \mathbb{Q}[M]$, with the obvious M-grading and Lie bracket defined as follows.

Definition 1.4. The skew-form $\langle \cdot, \cdot \rangle$ induces a Lie bracket on $\mathbb{Q}[M]$, with

$$[z^{m_1}, z^{m_2}] = \langle m_1, m_2 \rangle z^{m_1 + m_2}.$$

Remark 1.5. We can unwind the construction of θ_H for $H = H(z^m, t) \in \mathbb{Q}[z^m] \widehat{\otimes} \mathfrak{m}$ as follows, assuming that $H \equiv 0 \mod z^m$.

First, we introduce some additional notation. For $m \in M$, $\langle m, \cdot \rangle \in N$. Explicitly, if $m = ae_1 + be_2$, then $\langle m, \cdot \rangle = 3be_1^* - 3ae_2^*$. We write this as $\check{m} \in N$. Thus

$$[z^m, z^{m'}] = \check{m}(m')z^{m+m'}.$$

Writing $H = \sum_{k=1}^{\infty} h_k(t) z^{km}$, we then see that

$$[H, z^{m'}] = \sum_{k=1}^{\infty} h_k(t) k \check{m}(m') z^{km+m'} = \check{m}(m') z^{m'} \left(\sum_{k=1}^{\infty} k h_k(t) z^{km} \right).$$

Repeating, and noting that $[H, z^m] = 0$, we obtain

$$\theta_H(z^{m'}) = z^{m'} \exp\left(\check{m}(m') \sum_{k=1}^{\infty} k h_k(t) z^{km}\right).$$

If we set

$$(1.9) f := \exp\left(3\sum_{k=1}^{\infty} kh_k(t)z^{km}\right),$$

then we can write

$$\theta_H = \bar{\theta}_f$$
,

where

$$\bar{\theta}_f(z^{m'}) = z^{m'} f^{\check{m}(m')/3}.$$

The reason for the factor of 3 in the definition of f and dividing by 3 above is that if m is primitive, so is $\check{m}/3$.

Definition 1.6. For $\sigma = (x, y) \in M_{\mathbb{R}}$, define $\varphi_{\sigma} : M \to \mathbb{R}$ by

$$\varphi_{\sigma}(a,b) = 2(-ax-b).$$

Definition 1.7. A *(stability) scattering diagram* \mathfrak{D} for a Lie algebra \mathfrak{g} is a set of rays or lines whose support is contained in the closure \overline{U} of U (where U is defined in (1.7)), satisfying the following conditions:

- (1) For $(\mathfrak{d}, H_{\mathfrak{d}}) \in \mathfrak{D}$ and $\sigma \in \mathfrak{d} \cap U$, one has $\varphi_{\sigma}(m_{\mathfrak{d}}) > 0$.
- (2) For $(\mathfrak{d}, H_{\mathfrak{d}}) \in \mathfrak{D}$, let $\deg H_{\mathfrak{d}}$ be the smallest k for which $\pi_{m_{\mathfrak{d}}, k}(H_{\mathfrak{d}}) \neq 0$. Then for every compact set K in U and every $r \in \mathbb{R}_{\geq 0}$, the set of rays $(\mathfrak{d}, H_{\mathfrak{d}}) \in \mathfrak{D}$ such that there exists $\sigma \in \mathfrak{d} \cap K$ with $(\deg H_{\mathfrak{d}})\varphi_{\sigma}(m_{\mathfrak{d}}) \leq k$ is finite.

Definition 1.8. We define the *support* of \mathfrak{D} to be

$$Supp(\mathfrak{D})\!:=\!\bigcup_{\mathfrak{d}\in\mathfrak{D}}\mathfrak{d}$$

and define the *singular locus* of \mathfrak{D} to be

$$Sing(\mathfrak{D}) \coloneqq \bigcup_{\mathfrak{d} \in \mathfrak{D}} \partial \mathfrak{d} \cup \bigcup_{\substack{\mathfrak{d}_{1}, \mathfrak{d}_{2} \in \mathfrak{D} \\ \dim \mathfrak{d}_{1} \cap \mathfrak{d}_{2} = 0}} \mathfrak{d}_{1} \cap \mathfrak{d}_{2},$$

the union of endpoints of rays in $\mathfrak D$ and intersections of non-collinear rays in $\mathfrak D$.

Definition 1.9. For $x \in \text{Supp}(\mathfrak{D}) \setminus \text{Sing}(\mathfrak{D})$, we define

$$H_{\mathfrak{D},x} := \sum_{(\mathfrak{d},H_{\mathfrak{d}})\in\mathfrak{D},x\in\mathfrak{d}} H_{\mathfrak{d}}.$$

We define $Supp'(\mathfrak{D})$ to be the closure of the set

$$\{x \in \operatorname{Supp}(\mathfrak{D}) \setminus \operatorname{Sing}(\mathfrak{D}) | H_{\mathfrak{D},x} \neq 0\}.$$

Definition 1.10. We say two scattering diagrams \mathfrak{D}_1 and \mathfrak{D}_2 are *equivalent* if Supp'(\mathfrak{D}_1) = Supp'(\mathfrak{D}_2) and for any $x \in \text{Supp'}(\mathfrak{D}_i) \setminus (\text{Sing}(\mathfrak{D}_1) \cup \text{Sing}(\mathfrak{D}_2))$ we have

$$H_{\mathfrak{D}_1,x} = H_{\mathfrak{D}_2,x}$$
.

Definition 1.11. Let \mathfrak{D} be a stability scattering diagram, and $\sigma \in \operatorname{Supp}(\mathfrak{D})$. For $(\mathfrak{d}, H_{\mathfrak{d}}) \in \mathfrak{D}$ with $\sigma \in \mathfrak{d}$, write $H_{\mathfrak{d}}$ as a formal sum $\sum_{k \geq 1} H_{\mathfrak{d},k}$ where $H_{\mathfrak{d},k} \in \mathfrak{g}_{km_{\mathfrak{d}}}$. Then we write

$$H_{\mathfrak{d}}^{\sigma} := \sum_{k \geq 1} H_{\mathfrak{d},k} \, t^{\varphi_{\sigma}(km_{\mathfrak{d}})} \in \mathfrak{g} \widehat{\otimes} \mathfrak{m}.$$

Here we use the condition $\varphi_{\sigma}(m_{\vartheta}) > 0$ of Definition 1.7,(1).

We define the *local scattering diagram at* σ to be

$$\mathfrak{D}_{\sigma} := \{ (T_{\sigma}(\mathfrak{d}), H_{\mathfrak{d}}^{\sigma}) | (\mathfrak{d}, H_{\mathfrak{d}}) \in \mathfrak{D} \text{ such that } \sigma \in \mathfrak{d} \}.$$

Here, $T_{\sigma}(\mathfrak{d})$ denotes the tangent cone to \mathfrak{d} at σ . This coincides with the tangent line to \mathfrak{d} if $\sigma \in \operatorname{Int}(\mathfrak{d})$, and coincides with $\mathfrak{d} - \sigma$ if σ is the endpoint of \mathfrak{d} .

Definition 1.12. Let \mathfrak{D} be a stability scattering diagram and let $\sigma \in \operatorname{Sing}(\mathfrak{D}) \cap U$. For a given positive integer k, we write

$$\mathfrak{D}_{\sigma}^{k} := \{ (\mathfrak{d}, H_{\mathfrak{d}}^{\sigma}) | (\mathfrak{d}, H_{\mathfrak{d}}^{\sigma}) \in \mathfrak{D}_{\sigma}, H_{\mathfrak{d}}^{\sigma} \not\equiv 0 \mod \mathfrak{m}_{k} \}.$$

By the finiteness condition of Definition 1.7, $\mathfrak{D}_{\sigma}^{k}$ is a finite set.

(1) Let $\gamma:[0,1]\to M_{\mathbb{R}}$ be a small parameterized circle centred at σ with $\gamma(0)=\gamma(1)\in M_{\mathbb{R}}\setminus \mathrm{Supp}(\mathfrak{D})$. We define the *path-ordered product* $\theta_{\gamma,\mathfrak{D}_{\sigma}^k}:\mathfrak{g}\otimes R_k\to\mathfrak{g}\otimes R_k$ as follows. Let $(\mathfrak{d}_1,H_1),\ldots,(\mathfrak{d}_n,H_n)$ be the elements of \mathfrak{D}_{σ}^k traversed by γ , with $\gamma(t_i)\in\mathfrak{d}_i$, in the order traversed. We define

$$\theta_{\gamma,\mathfrak{D}_{\sigma}^{k}} := \theta_{H_{n}}^{\pm 1} \circ \cdots \theta_{H_{1}}^{\pm 1},$$

where the sign ± 1 is +1 provided $\check{m}(\gamma'(t_i)) < 0$.

- (2) We define $\theta_{\gamma,\mathfrak{D}_a}: \mathfrak{g}\widehat{\otimes}\widehat{R} \to \mathfrak{g}\widehat{\otimes}\widehat{R}$ as the limit of the $\theta_{\gamma,\mathfrak{D}_a^k}$.
- (3) We say $\mathfrak D$ is *consistent at* σ if $\theta_{\gamma,\mathfrak D_\sigma} = \mathrm{id}$.
- (4) For an open subset $V \subseteq M_{\mathbb{R}}$, we say \mathfrak{D} is *consistent inside* V if it is consistent at each $\sigma \in V \cap \operatorname{Sing}(\mathfrak{D})$.

We can now define the stability scattering diagram for \mathbb{P}^2 with respect to $\mathfrak{g} = \mathbb{Q}[M]$. This will be the scattering diagram written as $\mathfrak{D}^{\mathbb{P}^2}_{cl^+}$ in [7].

¹This is the opposite sign convention from [7, Def. 1.6], correcting an oversight in that paper.

Identifying $M_{\mathbb{R}}$ with the (x, y)-plane, we recall the open subset $U \subseteq M_{\mathbb{R}}$ given in (1.7). For $n \in \mathbb{Z}$, define two rays,

$$\mathfrak{d}_n^+ := \left((n, -n^2/2) - \mathbb{R}_{\geq 0}(-1, n), -\operatorname{li}_2(-z^{(-1, n)}) \right)
\mathfrak{d}_n^- := \left((n, -n^2/2) - \mathbb{R}_{\geq 0}(1, -n), -\operatorname{li}_2(-z^{(1, -n)}) \right)$$

where the dilogarithm is defined by

$$\operatorname{li}_2(z) = \sum_{k=1}^{\infty} \frac{z^k}{k^2}.$$

Set

$$\mathfrak{D}_{\mathrm{in}}^{\mathrm{stab}} := \{\mathfrak{d}_n^+, \mathfrak{d}_n^- | n \in \mathbb{Z}\}.$$

[7, Prop. 1.9], following [28, Thm. 6], proves the following statement:

Theorem 1.13. There exists a stability scattering diagram $\mathfrak{D}^{\text{stab}}$ consistent in U and equivalent to $\mathfrak{D}^{\text{stab}}_{\text{in}}$ in small neighbourhoods of the endpoints of the rays \mathfrak{d}^{\pm}_n . Further, this diagram is unique up to equivalence.

Note that the endpoints $(n, -n^2/2)$ of \mathfrak{d}_n^{\pm} lie in the boundary of \overline{U} , and thus there is no consistency for loops around these points, as they are not contained in U.

One of the main theorems of [7] relates the functions attached to rays of $\mathfrak{D}^{\text{stab}}$ to Euler characteristics of moduli spaces of stable objects in $D^b(\mathbb{P}^2)$. Explicitly, let $\sigma \in U$, and let $\gamma \in \Gamma$ as defined in (1.1). We may write γ either as (r, d, γ) or $(\operatorname{ch}_0, \operatorname{ch}_1, \operatorname{ch}_2)$.

Definition 1.14. For $\gamma = (r, d, \chi) \in \Gamma$ or \mathcal{E} an object of the derived category $D^b(\mathbb{P}^2)$ with invariants γ , we define:

(1) the *opposite vector* of γ or \mathcal{E} to be

$$(1.10) m_{\gamma} = m_{\mathcal{E}} := (r, -d) \in M.$$

(2) We define the line in $M_{\mathbb{R}}$

(1.11)
$$L_{\gamma} = L_{\mathcal{E}} := \{ (x, y) \in U \mid ry + dx + r + \frac{3}{2}d - \chi = 0 \}$$

$$= \{ (x, y) \in U \mid \operatorname{ch}_{0} y + \operatorname{ch}_{1} x = \operatorname{ch}_{2} \},$$

using (1.2). Note that m_{γ} is tangent to L_{γ} . The line L_{γ} can be viewed as the set of stability conditions $\sigma \in U$ for which the central charge Z_{γ}^{σ} of γ is purely imaginary.

An object \mathcal{E} with Chern character $\gamma = (\operatorname{ch}_0, \operatorname{ch}_1, \operatorname{ch}_2)$ is called an *object corresponding* to the line $L_{\gamma} = L_{\mathcal{E}}$.

(3) We denote by $\mathcal{M}_{\gamma}^{\sigma}$ the moduli space of *S*-equivalence classes of σ -semistable objects of class γ in \mathbb{P}^2 .

The following is [7, Thm. 5.10]:

Theorem 1.15. For a point $\sigma \in \text{Supp}(\mathfrak{D}^{\text{stab}}) \setminus \text{Sing}(\mathfrak{D}^{\text{stab}})$,

$$H_{\mathfrak{D}^{\mathrm{stab}},\sigma} = \sum_{\gamma:\sigma \in L_{\gamma}} (-1)^{(\gamma,\gamma)-1} \left(\sum_{\substack{\gamma' \in \Gamma_{\gamma} \\ \gamma = \ell \gamma'}} \frac{1}{\ell^{2}} I e_{\gamma',\sigma}^{-} \right) z^{m_{\gamma}}.$$

Here

$$\Gamma_{\gamma} = \{ \gamma' \in \Gamma \mid \gamma = \ell \gamma' \text{ for some } \ell \in \mathbb{Z}_{\geq 1} \}$$

and $Ie^-_{\gamma',\sigma}$ is a signed Euler characteristic of the intersection cohomology of $\mathcal{M}^{\sigma}_{\gamma'}$, see [7, §2.4].

For us, the precise definition of $Ie_{\gamma',\sigma}^-$ will not be important, other than the observation that if this number is non-zero, then $\mathcal{M}_{\gamma'}^-$ is non-empty.

Lemma 1.16. $\mathfrak{D}^{\text{stab}}$ is invariant under the affine linear transformation

$$T: M_{\mathbb{R}} \to M_{\mathbb{R}}, \quad T = \begin{pmatrix} 1 & 0 \\ -1 & 1 \end{pmatrix} \begin{pmatrix} x \\ y \end{pmatrix} + \begin{pmatrix} 1 \\ -1/2 \end{pmatrix}.$$

We define the action of T on a ray via $T(\mathfrak{d}, H(z^m)) = (T(\mathfrak{d}), H(z^{T(m)}))$.

Proof. To see this invariance, it is sufficient to note that $T(\mathfrak{d}_n^{\pm}) = \mathfrak{d}_{n+1}^{\pm}$ and then apply uniqueness of $\mathfrak{D}^{\text{stab}}$ as obtained from $\mathfrak{D}^{\text{stab}}_{\text{in}}$.

Remark 1.17. This affine linear transformation is induced by the action of the autoequivalence $T:D^b(\mathbb{P}^2)\to D^b(\mathbb{P}^2)$ given via $\otimes\mathcal{O}_{\mathbb{P}}(1)$. According to [7, Lem. 2.24], this autoequivalence acts on $\operatorname{Stab}(\mathbb{P}^2)$ via $(Z,\mathcal{A})\mapsto (Z\circ T^{-1},T(\mathcal{A}))$, and this action preserves the subset of $\operatorname{Stab}(\mathbb{P}^2)$ parameterized by $U\subseteq M_{\mathbb{R}}$. This action takes $\sigma\in U$ to $T(\sigma)$ with T as in Lemma 1.16.

Remark 1.18. For future reference, we note that

$$T^{d} \begin{pmatrix} x \\ y \end{pmatrix} = \begin{pmatrix} 1 & 0 \\ -d & 1 \end{pmatrix} \begin{pmatrix} x \\ y \end{pmatrix} + \begin{pmatrix} d \\ -d^{2}/2 \end{pmatrix}.$$

Remark 1.19. We note that $\mathfrak{D}^{\text{stab}}$ is also obviously invariant under the transformation $(x, y) \mapsto (-x, y)$.

Remark 1.20. In fact, in [7], Bousseau constructs a scattering diagram which he writes as $\mathfrak{D}_{u,v}^{\mathbb{P}^2}$. We will not give the definition here, as it is somewhat more complicated than $\mathfrak{D}^{\text{stab}}$. Crucially, however, rays in this scattering diagram encode more information about each moduli space $\mathcal{M}_{\gamma}^{\sigma}$, namely the Hodge polynomial associated to the intersection cohomology of $\mathcal{M}_{\gamma}^{\sigma}$. Since this Hodge polynomial is non-zero if $\mathcal{M}_{\gamma}^{\sigma}$ is non-empty,

the scattering diagram sees all non-empty moduli spaces. It is possible that in passing to $\mathfrak{D}^{\mathrm{stab}}$ we lose some information as some moduli spaces might have Euler characteristic zero. Bousseau's main result is in fact about $\mathfrak{D}^{\mathbb{P}^2}_{u,v}$, and the result for $\mathfrak{D}^{\mathrm{stab}}$ is then obtained after taking Euler characteristics. In particular, $\mathfrak{D}^{\mathbb{P}^2}_{u,v}$ is obtained from an intial scattering diagram $\mathfrak{D}^{\mathrm{in}}_{u,v}$ in the same way that $\mathfrak{D}^{\mathrm{stab}}$ is.

Most of the results of this paper stated for $\mathfrak{D}^{\mathrm{stab}}$ also hold for $\mathfrak{D}^{\mathbb{P}^2}_{u,v}$. Indeed, results about the non-existence of certain rays are proved by showing the corresponding moduli spaces are empty, and hence these rays don't exist in either $\mathfrak{D}^{\mathbb{P}^2}_{u,v}$ or $\mathfrak{D}^{\mathrm{stab}}$. Results about the existence of certain rays, however, are proven in $\mathfrak{D}^{\mathrm{stab}}$ using results about scattering, and this implies existence of rays in $\mathfrak{D}^{\mathbb{P}^2}_{u,v}$.

On the other hand, $\mathfrak{D}^{\text{stab}}$ is easier to work with as the type of scattering which occurs there has been much studied (and in particular the results of [26] can be easily applied) and is algorithmically simple to implement.

1.3. Wall-crossing and destablizing subobjects and quotient objects. The motivating question of this paper is to understand the behaviour of the moduli spaces $\mathcal{M}_{\gamma}^{\sigma}$ as σ varies. Here we explain how Bousseau's work gives us insight into this question. Consider a Chern character $\gamma \in \Gamma$. Suppose that this moduli space is non-empty for some $\sigma = (x_0, y_0) \in U$. Then it follows

from the Bogomolov-Gieseker inequality (Theorem 1.1) that the line L_{γ} intersects the boundary of \overline{U} , namely the parabola $y=-x^2/2$. Indeed, replacing y with $-x^2/2$ in the equation for L_{γ} , we obtain $-\mathrm{ch}_0 x^2/2 + \mathrm{ch}_1 x - \mathrm{ch}_2 = 0$, and this quadratic equation has discriminant $\mathrm{ch}_1^2 - 2\mathrm{ch}_0\mathrm{ch}_2$, which is non-negative by the Bogomolov-Gieseker inequality. In particular, we have solutions

$$x = \frac{\text{ch}_1}{\text{ch}_0} \pm \sqrt{\left(\frac{\text{ch}_1}{\text{ch}_0}\right)^2 - 2\frac{\text{ch}_2}{\text{ch}_0}}.$$

As a consequence, we can write $L_{\gamma} \cap \overline{U} = L_{\gamma}^+ \cup L_{\gamma}^-$, where L_{γ}^\pm is a ray with endpoint on $\partial \overline{U}$. From the above formula for the x-coordinate at the points of $L_{\gamma} \cap \partial \overline{U}$ and the formula (1.8) for Z^{σ} , we can choose L_{γ}^+ and L_{γ}^- so that for $\sigma \in \operatorname{Int}(L_{\gamma}^+)$, $Z^{\sigma}(\gamma) \in i\mathbb{R}_{>0}$ and for $\sigma \in \operatorname{Int}(L_{\gamma}^-)$, $Z^{\sigma}(\gamma) \in i\mathbb{R}_{<0}$. Note that replacing γ by $-\gamma$, which corresponds to a shift [1] in $D^b(\mathbb{P}^2)$, interchanges these two rays.

Assuming now that γ satisfies the Bogomolov-Gieseker inequality, we can write $L_{\gamma}^+ = p + \mathbb{R}_{\geq 0} m$ for some $m \in M$. For $\sigma = p + t m$ for t small, the moduli space $\mathcal{M}_{\gamma}^{\sigma}$ will be empty (assuming that L_{γ}^+ does not coincide with an initial ray), as follows from [7, Lemmas 4.8,4.10]. As t increases, the moduli space $\mathcal{M}_{\gamma}^{\sigma}$ may become non-empty. We call the point on L_{γ}^+ where this first occurs the first actual wall for γ . Further (actual) walls are points of L_{γ}^+ at which $\mathcal{M}_{\gamma}^{\sigma}$ changes again. This leads to the following definition.

Definition 1.21. Let γ be a Chern character, and let $\sigma_0 = L_{\gamma}^+ \cap \partial \overline{U}$. We define the *first generating* point of γ to be $\sigma_0 - t_0 m_{\gamma}$, where

$$t_0=\inf\{\,t\,|\,\sigma_0-t\,m_\gamma\in\mathfrak{d}\text{ for some }(\mathfrak{d},H_{\mathfrak{d}})\in\mathfrak{D}^{\mathrm{stab}}\text{ with }\mathfrak{d}\subseteq L_\gamma^+\}.$$

Note this only depends on γ up to positive multiples.

Note that this is not the usual picture for walls in stability moduli space. Rather, typically walls are viewed as codimension one sets in the space of stability conditions. *Potential walls* arise via a choice of (non-proportional) Chern characters γ_1, γ_2 , with the potential wall being

$$W_{\gamma_1,\gamma_2} := \{ \sigma \in U \mid \operatorname{Arg}(Z^{\sigma}(\gamma_1)) = \operatorname{Arg}(Z^{\sigma}(\gamma_2)) \}.$$

This is a conic section, see e.g., the proof of [7, Lem. 3.3]. Let σ_0 be the point of intersection between L_{γ_1} and L_{γ_2} . Then clearly $\sigma_0 \in W_{\gamma_1,\gamma_2}$. [7, Lem. 3.3] shows that the tangent line ℓ_{γ_1,γ_2} to W_{γ_1,γ_2} at σ_0 is given by the equation $\varphi_{\sigma_0} = 0$ (see Definition 1.6), after identifying the tangent space to U at σ_0 with $M_{\mathbb{R}}$. See Figure 1.

As in [7], we choose general stability conditions $\sigma_{\rm in}$ and $\sigma_{\rm out}$ sufficiently close to σ_0 and below and above ℓ_{γ_1,γ_2} respectively. This makes sense since ℓ_{γ_1,γ_2} is never vertical. Further, we may choose these two stability conditions to have the same x-coordinate, so that the hearts $\mathcal{A}^{\sigma_{\rm in}}$ and $\mathcal{A}^{\sigma_{\rm out}}$ of these stability conditions coincide, as the hearts only depend on the x-coordinate. Further, as explained in [7, §3.2], for any ray \mathfrak{d} coming into σ_0 , we have

(Note this is required by Definition 1.7,(1).)

Now fix $\gamma \in \Gamma$ satisfying the Bogomolov-Gieseker inequality, and let σ_0 be the intersection of L_{γ}^+ with a potential wall W_{γ_1,γ_2} as above. The key argument in [7, §3.5] makes use of the following. Let $\mathcal E$ be an object in the moduli space $\mathcal M_{\gamma}^{\sigma_{\text{out}}}$. If $\mathcal E$ is not stable with respect to σ_{in} , then σ_0 is an actual wall in our language. In this case, $\mathcal E$ has a Harder-Narasimhan filtration

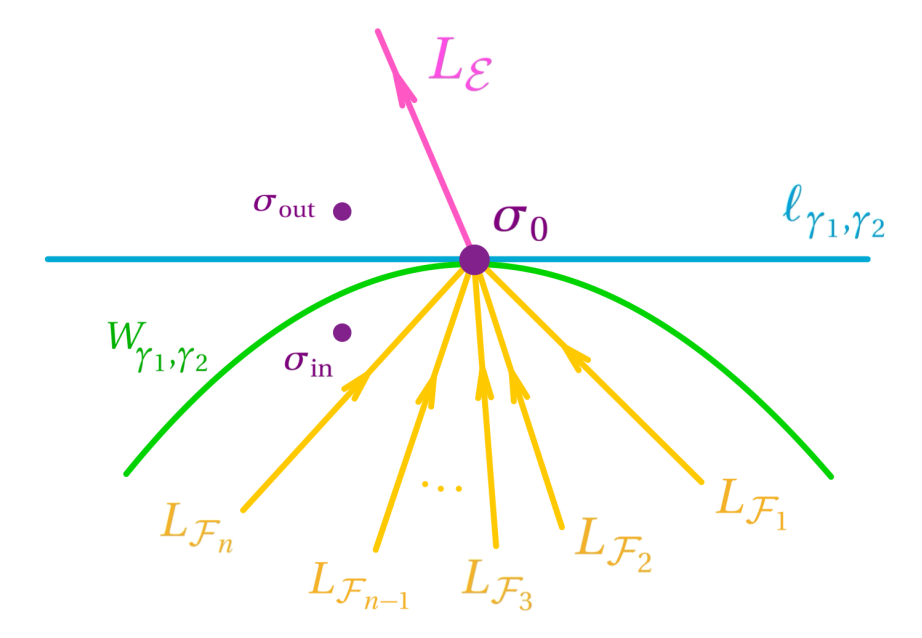


FIGURE 1

with respect to the stability condition $\sigma_{\rm in}$, with graded pieces of the filtration being $\mathcal{F}_1,\ldots,\mathcal{F}_n$, and with ${\rm Arg}(Z^{\sigma_{\rm in}}(\mathcal{F}_i))$ decreasing as i increases. In particular, \mathcal{F}_1 is a subobject of \mathcal{E} and \mathcal{F}_n is a quotient object. The lines $L_{\mathcal{F}_i}$ all pass through σ_0 , as the objects \mathcal{F}_i will all have the same slope as each other and as \mathcal{E} with respect to the stability condition σ_0 . Further, as the argument of the central charge is decreasing, $L_{\mathcal{F}_1}$ lies to the left of $L_{\mathcal{E}}$ (relative to the direction vector $-m_{\mathcal{E}}$) after passing σ_0 this intersection point, and $L_{\mathcal{F}_n}$ lies to the right, see Figure 1. Thus, we will refer to the subobject \mathcal{F}_1 as the *left generator* and the quotient object \mathcal{F}_n as the *right generator*. We also refer to these as *generators*. We call the point $\sigma_0 = L_{\mathcal{F}_1} \cap L_{\mathcal{F}_n}$, the *first generating point*.

We note that if γ_i is the Chern character of \mathcal{F}_i , then $\gamma = \sum_i \gamma_i$ and $m_{\gamma} = \sum_i m_{\gamma_i}$. Further, m_{γ} is a positive rational linear combination of m_{γ_1} and m_{γ_n} .

This gives us the following procedure to visualize how various sheaves are generated by the scattering process. For a semistable object $\mathcal{F} \in \mathcal{A}^{\sigma}$ with $\sigma \in L_{\mathcal{F}}$, define the line segment $E(\mathcal{F}, \sigma) \subseteq L_{\mathcal{F}}$ to be the line segment with endpoints σ and $\sigma + \alpha m_{\mathcal{F}}$, where

$$\alpha := \sup \{ \alpha' \mid \mathcal{F} \text{ is } \sigma + \beta m_{\mathcal{F}} \text{-semistable for all } 0 \le \beta \le \alpha' \}.$$

Now given $\mathcal{E} \in \mathcal{A}^{\sigma_0}$ a σ_0 -semistable object, let $E_0 = E(\mathcal{E}, \sigma_0)$, and let σ_1 be the other endpoint of E_0 . Then \mathcal{E} is unstable for a stability condition $\sigma_1 + \epsilon m_{\mathcal{E}}$ for small $\epsilon > 0$, and let \mathcal{Q}_1 be the right generator in the sense of §1.3. We proceed similarly, taking $E_1 = E(\mathcal{Q}_1, \sigma_1)$. Let σ_2 be the other endpoint of E_1 . We continue in this fashion, always using the right generator. Because each of these line segments are contained in rays of $\mathfrak{D}_{u,v}^{\mathbb{P}^2}$ as discussed in Remark 1.20, as the moduli spaces of \mathcal{Q}_i are non-empty for stability conditions in the interior of E_i , we see that this process must terminate when we reach some $\sigma_n = (d, -d^2/2)$ for some d. In particular, this gives a sequence of successive quotient objects.

Similarly, we can use the left generators to get a different sequence of edges and this time a sequence of subobjects S_i . See Figure 2.

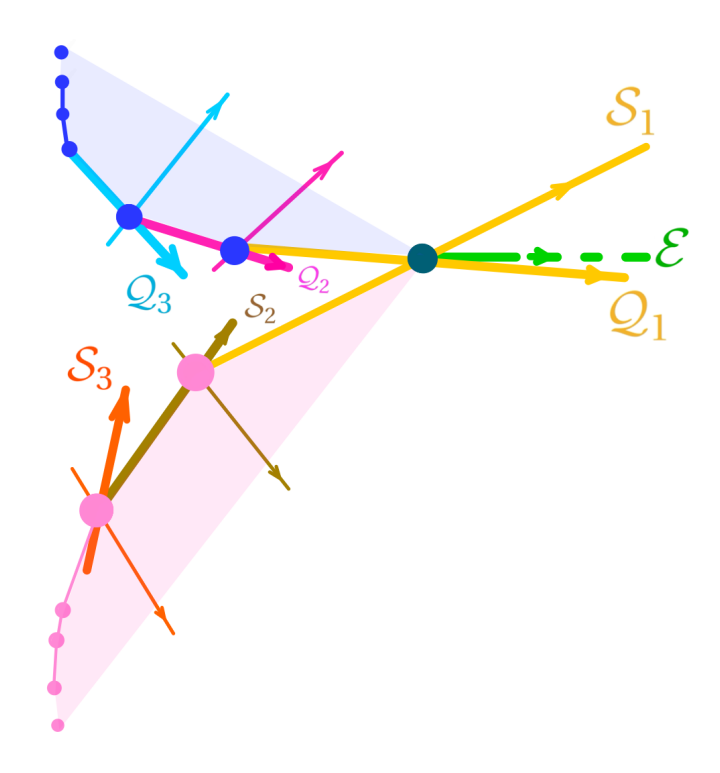


FIGURE 2. The repeated subobjects and the repeated quotients.

2. STRUCTURE OF THE SCATTERING DIAGRAM: THE DISCRETE REGION

In this section we discuss the discrete region of $\mathfrak{D}^{\mathrm{stab}}$, defining the set of discrete rays $\mathfrak{D}_{\mathrm{discrete}} \subseteq \mathfrak{D}^{\mathrm{stab}}$ and showing that this gives a complete description of $\mathfrak{D}^{\mathrm{stab}}$ in a region R_{Δ} which decomposes into an (infinite) union of triangular chambers of $\mathfrak{D}^{\mathrm{stab}}$. The results in this section partially overlap with results of [34], but we need the refined description here, and our proofs are completely different. We give dual descriptions of the triangles, first by describing the rays which bound them via an inductive process, and second by describing their vertices in terms of exceptional bundles.

2.1. The discrete rays of $\mathfrak{D}^{\text{stab}}$ and the triangles.

Construction 2.1. Let \mathcal{T} be an infinite binary tree with one root w_0 and every vertex having two children. Label each edge of the tree as being either *hybrid* or *outgoing*. This is done so that each edge connected to w_0 is hybrid, but the two edges attaching any other vertex w to its children consist of one hybrid and one outgoing edge. See Figure 3.

We will associate a triangle $\Delta_w \subseteq M_\mathbb{R}$ for each vertex w of \mathcal{T} . These triangles will be constructed inductively, starting with Δ_{w_0} . The tree \mathcal{T} can then be thought of as being dual to a two-dimensional simplicial complex composed of these triangles. The vertices of \mathcal{T} correspond to triangles, while edges of \mathcal{T} with endpoints w_1, w_2 correspond to an edge $\Delta_{w_1} \cap \Delta_{w_2}$ of both triangles. In addition, for each vertex w which is not the root, we will associate a ray

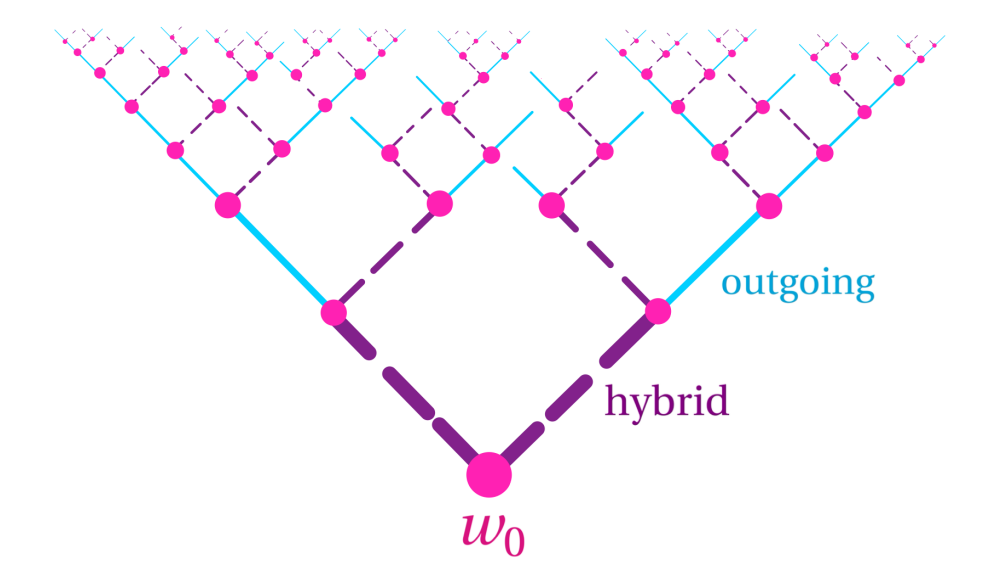


Figure 3. The infinite binary tree \mathcal{T} . The hybrid edges are depicted by dashed lines.

 \mathfrak{d}_w . Once we do this, we may define

(2.1)
$$\mathfrak{D}_{\text{discrete}}^{0} := \{\mathfrak{d}_{w} \mid w \neq w_{0} \text{ a vertex of } \mathcal{T}\},$$
$$\mathfrak{D}_{\text{discrete}} := \bigcup_{k \in \mathbb{Z}} T^{k}(\mathfrak{D}_{\text{discrete}}^{0}),$$

where T is as defined in Lemma 1.16. The boundary of Δ_w consists of three intervals each contained in a ray of $\{\mathfrak{d}_{-1}^+,\mathfrak{d}_1^-\}\cup\mathfrak{D}_{\mathrm{discrete}}^0$, except for Δ_{w_0} , which is slightly special. Explicitly, Δ_{w_0} is the triangle

(2.2)
$$\Delta_{w_0} := \operatorname{Conv}((-1/2, 0), (1/2, 0), (0, 1/2)).$$

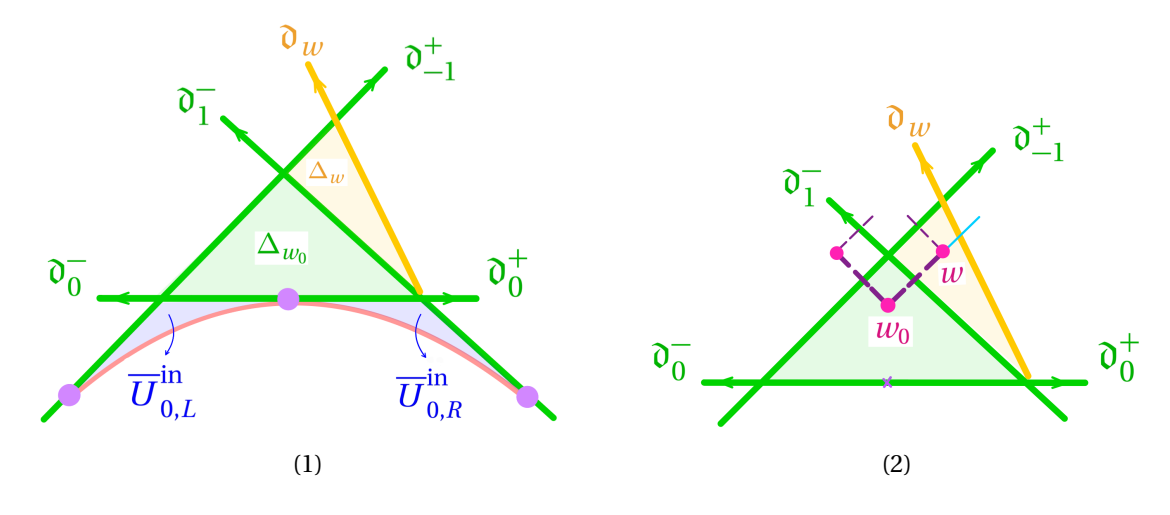


FIGURE 4

Note that the two edges of this triangle with endpoint (0, 1/2) are contained in \mathfrak{d}_{-1}^+ and \mathfrak{d}_{1}^- , while the lower edge with endpoints $(\pm 1/2, 0)$ is contained in $\mathfrak{d}_{0}^+ \cup \mathfrak{d}_{0}^-$. See Figure 4.

We orient each ray \mathfrak{d} in the direction pointing out from the endpoint of the ray, i.e., in the direction of the direction vector $-m_{\mathfrak{d}}$. This induces orientations on edges of triangles

contained in these rays. We classify vertices of a given triangle based on the orientations of the edge of the triangle. We say a vertex is *outgoing* if its adjacent edges are oriented away from the vertex. We say a vertex is *incoming* if the adjacent edges are oriented towards the vertex. Otherwise, the vertex is said to be *hybrid*.

We note that Δ_{w_0} has two hybrid vertices and one incoming vertex, while it will be clear by the inductive construction that all other triangles will have one vertex of each type.

For a vertex v of Δ_w , let m_1 , m_2 be primitive tangent vectors to the edges adjacent to v. We define the *determinant* of the vertex v to be

$$(2.3) D_v := |m_1 \wedge m_2|,$$

i.e., the absolute value of the determinant of the 2×2 matrix with rows given by m_1, m_2 . A priori, D_v depends not just on v but the triangle Δ_w it is a vertex of. In Proposition 2.16, we will show that in fact D_v only depends on the x-coordinate of $v \in M_{\mathbb{R}}$. If v is clear, for simplicity, we denote the determinant by D.

Given a triangle Δ_w , let v be the unique incoming vertex, and let E_1, E_2 be the adjacent edges. We call E_i hybrid if its other vertex is hybrid, and *outgoing* if its other vertex is outgoing. We may then equate E_1, E_2 with the edges of \mathcal{T} attaching w to its two children, w_1, w_2 , in a way which respects the labeling of hybrid and outgoing.

Denote by v_i the other vertex of E_i , and by \mathfrak{d}_i the ray containing E_i . Let m_i be the primitive tangent vector to E_i , oriented in the opposite direction of E_i (hence m_i agrees with the opposite vector $m_{\mathfrak{d}_i}$). Let E be the remaining edge of Δ_w . To obtain the triangle Δ_{w_j} , let j' be such that $\{j,j'\}=\{1,2\}$. Let m be a primitive tangent vector to E pointing towards v_i . Define

$$\mathfrak{d}_{w_j} := \left((v_j - \mathbb{R}_{\geq 0} (3D_{v_j} m_j - m), -\operatorname{li}_2 (-z^{3D_{v_j} m_j - m}) \right).$$

Let v_i' be the intersection of the ray $\mathfrak{d}_{j'}$ and the ray \mathfrak{d}_{w_i} . We then define

$$\Delta_{w_j} := \operatorname{Conv}(E_j \cup \{v_j'\}),$$

where Conv denotes convex hull. See Figure 5.

Note that the vertices of Δ_{w_j} are v, v_j and v'_j , and the edge joining v and v'_j is contained in the ray $\mathfrak{d}_{j'}$. Further, v'_i is now (in Δ_{w_i}) an incoming vertex and v is a hybrid vertex.

Definition 2.2 (Mutation). We call the construction of Δ_{w_j} from Δ_w the *mutation of* Δ_w *at* the vertex $v_{j'}$ or the *mutation of* Δ_w along the ray \mathfrak{d}_j , so that \mathfrak{d}_j remains an edge during the mutation process. Also, sometimes we call \mathfrak{d}_{w_j} the *mutation of* \mathfrak{d}_j *at* v_j *or along* $\mathfrak{d}_{j'}$.

2.2. **Moduli emptiness of the triangles.** In this subsection, we will connect the triangles constructed in the previous subsection to strong exceptional triples. This will allow us, in particular, to give a proof of Theorem C(i), as well as give a powerful additional tool for understanding $\mathfrak{D}^{\text{stab}}$.

We begin by recalling basics about exceptional bundles on \mathbb{P}^2 , drawing from [15], [18], [37].

- **Definition 2.3.** (1) An *exceptional bundle* on \mathbb{P}^2 is a bundle \mathcal{E} such that $\operatorname{Hom}(\mathcal{E},\mathcal{E}) = \mathbb{C}$ and $\operatorname{Ext}^1(\mathcal{E},\mathcal{E}) = \operatorname{Ext}^2(\mathcal{E},\mathcal{E}) = 0$.
 - (2) An ordered tuple of exceptional bundles $(\mathcal{E}_0, \dots, \mathcal{E}_n)$ is a *exceptional collection* if we have $\operatorname{Ext}^{\bullet}(\mathcal{E}_i, \mathcal{E}_i) = 0$ for i > j.
 - (3) An exceptional collection is a strong exceptional collection if $\operatorname{Ext}^k(\mathcal{E}_i, \mathcal{E}_i) = 0$ for k > 0.

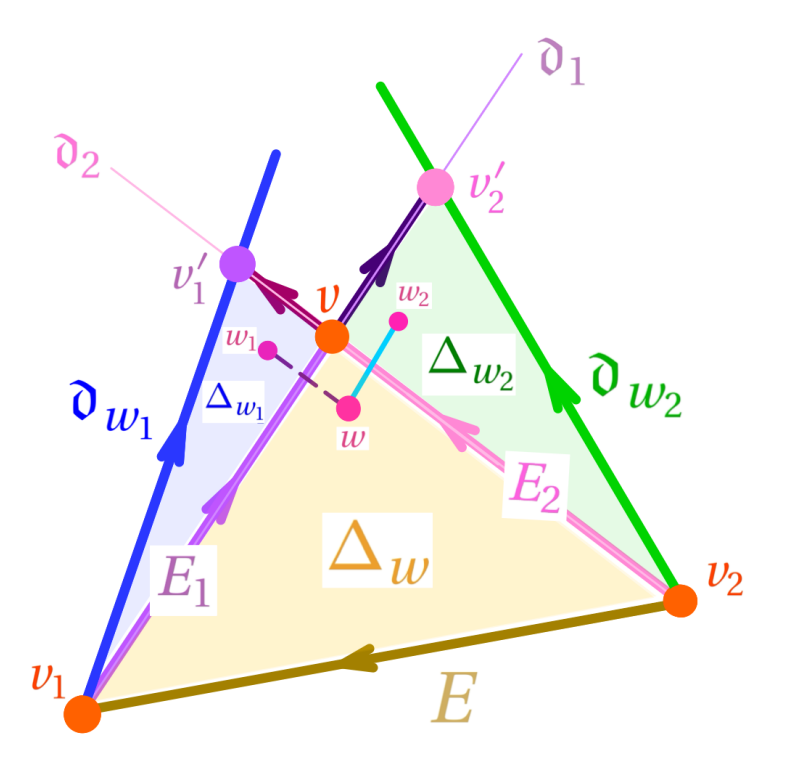


FIGURE 5. Δ_w along with Δ_{w_1} and Δ_{w_2} . Note that E_1 is hybrid and E_2 is outgoing. Part of the tree corresponding to this diagram is also pictured.

Given a strong exceptional pair $(\mathcal{E}, \mathcal{F})$, one defines the left and right mutations via the exact sequences

$$\begin{split} 0 \to & \mathcal{L}_{\mathcal{E}} \mathcal{F} \to \text{Hom}(\mathcal{E}, \mathcal{F}) \otimes \mathcal{E} \to \mathcal{F} \to 0, \\ 0 \to & \mathcal{E} \to \text{Hom}(\mathcal{E}, \mathcal{F})^* \otimes \mathcal{F} \to \mathcal{R}_{\mathcal{F}} \mathcal{E} \to 0, \end{split}$$

with the second and first non-zero maps in the two rows respectively given canonically by evaluation.

It is well-known (see [18],[37]) that all strong exceptional collections on \mathbb{P}^2 can be produced by a process of mutation, starting an *initial exceptional collection* with $(\mathcal{E}_0,\mathcal{E}_1,\mathcal{E}_2) = (\mathcal{O}(m),\mathcal{O}(m+1),\mathcal{O}(m+2))$, replacing at each step a strong exceptional collection $\mathcal{C} = (\mathcal{E}_0,\mathcal{E}_1,\mathcal{E}_2)$ with either

$$\mathcal{L}_{\mathcal{C}} := (\mathcal{E}_0, \mathcal{L}_{\mathcal{E}_1} \mathcal{E}_2, \mathcal{E}_1) \text{ or } \mathcal{R}_{\mathcal{C}} := (\mathcal{E}_1, \mathcal{R}_{\mathcal{E}_1} \mathcal{E}_0, \mathcal{E}_2).$$

We recall a few facts. For a sheaf \mathcal{E} , as usual we write the slope $\mu(\mathcal{E}) = d(\mathcal{E})/r(\mathcal{E})$. Note that the slope triple for the initial exceptional collection is $(\mu_0, \mu_1, \mu_2) = (m, m+1, m+2)$.

Lemma 2.4 (Properties of strong exceptional triples). Let $C = (\mathcal{E}_0, \mathcal{E}_1, \mathcal{E}_2)$ be a strong exceptional triple with slopes μ_0, μ_1, μ_2 , ranks r_0, r_1, r_2 , and first Chern classes d_0, d_1, d_2 . Then

- (1) The rank triple of $\mathcal{L}_{\mathcal{C}}$ is $(r_0, 3r_0r_1 r_2, r_1)$ and the rank triple of $\mathcal{R}_{\mathcal{C}}$ is $(r_1, 3r_1r_2 r_0, r_2)$.
- (2) $\mu_0 < \mu_1 < \mu_2$.
- (3) Provided that C is not an initial exceptional collection, then

$$\mu_1 - \mu_0 \le 1/2$$
, $\mu_2 - \mu_1 \le 1/2$.

(4) There are exact sequences

$$0 \to \mathcal{L}_{\mathcal{E}_{1}} \mathcal{E}_{2} \to \operatorname{Hom}(\mathcal{E}_{1}, \mathcal{E}_{2}) \otimes \mathcal{E}_{1} \to \mathcal{E}_{2} \to 0,$$

$$0 \to \mathcal{E}_{0} \to \operatorname{Hom}(\mathcal{E}_{0}, \mathcal{E}_{1})^{*} \otimes \mathcal{E}_{1} \to \mathcal{R}_{\mathcal{E}_{1}} \mathcal{E}_{0} \to 0,$$

$$0 \to \mathcal{E}_{2}(-3) \to \operatorname{Hom}(\mathcal{E}_{2}(-3), \mathcal{E}_{0})^{*} \otimes \mathcal{E}_{0} \to \mathcal{L}_{\mathcal{E}_{1}} \mathcal{E}_{2} \to 0,$$

$$0 \to \mathcal{R}_{\mathcal{E}_{3}} \mathcal{E}_{0} \to \operatorname{Hom}(\mathcal{E}_{2}, \mathcal{E}_{0}(3)) \otimes \mathcal{E}_{2} \to \mathcal{E}_{0}(3) \to 0.$$

- (5) $\dim \operatorname{Hom}(\mathcal{E}_0, \mathcal{E}_1) = 3(d_1 r_0 d_0 r_1)$ and $\dim \operatorname{Hom}(\mathcal{E}_1, \mathcal{E}_2) = 3(d_2 r_1 d_1 r_2)$. Also, $\dim \operatorname{Hom}(\mathcal{E}_2(-3), \mathcal{E}_0) = \dim \operatorname{Hom}(\mathcal{E}_2, \mathcal{E}_0(3)) = 3(3r_0 r_2 + d_0 r_2 d_2 r_0)$.
- (6) For any exceptional bundle with Chern character (r, d, e), we have $r^2 d^2 + 2re = 1$. Further, gcd(r, d) = 1.
- (7) There is at most one exceptional bundle of a given slope.
- (8) For \mathcal{E} an exceptional bundle, there is at most one strong exceptional triple $(\mathcal{F}_0, \mathcal{E}, \mathcal{F}_2)$ containing \mathcal{E} as its middle member.

Proof. (1) is standard, see e.g., [37, Thm. 4.2,3)]. For (2), the statement is certainly true for an initial triple. The proof of [37, Thm. 4.3(3)] shows in any event that the slopes satisfy, for some odd integer a and non-negative integer b, the equalities

(2.5)
$$\mu_0 = \varepsilon \left(\frac{a-1}{2^b} \right), \quad \mu_1 = \varepsilon \left(\frac{a}{2^b} \right), \quad \mu_2 = \varepsilon \left(\frac{a+1}{2^b} \right),$$

where ε is defined in [15, §5.1]. Note $\mu_0 < \mu_2$ follows inductively from the construction of a mutation of the triple, and by definition of ε , $\mu_1 = \mu_0.\mu_2$, where this notation is as defined in [15, §5.1]. By [15, Prop. (5.1)], $\mu_0 < \mu_0.\mu_2 < \mu_2$, hence the claim in (2).

(3) now follows from [15, Lem. (5.4)].

The first two exact sequences of (4) are the definitions of the mutation, and the last two are [37, Thm. 4.2,2)], correcting the obvious typographical errors.

(5) is [37, Lem. 4.1,2),5)], bearing in mind the vanishing of Ext's required for a strong exceptional collection.

For (6), we have for an exceptional bundle $1 = \chi(\mathcal{E}, \mathcal{E})$, and the claimed equality then follows from Riemann-Roch (1.5). Since $e \in \mathbb{Z}/2$, the equality immediately implies $\gcd(r, d) = 1$.

(7) is [15, Lemme (4.3)].

For (8), note that (2.5) implies that the slopes of \mathcal{F}_0 and \mathcal{F}_2 are determined by the slope of \mathcal{E} . The result then follows from (7).

Definition 2.5 (Associated vertex to an exceptional object). For \mathcal{E} an object of rank $r \neq 0$, first Chern class d, and Euler characteristic χ , define

$$(2.6) V_{\mathcal{E}} := \left(\frac{d}{r} - \frac{3}{2}, \frac{3d - \chi}{r}\right) \in M_{\mathbb{R}}.$$

Given a strong exceptional triple $\mathcal{C} = (\mathcal{E}_0, \mathcal{E}_1, \mathcal{E}_2)$, we define $\Delta_{\mathcal{C}}$ to be the triangle in $M_{\mathbb{R}}$ with vertices $V_{\mathcal{E}_0}$, $V_{\mathcal{E}_1}$, $V_{\mathcal{E}_2}$.

Example 2.6. Starting with $C = (\mathcal{O}, \mathcal{O}(1), \mathcal{O}(2))$, we have $\mathcal{R}_C = (\mathcal{O}(1), \mathcal{T}_{\mathbb{P}^2}, \mathcal{O}(2))$. The vertices of $\Delta_{\mathcal{R}_C}$ are (-1/2, 0), (0, 1/2) and (1/2, 0). We call this triangle an *initial triangle*.

The following theorem generalizes [7, Lem. 4.8], and the proof is very similar.

Theorem 2.7 (Moduli emptiness). Let C be a strong exceptional triple not equal to $(\mathcal{O}(m), \mathcal{O}(m+1), \mathcal{O}(m+2))$ for any m, i.e., not an initial exceptional collection. Then for σ in the interior of an edge of Δ_C , we have

$$H_{\Omega \text{stab }\sigma} = -\text{li}_2(-z^{m_F})$$

for some object $\mathcal{F} = \mathcal{E}$ or $\mathcal{E}[1]$, for \mathcal{E} an exceptional bundle. Further, for any $\sigma \in \operatorname{Int}(\Delta_{\mathcal{C}})$, there are no stable objects \mathcal{E} in \mathcal{A}^{σ} with $\operatorname{Re} Z^{\sigma}(\gamma(\mathcal{E})) = 0$.

Proof. **Step I.** *Identifying* $D^b(\mathbb{P}^2)$ *with a quiver representation category.* Since $\mathcal{C} = (\mathcal{E}_0, \mathcal{E}_1, \mathcal{E}_2)$ is not an initial exceptional collection, we can write it as the mutation of another strong exceptional collection $\mathcal{C}' = (\mathcal{E}'_0, \mathcal{E}'_1, \mathcal{E}'_2)$.

Let
$$\mathbf{T} = \mathcal{E}_0 \oplus \mathcal{E}_1 \oplus \mathcal{E}_2$$
, and let

$$A_0 := \operatorname{Hom}(\mathbf{T}, \mathbf{T})^{\operatorname{op}}.$$

Let A_0 be the abelian category of finitely generated left A_0 -modules. By a result due to Bondal, see [33, Thm. 3.11], there is an equivalence of categories

$$D^b(\mathbb{P}^2) \to D^b(\mathcal{A}_0), \quad E \mapsto \mathbf{R} \operatorname{Hom}(\mathbf{T}, E).$$

This allows us to view A_0 as a subcategory of $D^b(\mathbb{P}^2)$.

We note that A_0 is the quotient of the path algebra associated to a quiver with vertices v_0, v_1, v_2 and with dim $\text{Hom}(\mathcal{E}_i, \mathcal{E}_{i+1})$ arrows from v_{i+1} to v_i . We may label these arrows with a choice of basis $\{e_{i,j}\}$ for $\text{Hom}(\mathcal{E}_i, \mathcal{E}_{i+1})$. We divide out by an ideal of relations coming from the kernel of the composition map

$$\operatorname{Hom}(\mathcal{E}_1, \mathcal{E}_2) \otimes \operatorname{Hom}(\mathcal{E}_0, \mathcal{E}_1) \to \operatorname{Hom}(\mathcal{E}_0, \mathcal{E}_2).$$

In other words, if $\sum_{j_1,j_0} c_{j_1,j_0} e_{1,j_1} \otimes e_{0,j_0}$ lies in the kernel, then we include the corresponding linear combination of paths $\sum_{j_1,j_0} c_{j_1,j_0} e_{1,j_1} e_{0,j_0}$ in the ideal. Thus a finite-dimensional left A_0 -module consists of the data of finite-dimensional \mathbb{C} -vector spaces V_0, V_1, V_2 , and for every arrow between v_i and v_j a linear transformation $V_i \to V_j$. These must satisfy the given relations.

Note that A_0 then has simple objects S_0 , S_1 , S_2 with dimension vectors (1,0,0), (0,1,0) and (0,0,1) respectively, with S_j given by $V_j = \mathbb{C}$ and $V_k = 0$, $j \neq k$.

Step II. Identifying simple objects. We analyze right and left mutations separately.

Right mutations. Suppose $C = \mathcal{R}_{C'}$. In this case

$$(\mathcal{E}_0,\mathcal{E}_1,\mathcal{E}_2) = (\mathcal{E}_1',\mathcal{R}_{\mathcal{E}_1'}\mathcal{E}_0',\mathcal{E}_2').$$

The following triple

$$(S_0, S_1, S_2) = (E'_1, E'_0[1], E'_2(-3)[2])$$

corresponds to the three simple objects. To see this, we just need to show that \mathbf{R} Hom(\mathbf{T} , \mathcal{S}_i) defines the A_0 -module S_i for i=1,2,3. In other words, we need to check that

$$\operatorname{Ext}^{k}(\mathcal{E}_{i}, \mathcal{S}_{j}) = \begin{cases} 0 & \text{if } k \neq 0 \text{ or } i \neq j \\ \mathbb{C} & k = 0, i = j \end{cases}$$

These are all mostly straightforward using the fact that \mathcal{C} and \mathcal{C}' are strong exceptional collections. For example, $\operatorname{Ext}^*(\mathcal{E}_0,\mathcal{S}_0)=\operatorname{Ext}^*(\mathcal{E}_1',\mathcal{E}_1')$ which is \mathbb{C} in degree 0 and 0 otherwise. On the other hand, $\operatorname{Ext}^*(\mathcal{E}_0,\mathcal{S}_2)=\operatorname{Ext}^*(\mathcal{E}_1',\mathcal{E}_2'(-3)[2])=\operatorname{Ext}^{*+2}(\mathcal{E}_1',\mathcal{E}_2'(-3))=\operatorname{Ext}^{-*}(\mathcal{E}_2',\mathcal{E}_1')^\vee=0$ by Serre duality and again the fact that \mathcal{C}' is an strong exceptional collection.

The only slightly subtle calculation is that of $\operatorname{Ext}^*(\mathcal{E}_1,\mathcal{S}_1) = \operatorname{Ext}^{*+1}(\mathcal{R}_{\mathcal{E}_1'}\mathcal{E}_0',\mathcal{E}_0')$. Applying $\operatorname{Ext}^*(\cdot,\mathcal{E}_0')$ to the defining exact sequence for $\mathcal{R}_{\mathcal{E}_1'}\mathcal{E}_0'$, we have a long exact sequence

 $\rightarrow \operatorname{Hom}(\mathcal{E}_0',\mathcal{E}_1')^* \otimes \operatorname{Ext}^i(\mathcal{E}_1',\mathcal{E}_0') \rightarrow \operatorname{Ext}^i(\mathcal{E}_0',\mathcal{E}_0') \rightarrow \operatorname{Ext}^{i+1}(\mathcal{R}_{\mathcal{E}_1'}\mathcal{E}_0',\mathcal{E}_0') \rightarrow \operatorname{Hom}(\mathcal{E}_0',\mathcal{E}_1')^* \otimes \operatorname{Ext}^{i+1}(\mathcal{E}_1',\mathcal{E}_0') \rightarrow \operatorname{Hom}(\mathcal{E}_0',\mathcal{E}_1')^* \otimes \operatorname{Ext}^i(\mathcal{E}_1',\mathcal{E}_0') = \operatorname{Hom}(\mathcal{E}_0',\mathcal{E}_1')^* \otimes \operatorname{Ext}^i(\mathcal{E}_1',\mathcal{E}_0'). \text{ Since } \operatorname{Ext}^*(\mathcal{E}_1',\mathcal{E}_0') = 0 \text{ and } \mathcal{E}_0' \text{ is exceptional, we obtain}$

$$\operatorname{Ext}^{i}(\mathcal{E}_{1},\mathcal{S}_{1}) = \begin{cases} \mathbb{C} & i = 0\\ 0 & i \neq 0. \end{cases}$$

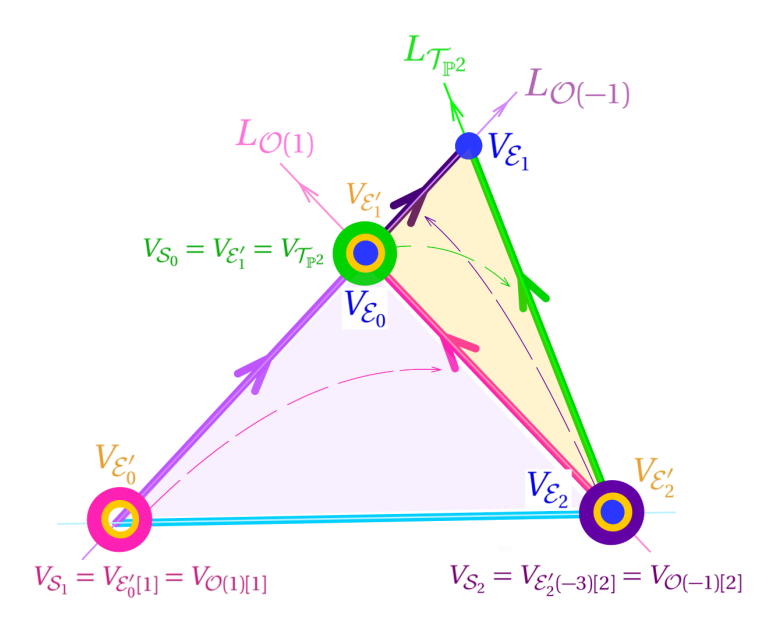


FIGURE 6. Right mutation of the central initial triangle. Dashed arrows show the corresponding edges to the simple vertices V_{S_i} . Here, $\mathcal{E}_0 = \mathcal{T}_{\mathbb{P}^2}$, $\mathcal{E}_2 = \mathcal{O}(2)$, and \mathcal{E}_1 is an object of Chern character (5, 8, 4).

Left mutations. Suppose $C = \mathcal{L}_{C'}$. In this case

$$(\mathcal{E}_0,\mathcal{E}_1,\mathcal{E}_2) = (\mathcal{E}_0',\mathcal{L}_{\mathcal{E}_1'}\mathcal{E}_2',\mathcal{E}_1').$$

Now the simples are

$$(S_0, S_1, S_2) = (E'_0, E'_2(-3)[1], E'_1(-3)[2]).$$

This is checked similarly.

Step III. The central charges of the simple objects and the categories $\mathcal{A}^{\sigma}[Z^{\sigma}, \phi]$. Write $(r_i, d_i, \chi_i) = (r(\mathcal{E}_i), d(\mathcal{E}_i), \chi(\mathcal{E}_i))$ and $(r'_i, d'_i, \chi'_i) = (r(\mathcal{S}_i), d(\mathcal{S}_i), \chi(\mathcal{S}_i))$. Following (1.11), set

$$L_i = L_{(r_i',d_i',\chi_i')} = L_{\mathcal{S}_i}.$$

Recall from (1.8) that, with $\sigma = (x, y)$,

(2.7)
$$Z^{\sigma}(S_j) = r'_j y + d'_j x + r'_j + \frac{3}{2} d'_j - \chi'_j + i(d'_j - r'_j x) \sqrt{x^2 + 2y}.$$

On the other hand, by the calculations of $\operatorname{Ext}^i(\mathcal{E}_j, \mathcal{S}_k)$ of Step II for the first equality and Riemann-Roch (1.5) for the second,

(2.8)
$$\delta_{ij} = \chi(\mathcal{E}_i, \mathcal{S}_j) = -3d_i r'_j - r_i r'_j - d_i d'_j + r_i \chi'_j + \chi_i r'_j$$

where δ_{ij} is the Kronecker delta. Note that

$$(2.9) -r_i \operatorname{Re} Z^{V_{\mathcal{E}_i}}(\mathcal{S}_j) = -r_i r_j' \frac{3d_i - \chi_i}{r_i} - r_i d_j' \left(\frac{d_i}{r_i} - \frac{3}{2}\right) - r_i r_j' - \frac{3}{2} r_i d_j' + r_i \chi_j'$$

$$= \chi(\mathcal{E}_i, \mathcal{S}_j).$$

Thus, if $\{i, j, k\} = \{0, 1, 2\}$, we see that $V_{\mathcal{E}_i} = L_j \cap L_k$ and that

In particular, the L_i are the extensions of the three edges of Δ_C to lines.

We first show that if $\sigma \in \operatorname{Int}(\Delta_{\mathcal{C}})$, then there are no stable objects \mathcal{E} in \mathcal{A}^{σ} with $\operatorname{Re} Z^{\sigma}(\mathcal{E}) = 0$. This was already shown for the triangles obtained when \mathcal{C}' is an initial strong exceptional triple in [7, Lemma 4.8], and therefore we will assume that \mathcal{C}' is not an initial triple. This will enable us to avoid a special case.

Recall from [7, Section 4.3], the construction of a new stability condition $(Z[\phi], \mathcal{A}[Z,\phi])$ from a stability condition (Z,\mathcal{A}) for $\phi \in \mathbb{R}$. One defines $Z[\phi](\gamma) := e^{-i\pi\phi}Z(\gamma)$. Let \mathcal{Q}_{ϕ} be the subcategory of \mathcal{A} generated via extensions of the semistable objects \mathcal{E} with $\frac{1}{\pi}\operatorname{Arg}Z(\mathcal{E}) > \phi$, and \mathcal{F}_{ϕ} the subcategory of \mathcal{A} similarly generated by the semistable objects \mathcal{E} with $\frac{1}{\pi}\operatorname{Arg}Z(\mathcal{E}) \leq \phi$. Then denoting $\mathcal{H}_{\mathcal{A}}^i$ the cohomology functors with respect to the bounded t-structure of heart \mathcal{A} , the category $\mathcal{A}[Z,\phi]$ is the subcategory of $D^b(\mathbb{P}^2)$ of objects with $\mathcal{H}_{\mathcal{A}}^i = 0$ for $i \neq -1,0$, $\mathcal{H}_{\mathcal{A}}^{-1}$ an object of \mathcal{F}_{ϕ} , and $\mathcal{H}_{\mathcal{A}}^0$ an object of \mathcal{Q}_{ϕ} .

We can write $(x, y) = \sigma \in \operatorname{Int}(\Delta_{\mathcal{C}})$ as $\sum_{i=0}^{2} a_i V_{\mathcal{E}_i}$ for $a_i > 0$, $a_0 + a_1 + a_2 = 1$. Then $\sum_{i=0}^{2} a_i \operatorname{Re} Z^{V_{\mathcal{E}_i}}(\mathcal{E}) = \operatorname{Re} Z^{\sigma}(E)$, so by (2.10),

(2.11)
$$\operatorname{Re} Z^{\sigma}(S_i) < 0 \text{ for } i = 0, 1, 2.$$

We also need to understand the sign of $\operatorname{Im} Z^{\sigma}(\mathcal{S}_i)$, which requires slightly different analyses in the left and right mutation cases. Note that the sign of $\operatorname{Im} Z^{\sigma}(\mathcal{S}_i)$ agrees with the sign of $\operatorname{sign}(r'_j) \left(\frac{d'_j}{r'_j} - x \right)$, and d'_j/r'_j is the slope of \mathcal{S}_i . (Bear in mind that the rank of $\mathcal{E}[1]$ is the negative of the rank of \mathcal{E}).

The right mutation case. Suppose $\mathcal{C}=\mathcal{R}_{\mathcal{C}'}$. Let μ_i' be the slope of \mathcal{E}_i' . Then the slopes of \mathcal{S}_i , i=0,1,2, are μ_1' , μ_0' , $\mu_2'-3$ respectively. Note further that by the definition of $V_{\mathcal{E}_i}$ and Lemma 2.4, (2), $\mu_0-3/2 < x < \mu_2-3/2$, or $\mu_1'-3/2 < x < \mu_2'-3/2$. By Lemma 2.4, (3), $\mu_2'-\mu_1'=\mu_2-\mu_0 \le 1$. Thus we have

(2.12)
$$\mu_1' > x, \quad \mu_2' - 3 < x.$$

Provided that \mathcal{C}' was not an initial exceptional collection, then again $\mu_2' - \mu_0' \leq 1$ and

(2.13)
$$\mu_0' > x$$
.

Thus we see that (taking into account the shift and twist on S_1, S_2)

$$\operatorname{Im} Z^{\sigma}(S_0) > 0$$
, $\operatorname{Im} Z^{\sigma}(S_1) < 0$, $\operatorname{Im} Z^{\sigma}(S_2) < 0$.

Note further that the inequalities (2.12), (2.13) imply that $\mathcal{E}_0', \mathcal{E}_1' \in \mathcal{A}^{\sigma}$ and $\mathcal{E}_2'(-3)[1] \in \mathcal{A}^{\sigma}$.

Putting this all together, taking $\phi = 1/2$, we see that $\mathcal{E}'_1 \in \mathcal{Q}_{\phi}$, $\mathcal{E}'_0 \in \mathcal{F}_{\phi}$ (remembering that $\mathcal{S}_1 = \mathcal{E}'_0[1]$), $\mathcal{E}'_2(-3)[1] \in \mathcal{F}_{\phi}$, so we get $\mathcal{S}_i \in \mathcal{A}^{\sigma}[Z^{\sigma}, \phi]$.

The left mutation case. Suppose $C = \mathcal{L}_{C'}$ with C' not an initial collection.

Similarly as in the right mutation case, we obtain

$$\operatorname{Im} Z^{\sigma}(S_0) > 0$$
, $\operatorname{Im} Z^{\sigma}(S_1) > 0$, $\operatorname{Im} Z^{\sigma}(S_2) < 0$.

In addition, $\mathcal{E}'_0 \in \mathcal{A}^{\sigma}$ and $\mathcal{E}'_1(-3)[1], \mathcal{E}'_2(-3)[1] \in \mathcal{A}^{\sigma}$.

Putting this together, taking $\phi = 1/2$, we see that $\mathcal{E}'_0, \mathcal{E}'_2(-3)[1] \in \mathcal{Q}_{\phi}, \mathcal{E}'_1(-3)[1] \in \mathcal{F}_{\phi}$, so we get $\mathcal{S}_i \in \mathcal{A}^{\sigma}[Z^{\sigma}, \phi]$.

Step IV. Completing the argument. We may now finish the argument as in the proof of [7, Lemma 4.8]. In both cases, $\mathcal{A}^{\sigma}[Z^{\sigma}, \phi]$ contains the simple objects of the quiver representation category \mathcal{A}_0 and $\frac{1}{\pi}\operatorname{Arg}Z^{\sigma}[\phi](\mathcal{S}_i)\in(0,1)$. Further, $(\mathcal{S}_0,\mathcal{S}_1,\mathcal{S}_2)$ form a complete Ext-exceptional collection in the sense of [33, Def. 3.10]. Thus by [33, Lem. 3.16], $\mathcal{A}^{\sigma}[Z^{\sigma}, \phi] = \mathcal{A}_0$. We deduce that the central charge with respect to $Z^{\sigma}[\phi]$ of any stable object in $\mathcal{A}^{\sigma}[Z^{\sigma}, \phi]$, being a nonnegative linear combination of the central charges of the \mathcal{S}_i , lie in the open upper half-plane. Correspondingly, any stable object of \mathcal{A}^{σ} has Z^{σ} -central charge lying in the open left half-plane, and hence has negative real part. In particular, the real part of the central charge is non-zero. This proves the emptiness of $\operatorname{Int}(\Delta_{\mathcal{C}})$.

If instead σ lies in the interior of an edge of $\Delta_{\mathcal{C}}$, say contained in the line L_i , containing $V_{\mathcal{E}_j}$, $V_{\mathcal{E}_k}$, $\{i,j,k\}=\{0,1,2\}$, then $\operatorname{Re} Z^{\sigma}(\mathcal{S}_i)=0$. Further, the argument above in the two cases still shows that $\mathcal{S}_i \in \mathcal{A}^{\sigma}[Z^{\sigma},1/2]$; indeed, the inequalities (2.12), (2.13) remain strict inequalities, as well as the analogous inequalities in the left mutation case. Since \mathcal{S}_i is simple, it must be stable. Thus \mathcal{S}_i corresponds to a stable object in \mathcal{A}^{σ} , necessarily (a shift) of an exceptional bundle. So there is a one-point moduli space and the edge is thus contained in a non-trivial ray. The precise form of the function attached to the ray then follows from Theorem 1.15. \square

Remark 2.8. For future reference, we observe that in Step III of the proof, the object of \mathcal{A}^{σ} corresponding to \mathcal{S}_0 is \mathcal{E}_0 in both the left and right mutation cases. The object corresponding to \mathcal{S}_2 in \mathcal{A}^{σ} is $\mathcal{E}_2(-3)[1]$ in both cases.

Remark 2.9. The object S_1 cannot be read off from the strong exceptional collection C, as it depends on whether C is obtained by right or left mutation. However, $S_1 = \mathcal{E}_0'[1]$ or $\mathcal{E}_2'(-3)[1]$ in the right or left mutation case, and thus in either case $r_1' < 0$. From (2.7), (2.8) and (2.9), we then see that $V_{\mathcal{E}_1}$ always lies above the line $L_{\mathcal{S}_i}$. Thus $V_{\mathcal{E}_1}$ always lies above the line containing $V_{\mathcal{E}_0}$, $V_{\mathcal{E}_2}$.

Definition 2.10 (Vertex-line duality). Let \mathcal{E}_i , i = 0, 1, 2, be as in the proof of Theorem 2.7. We say that the vertex $V = V_{\mathcal{E}_i}$ (defined in Definition 2.5) is the *dual vertex to* \mathcal{E}_i , or the *dual vertex to* $\mathcal{L}_{\mathcal{E}_i}$. On the other hand, \mathcal{E}_i , or $\mathcal{L}_{\mathcal{E}_i}$ is called the *dual object/line to* $V_{\mathcal{E}_i}$.

Recall the tree \mathcal{T} of Construction 2.1. Write \mathcal{T}_E for a copy of this tree. We decorate each vertex $w \in V(\mathcal{T}_E)$ with a strong exceptional triple $\mathcal{C}(w)$ in the following way. First, we assign to the root of \mathcal{T}_E the strong exceptional triple $(\mathcal{O}(1), \mathcal{T}_{\mathbb{P}^2}, \mathcal{O}(2))$. Inductively, if $\mathcal{C}(w)$ has been defined, we assign the triples $\mathcal{L}_{\mathcal{C}(w)}$ and $\mathcal{R}_{\mathcal{C}(w)}$ to the two children of w.

We now identify the triangles constructed algorithmically in Construction 2.1 with the triangles associated to strong exceptional triples.

Theorem 2.11. (1) There exists an isomorphism $\eta_E : \mathcal{T} \to \mathcal{T}_E$ so that for w a vertex of \mathcal{T} , $\Delta_w = \Delta_{\mathcal{C}(\eta_E(w))}$.

- (2) This isomorphism has the property that if $C(\eta_E(w)) = (\mathcal{E}_0, \mathcal{E}_1, \mathcal{E}_2)$, then $V_{\mathcal{E}_1}$ is the incoming vertex of Δ_w .
- (3) Except for the horizontal edge of Δ_{w_0} , which is contained in $\mathfrak{d}_0^- \cup \mathfrak{d}_0^+$, every edge E of every triangle Δ_w is contained in precisely one ray (\mathfrak{d}, H_0) of $\{\mathfrak{d}_{-1}^+, \mathfrak{d}_{-1}^-\} \cup \mathfrak{D}_{\text{discrete}}^0$.

Furthermore, if $\sigma \in U \subseteq M_{\mathbb{R}}$ lies in the interior of E, then $H_{\mathfrak{d}} = H_{\mathfrak{D}^{\text{stab}},\sigma}$, in the sense of Definition 1.9.

Proof. We construct η_E inductively, and prove statement (2) at the same time. We check most of (3) after this is done.

Step I. The base case. The base case is the vertex w_0 . From Example 2.6, we have that $\Delta_{w_0} = \Delta_{\mathcal{C}}$ with $\mathcal{C} = (\mathcal{O}(1), \mathcal{T}_{\mathbb{P}^2}, \mathcal{O}(2))$. Note that $V_{\mathcal{T}_{\mathbb{P}^2}}$ is the incoming vertex of Δ_{w_0} and Δ_{w_0} has a horizontal edge E contained in a union of the two rays \mathfrak{d}_0^- and \mathfrak{d}_0^+ . [7, Lem. 4.11] shows that $H_{\mathfrak{D}^{\mathrm{Stab}},\sigma}$ agrees with the attached wall functions to \mathfrak{d}_0^\pm for σ lying in $\mathrm{Int}(E) \cap \mathrm{Int}(\mathfrak{d}_0^\pm)$. Except for the uniqueness statements, this shows (3) for $\sigma \in E \cap U$.

Step II. The induction step. Now assume that for a vertex $w \in V(\mathcal{T})$, we have an assignment $\eta_E(w) \in V(\mathcal{T}_M)$ so that $\Delta_w = \Delta_{\mathcal{C}(w)}$, with $\mathcal{C}(w) = (\mathcal{E}_0, \mathcal{E}_1, \mathcal{E}_2)$ and $V_{\mathcal{E}_1}$ the incoming vertex of Δ_w . Let $\mathcal{S}_0, \mathcal{S}_1, \mathcal{S}_2$ be the corresponding simple objects as described in Step II of the proof of Theorem 2.7, so that $V_{\mathcal{E}_i} \in L_{\mathcal{S}_i}$ for $i \neq j$.

From the precise description of the \mathcal{S}_i in the right and left mutation cases, we see that the edges of $\Delta_{\mathcal{C}(w)}$ joining $V_{\mathcal{E}_1}$ to $V_{\mathcal{E}_0}$ and $V_{\mathcal{E}_2}$ are contained in the lines $L_{\mathcal{E}_2(-3)[1]}$ and $L_{\mathcal{E}_0}$ respectively, see Remark 2.8. Again, from the explicit description of the simples for $\mathcal{R}_{\mathcal{C}(w)}$ and $\mathcal{L}_{\mathcal{C}(w)}$, one sees that $V_{\mathcal{R}_{\mathcal{E}_1}\mathcal{E}_0}$ is also contained in the line $L_{\mathcal{E}_2(-3)[1]}$ and the vertex $V_{\mathcal{L}_{\mathcal{E}_1}\mathcal{E}_2}$ is also contained in the line $L_{\mathcal{E}_0}$. Further, the edge joining $V_{\mathcal{E}_0}$ and $V_{\mathcal{L}_{\mathcal{E}_1}\mathcal{E}_2}$ is contained in $L_{\mathcal{E}_1(-3)[1]}$ and the edge joining $V_{\mathcal{E}_2}$ and $V_{\mathcal{R}_{\mathcal{E}_1}\mathcal{E}_0}$ is contained in $\mathcal{L}_{\mathcal{E}_1}$. See Figure 7.

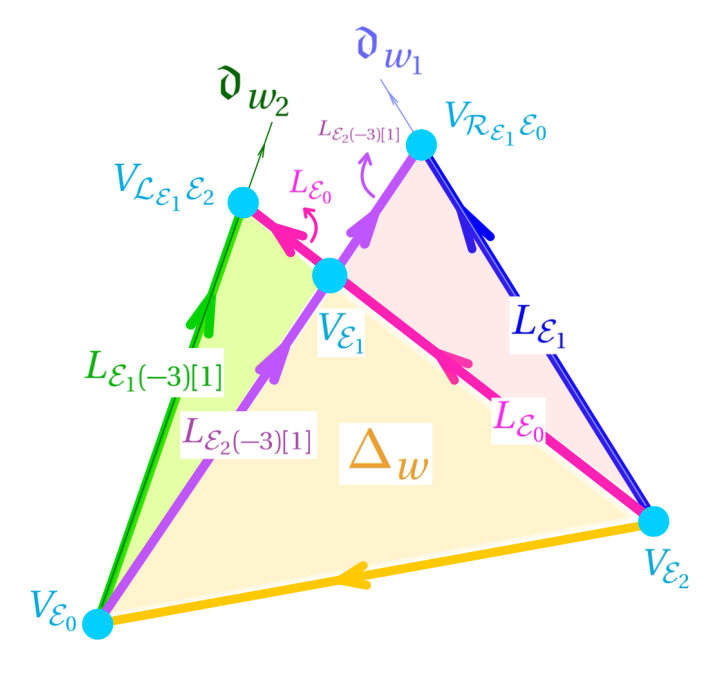


FIGURE 7

Since we have assumed that $V_{\mathcal{E}_1}$ is the incoming vertex, in the language of Construction 2.1, we have $v = V_{\mathcal{E}_1}$, and can take $v_1 = V_{\mathcal{E}_0}$, $v_2 = V_{\mathcal{E}_2}$. Again in the notation of Construction 2.1, m_i is a primitive tangent vector to the edge joining v to v_i , oriented from v to v_i . Then we see that

$$m_1 = m_{\mathcal{E}_2(-3)[1]} = (-r(\mathcal{E}_2(-3)), d(\mathcal{E}_2(-3))), \quad m_2 = m_{\mathcal{E}_0} = (r(\mathcal{E}_0), -d(\mathcal{E}_0)),$$

recalling the notation of (1.10). To see these equalities, first note that the opposite vectors $m_{\mathcal{E}_2(-3)[1]}$ and $m_{\mathcal{E}_0}$ are tangent to $L_{\mathcal{E}_2(-3)[1]}$ and $L_{\mathcal{E}_0}$ respectively. They are have the same orientation as m_1 and m_2 by the fact that the x-coordinates of v_1 , v, v_2 are increasing by Lemma 2.4(2). Finally, they are primitive by Lemma 2.4,(6).

We may order the children w_1 , w_2 of w so that Δ_{w_j} is the mutation of Δ_w at v_j . We will define $\eta_E(w_1) := \mathcal{R}_{\mathcal{C}(w)}$ and $\eta_E(w_2) = \mathcal{L}_{\mathcal{C}(w)}$. Thus we need to check that $\Delta_{w_i} = \Delta_{\mathcal{C}(\eta_E(w_i))}$.

Further analysis requires two cases, depending on whether $(\mathcal{E}_0, \mathcal{E}_1, \mathcal{E}_2)$ is obtained as a right or left mutation from $(\mathcal{E}'_0, \mathcal{E}'_1, \mathcal{E}'_2)$.

Right mutation. Suppose $(\mathcal{E}_0, \mathcal{E}_1, \mathcal{E}_2) = (\mathcal{E}'_1, \mathcal{R}_{\mathcal{E}'_1} \mathcal{E}'_0, \mathcal{E}'_2)$. Then the edge of Δ_w joining $V_{\mathcal{E}_0}$ and $V_{\mathcal{E}_2}$ is $L_{\mathcal{E}'_0[1]}$, see Remark 2.9. A primitive tangent vector to this edge, pointing from v_1 to v_2 , is

$$m = m_{\mathcal{E}'_0} = (r(\mathcal{E}'_0), -d(\mathcal{E}'_0)).$$

If we mutate Δ_w at the vertex v_1 , we obtain the triangle Δ_{w_1} with vertices $V_{\mathcal{E}_1}$, $V_{\mathcal{E}_2}$, and the third vertex at the intersection of $L_{\mathcal{E}_2(-3)[1]}$ and $\mathfrak{d}_{w_1} = V_{\mathcal{E}_2} - \mathbb{R}_{\geq 0}(3D_{v_2}m_2 - m)$. If we show that this intersection is $V_{\mathcal{R}_{\mathcal{E}_1}\mathcal{E}_0}$, this will show that $\Delta_{w_1} = \Delta_{\mathcal{R}_{\mathcal{C}(w)}}$ as needed. Thus it is sufficient to show that \mathfrak{d}_{w_1} is contained in the line $L_{\mathcal{E}_1}$, i.e., that the tangent vector to $L_{\mathcal{E}_1}$ oriented from $V_{\mathcal{R}_{\mathcal{E}_1}\mathcal{E}_0}$ to $V_{\mathcal{E}_2} = v_2$ is $3D_{v_2}m_2 - m$. Put another way, we require

$$(2.14) m_{\mathcal{E}_1} = 3D_{\nu_2} m_{\mathcal{E}_0} - m_{\mathcal{E}_0'}$$

However, using $\mathcal{E}'_1 = \mathcal{E}_0$, we have the second exact sequence of Lemma 2.4(4) is

$$0 \to \mathcal{E}'_0 \to \text{Hom}(\mathcal{E}'_0, \mathcal{E}_0)^* \otimes \mathcal{E}_0 \to \mathcal{E}_1 \to 0.$$

By Lemma 2.4,(5), dim Hom $(\mathcal{E}_0',\mathcal{E}_0)=3(d(\mathcal{E}_0)r(\mathcal{E}_0')-d(\mathcal{E}_0')r(\mathcal{E}_0))=3|m\wedge m_2|=3D_{\nu_2}.$ Then (2.14) follows from the exact sequence.

Similarly, if instead we mutate Δ_w at the vertex v_2 to get the triangle Δ_{w_2} , we wish to show $\Delta_{w_2} = \Delta_{\mathcal{L}_{\mathcal{C}(w)}}$. For this analysis, we need to change the orientation of m, replacing it with

$$m = m_{\mathcal{E}'_0[1]} = \left(-r(\mathcal{E}'_0), d(\mathcal{E}'_0)\right).$$

Noting that $\mathfrak{d}_{w_2} = V_{\mathcal{E}_0} - \mathbb{R}_{\geq 0}(3D_{v_1}m_1 - m)$, we need to show that $\mathfrak{d}_{w_2} \subseteq L_{\mathcal{E}_1(-3)[1]}$, i.e., that

$$(2.15) m_{\mathcal{E}_1(-3)[1]} = 3D_{\nu_1} m_{\mathcal{E}_2(-3)[1]} - m_{\mathcal{E}_0'[1]}.$$

By twisting the fourth exact sequence of Lemma 2.4(4) by -3, we get the exact sequence

$$0 \to \mathcal{E}_1(-3) \to \operatorname{Hom}(\mathcal{E}_2, \mathcal{E}_0'(3)) \otimes \mathcal{E}_2(-3) \to \mathcal{E}_0' \to 0.$$

By Lemma 2.4,(5),

$$\dim \operatorname{Hom}(\mathcal{E}_{2}, \mathcal{E}'_{0}(3)) = 3 \left[3r(\mathcal{E}_{2})r(\mathcal{E}'_{0}) + d(\mathcal{E}'_{0})r(\mathcal{E}_{2}) - d(\mathcal{E}_{2})r(\mathcal{E}'_{0}) \right]$$

$$= 3 \left[d(\mathcal{E}'_{0})r(\mathcal{E}_{2}) - r(\mathcal{E}'_{0}) \left(d(\mathcal{E}_{2}) - 3r(\mathcal{E}_{2}) \right) \right]$$

$$= 3 \left[d(\mathcal{E}'_{0})r(\mathcal{E}_{2}(-3)) - r(\mathcal{E}'_{0})d(\mathcal{E}_{2}(-3)) \right]$$

$$= 3|m_{1} \wedge m|$$

$$= 3D_{\nu_{1}}.$$

Thus the exact sequence implies the desired equality on tangent vectors again.

Left mutation. Suppose instead that $(\mathcal{E}_0, \mathcal{E}_1, \mathcal{E}_2) = (\mathcal{E}'_0, \mathcal{L}_{\mathcal{E}'_1} \mathcal{E}'_2, \mathcal{E}'_1)$. Then the edge of Δ_w joining $V_{\mathcal{E}_0}$ and $V_{\mathcal{E}_2}$ is $L_{\mathcal{E}'_2(-3)[1]}$, again by Remark 2.9, and a primitive tangent vector to this edge, pointing from v_1 to v_2 , is

$$m = m_{\mathcal{E}'_2(-3)} = (r(\mathcal{E}'_2(-3)), -d(\mathcal{E}'_2(-3))).$$

If we mutate Δ_w at the vertex v_1 to get the triangle Δ_{w_1} , we have as previously $\mathfrak{d}_{w_1} = V_{\mathcal{E}_2} - \mathbb{R}_{\geq 0}(3D_{v_2}m_2 - m)$ and we need to show that $\mathfrak{d}_{w_1} \subseteq L_{\mathcal{E}_1}$, i.e., that

$$(2.17) m_{\mathcal{E}_1} = 3D_{\nu_2} m_{\mathcal{E}_0} - m_{\mathcal{E}_2'(-3)}.$$

As in the right mutation case, this follows from the third exact sequence of Lemma 2.4(4).

If instead we mutate Δ_w at the vertex v_2 to get the triangle Δ_{w_2} , we need to change the orientation of m, replacing it with

$$m = m_{\mathcal{E}'_2(-3)[1]} = (-r(\mathcal{E}'_2(-3)), d(\mathcal{E}'_2(-3))).$$

We have as previously $\mathfrak{d}_{w_2} = V_{\mathcal{E}_0} - \mathbb{R}_{\geq 0}(3D_{\nu_1}m_1 - m)$ and need to show that $\mathfrak{d}_{w_2} \subseteq L_{\mathcal{E}_1(-3)[1]}$, i.e., that

$$(2.18) m_{\mathcal{E}_1(-3)[1]} = 3D_{\nu_1} m_{\mathcal{E}_2(-3)[1]} - m_{\mathcal{E}_2'(-3)[1]}.$$

This time this follows by twisting the first exact sequence of Lemma 2.4(4) by -3.

Step III. *Proof of* (3). Let Δ_w be a triangle as above, with $(\mathcal{E}_0, \mathcal{E}_1, \mathcal{E}_2)$ the corresponding strong exceptional collection. By the inductive construction of the triangles, Construction 2.1, the edge E_i joining v to v_i , i = 1, 2, is contained in a ray $(\mathfrak{d}_i, H_{\mathfrak{d}_i})$ of $\{\mathfrak{d}_{-1}^+, \mathfrak{d}_1^-\} \cup \mathfrak{D}_{\text{discrete}}^0$, with $H_{\mathfrak{d}_i} = -\text{li}_2(-z^{m_i})$. But by Remark 2.8 and Theorem 2.7, this agrees with $H_{\mathfrak{D}_{\text{stab}},\sigma}$ for $\sigma \in \text{Int}(E_i)$.

It remains to show uniqueness of this ray. We first observe that if an edge of a triangle is contained in some $L_{\mathcal{E}}$ for \mathcal{E} an exceptional bundle, in fact \mathcal{E} is uniquely determined. Indeed, the slope of \mathcal{E} is determined by the slope of the line $L_{\mathcal{E}}$, and \mathcal{E} is uniquely determined by its slope by Lemma 2.4,(7).

We have seen in Step II that every ray of $\mathfrak{D}^0_{\text{discrete}}$ is contained in a line of the form $L_{\mathcal{E}}$ or $L_{\mathcal{E}(-3)[1]}$ for $V_{\mathcal{E}}$ an incoming vertex of a triangle Δ_w , or equivalently, the middle member of a strong exceptional triple. The middle member of the triple uniquely determines the strong exceptional triple by Lemma 2.4,(8) hence the triangle. Note that the ray is contained in a line of the form $L_{\mathcal{E}}$ if its direction vector has negative x-coordinate and is contained in a line of the from $L_{\mathcal{E}(-3)[1]}$ if its direction vector has positive x-coordinate. Thus the map which assigns to $(\mathfrak{d},H_{\mathfrak{d}})\in \mathfrak{D}^0_{\text{discrete}}$ the unique exceptional bundle \mathcal{E} or shifted exceptional bundle $\mathcal{E}[1]$ with $\mathfrak{d}\subseteq L_{\mathcal{E}}$ is an injective map into the set of exceptional bundles and their shifts. In particular, an edge of a triangle Δ_w cannot be contained in two different such rays. Note also that none of the exceptional bundles which appear in the image of this map are line bundles. Since the exceptional bundles whose corresponding lines contain \mathfrak{d}^+_{-1} and \mathfrak{d}^-_{1} are the line bundles $\mathcal{O}(-1)$ and $\mathcal{O}(1)$ respectively, we see that no edge of any triangle Δ_w can be contained in more than one ray of $\{\mathfrak{d}^+_{-1},\mathfrak{d}^-_{1}\}\cup\mathfrak{D}^0_{\text{discrete}}$. This complete the proof of (3).

Corollary 2.12 (Collection of triangles). (1) The collection of triangles $\{\Delta_w | w \in V(\mathcal{T})\}$ forms a triangulation of the region

$$R^0_{\Delta} := \bigcup_{w \in V(\mathcal{T})} \Delta_w.$$

(2) The collection of triangles $\{T^k(\Delta_w)|w\in V(\mathcal{T}), k\in\mathbb{Z}\}$ forms a triangulation of the region

$$R_{\Delta} := \bigcup_{k \in \mathbb{Z}} T^k(R_{\Delta}^0).$$

(3) $T^k(R^0_\Delta) = R_\Delta \cap \{(x, y) \in M_\mathbb{R} \mid (k-1)/2 \le x \le (k+1)/2\}.$

Proof. For (1), by Theorem 2.11, it is enough to observe that $\bigcup_{w \in V(\mathcal{T}_M)} \Delta_{\mathcal{C}(w)}$ is triangulated by $S := \{\Delta_{\mathcal{C}(w)} | w \in V(\mathcal{T}(M))\}$. By construction, each triangle $\Delta_{\mathcal{C}(w)}$ meets three other triangles in S along the three edges of $\Delta_{\mathcal{C}(w)}$ determined by the parent and the two children of w. There is of course one exception, namely when $w = w_0$ is the root, in which case there are only two triangles. To show S triangulates the given region, we just need to check that for any other triangle Δ of S, $\Delta \cap \Delta_{\mathcal{C}(w)}$ is a face of both if non-empty. However, if this intersection is not a face, then one of the edges of Δ must meet the interior of either $\Delta_{\mathcal{C}(w)}$ or one of the three adjacent triangles. However, since the edges of Δ are contained in non-trivial rays of $\mathfrak{D}^{\text{stab}}$ and the interior of the triangles $\Delta_{\mathcal{C}(w)}$ contain no non-trivial rays of $\mathfrak{D}^{\text{stab}}$, this is not possible. Again, there is a special case if $w = w_0$, in which case the edge with vertices (-1/2,0),(1/2,0) does not have an adjacent triangle. But the region below this edge also does not contain any rays, by [7, Lem 4.10] (where this region is split into two regions $\overline{U}_{0,L}^{\text{in}}$ and $\overline{U}_{0,R}^{\text{in}}$, see Figure 4(1)). This proves (1).

For (2), every non-initial strong exceptional collection is a twist of a non-initial strong exceptional collection obtained from mutating $(\mathcal{O}(1), \mathcal{T}_{\mathbb{P}^2}, \mathcal{O}(2))$. Thus the collection of triangles $\{T^k(\Delta_w)|\ w\in V(\mathcal{T})\}$ coincides with the collection of triangles

 $\{\Delta_{\mathcal{C}} | \mathcal{C} \text{ is a non-initial strong exceptional collection} \}.$

Given the previous paragraph, this clearly triangulates R_{Δ} .

For (3), it is sufficient to note that the initial triangle Δ_{w_0} has x-coordinate lying in [-1/2, 1/2], and by Lemma 2.4,(2), Definition 2.5, and Theorem 2.11, all vertices of triangles obtained via mutation from Δ_{w_0} also have x-coordinate lying in [-1/2, 1/2].

The following now follows immediately from Theorem 2.11(3):

Corollary 2.13. The two scattering diagrams $\mathfrak{D}^{\text{stab}}$ and $\mathfrak{D}^{\text{stab}}_{\text{in}} \cup \mathfrak{D}_{\text{discrete}}$ are equivalent in R_{Δ} .

2.3. **Determinants of vertices and Markov numbers.** We recall a Markov triple (x, y, z) is a triple of positive integers satisfying the equation

$$x^2 + y^2 + z^2 = 3xyz$$
.

Given a Markov triple (x, y, z), any permutation is also a Markov triple. Also, if (x, y, z) is a Markov triple, then so is (x, y, 3xy - z); this is *the mutation of* (x, y, z) *at* z. The mutations at x and y are defined similarly. The Markov tree is obtained by taking as vertices Markov triples up to permutation, and connecting two Markov triples by an edge if they are related by permutation and one mutation. The Markov tree has one univalent vertex, corresponding to (1,1,1), an adjacent bivalent vertex, corresponding to (1,1,2), also adjacent to (1,2,5). All remaining vertices, including (1,2,5), are trivalent.

Definition 2.14. We define a modified Markov tree \mathcal{T}_M as follows. Let \mathcal{T}' be the subtree obtained by deleting the two vertices (1,1,1) and (1,1,2). Take two copies of \mathcal{T}' and attach them to a vertex labeled with (1,1,2), to obtain an infinite binary tree with root given by (1,1,2). We call this tree \mathcal{T}_M .

Lemma 2.15. There is an isomorphism $\eta_M : \mathcal{T}_E \to \mathcal{T}_M$ with the property that for $w \in V(\mathcal{T}_E)$ with $\mathcal{C}(w) = (\mathcal{E}_0, \mathcal{E}_1, \mathcal{E}_2)$, the Markov triple (x, y, z) associated to the vertex $\eta_M(w)$ is a permutation of $(r(\mathcal{E}_0), r(\mathcal{E}_1), r(\mathcal{E}_2))$.

Proof. This is well-known, and follows immediately inductively. The base case is just fact that the rank triple of $C(w_0) = (\mathcal{O}(1), \mathcal{T}_{\mathcal{P}^2}, \mathcal{O}(2))$ is (1, 2, 1) and the induction step is Lemma 2.4,(1). \square

Lemma 2.16. For $w \in V(\mathcal{T})$, let v be a vertex of Δ_w , and let D_v (as defined in (2.3)) be calculated using the triangle Δ_w . Then there is an exceptional bundle \mathcal{E} such that $V_{\mathcal{E}} = v$ and $D_v = r(\mathcal{E})$. Further, if v = (x, y), then D_v is the denominator of the rational number x + 3/2 written in reduced form. In particular, D_v only depends on v.

Proof. We proceed by induction. The root $w=w_0$ of \mathcal{T} corresponds to the triangle of (2.2), and also has vertices $V_{\mathcal{O}(1)}, V_{\mathcal{T}_{\mathbb{P}^2}}, V_{\mathcal{O}(2)}$ by Example 2.6. The primitive tangent vectors at the vertex $v=(0,1/2)=V_{\mathcal{T}_{\mathbb{P}^2}}$ are (1,-1) and (-1,-1), $D_v=|(1,-1)\wedge(-1,-1)|=2=\mathrm{rank}(\mathcal{T}_{\mathbb{P}^2})$. The determinants of the vertices $(\pm 1/2,0)$ are similarly calculated to be 1, the ranks of $\mathcal{O}(1)$ and $\mathcal{O}(2)$.

For the induction step, suppose that we have shown the statement for a given triangle Δ_w , $w \in V(\mathcal{T})$. Let w' be a child of w, and assume first that $\mathcal{C}(\eta_E(w'))$ obtained via left mutation. Thus by Theorem 2.11, if $\mathcal{C}(\eta_E(w)) = (\mathcal{E}_0, \mathcal{E}_1, \mathcal{E}_2)$, then Δ_w has vertices $V_{\mathcal{E}_0}$, $V_{\mathcal{E}_1}$, $V_{\mathcal{E}_2}$ and $\Delta_{w'}$ as vertices $V_{\mathcal{E}_0}$, $V_{\mathcal{L}_{\mathcal{E}_1}\mathcal{E}_2}$, $V_{\mathcal{E}_1}$. Consulting Figure 7, we see that the number $D_{V_{\mathcal{E}_1}}$ is the same when calculated in either Δ_w or $\Delta_{w'}$ as it involves the wedge product of the same primitive tangent vectors.

On the other hand, we note that in the notation of the proof of Theorem 2.11, by (2.15) and (2.18) we have that $3D_{V_{\mathcal{E}_0}}m_1-m=m_{\mathcal{E}_1(-3)[1]}$. Thus by Lemma 2.4,(6), $3D_{V_{\mathcal{E}_0}}m_1-m$ is primitive. So we may compute $D_{V_{\mathcal{E}_0}}$ in the triangle $\Delta_{w'}$ as

$$|m_1 \wedge (3D_{V_{\mathcal{E}_0}} m_1 - m)| = |m_1 \wedge m| = D_{V_{\mathcal{E}_0}},$$

the latter computed in Δ_w . Thus $D_{V_{\mathcal{E}_0}}$, $D_{V_{\mathcal{E}_1}}$ are unchanged between the two triangles, and it remains to compute $D_{V_{\mathcal{L}_{\mathcal{E}_1}\mathcal{E}_2}}$. This is then $|m_2 \wedge (3D_{V_{\mathcal{E}_0}}m_1-m)|$. We note that $m_2 \wedge m_1$ and $m_2 \wedge m$ have the same sign with our orientation conventions. See Figure 8 (2). Thus we obtain $D_{V_{\mathcal{L}_{\mathcal{E}_1}\mathcal{E}_2}} = 3D_{V_{\mathcal{E}_0}}D_{V_{\mathcal{E}_1}} - D_{V_{\mathcal{E}_2}} = \mathrm{rank}(\mathcal{L}_{\mathcal{E}_1}\mathcal{E}_2)$ by Lemma 2.4,(1) and the induction hypothesis. This is sufficient to prove the induction step for right mutations.

The argument assuming $C(\eta_E(w'))$ is obtained via right mutation of $C(\eta(w))$ is the same, this time using (2.14) and (2.17).

Remark 2.17. In particular, this shows that for a triangle Δ_w with vertices v_0 , v_1 , v_2 , the triple $(D_{v_0}, D_{v_1}, D_{v_2})$ forms a Markov triple. See Figure 8.

Proposition 2.18. Let w be a vertex of \mathcal{T} with $w \neq w_0$. Let D, D'' and D' be the determinants of the incoming, hybrid and outgoing vertices of Δ_w respectively. Then D > D'' > D'.

Proof. From Lemma 2.4,(1), one sees inductively that for a strong exceptional triple $\mathcal{C} = (\mathcal{E}_0, \mathcal{E}_1, \mathcal{E}_2)$, we have $r(\mathcal{E}_1) \geq r(\mathcal{E}_0)$, $r(\mathcal{E}_2)$, with equality if and only if \mathcal{C} is an initial strong exceptional triple. Since $V_{\mathcal{E}_1}$ is always the incoming vertex of the corresponding triangle $\Delta_{\mathcal{C}}$, we see that D > D', D''. The ordering of D' and D'' is proved inductively by observing, e.g., from Figure 7, that if w_1, w_2 are the children of w in \mathcal{T} , then the incoming vertex of Δ_w becomes a hybrid vertex of Δ_{w_i} , while the outgoing vertex of Δ_w becomes the outgoing vertex of one of Δ_{w_1} , Δ_{w_2} , and the hybrid vertex of Δ_w becomes the outgoing vertex of the other one of Δ_{w_1} , Δ_{w_2} .

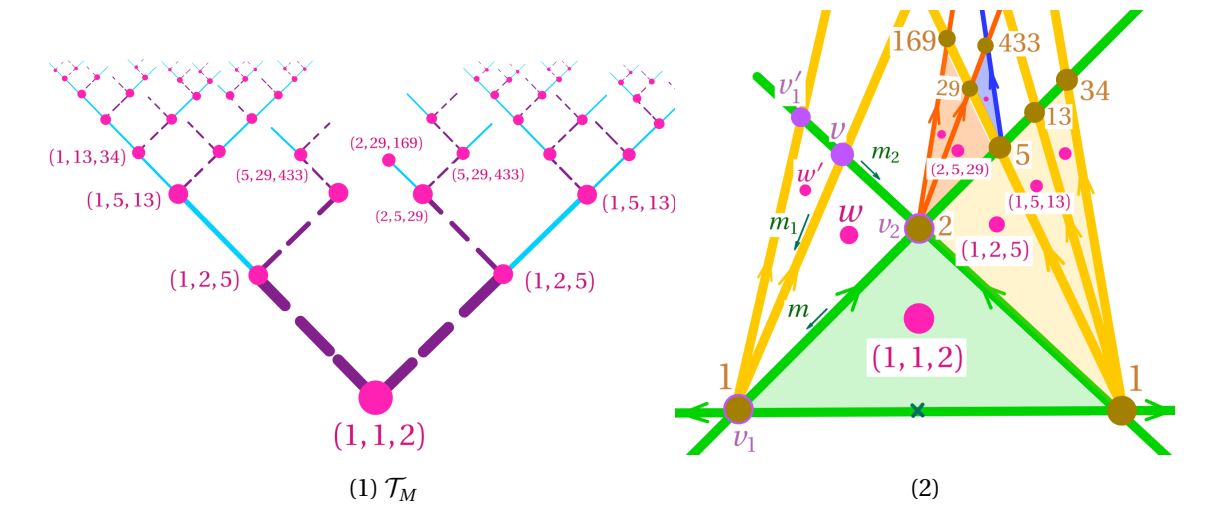


FIGURE 8. (1) The corresponding Markov tree \mathcal{T}_M to \mathcal{T} in Figure 3. (2) The corresponding triangles to \mathcal{T}_M : The numbers at the vertices are determinants at each vertex, and each triangle corresponds to a Markov triple given by the determinants at each of its vertices.

2.4. The structure of scattering at discrete points of \mathfrak{D}^{stab} . The discrete region of \mathfrak{D}^{stab} consists of triangles, and each vertex of each triangle has two rays coming into the vertex. This will always produce scattering of a standard, now much-studied form. We review this here.

We first recall a slightly different notion of scattering diagram in $M_{\mathbb{R}}$ than that of §1.2. A ray or line is of the form $(\mathfrak{d},f_{\mathfrak{d}})$ with \mathfrak{d} as in Definition 1.2, but $f_{\mathfrak{d}}(z^{m_{\mathfrak{d}}},t_{1},t_{2})\in \mathbb{Q}[M][[t_{1},t_{2}]]$ is a formal power series which satisfies $f_{\mathfrak{d}}\equiv 1 \mod (t_{1},t_{2})$ and $f_{\mathfrak{d}}\equiv 1 \mod z^{m_{\mathfrak{d}}}$. Given a scattering diagram \mathfrak{D} consisting of such rays and a path γ as in Definition 1.12, we may define the path-ordered product $\theta_{\gamma,\mathfrak{D}}:\mathbb{Q}[M][[t_{1},t_{2}]]\to \mathbb{Q}[M][[t_{1},t_{2}]]$ by taking a composition of automorphisms associated to the rays or lines crossed by γ . If at time $t_{\mathfrak{d}}$ the path γ crosses $(\mathfrak{d},f_{\mathfrak{d}})$, and $n\in N$ is the unique primitive element annihilating $m_{\mathfrak{d}}$ and with $\langle n,\gamma'(t_{\mathfrak{d}})\rangle < 0$, then the associated automorphism is given by $z^{m'}\mapsto z^{m'}f_{\mathfrak{d}}^{\langle n,m'\rangle}$.

Given a scattering diagram \mathfrak{D} , it is *consistent* if $\theta_{\gamma,\mathfrak{D}}$ is the identity for any loop for which $\theta_{\gamma,\mathfrak{D}}$ is defined. If \mathfrak{D} is a scattering diagram, there is a consistent scattering diagram $\mathsf{S}(\mathfrak{D})$ containing \mathfrak{D} and such that $\mathsf{S}(\mathfrak{D}) \setminus \mathfrak{D}$ consists only of rays. Again, this is [28, Thm. 6] or [21, Thm. 1.4].

Definition 2.19. Let *D* be a positive integer. Define the sequence of integers $R_i(D)$ for $i \ge 0$ recursively by

$$R_0(D) = 0$$
, $R_1(D) = 1$, $R_i(D) = 3DR_{i-1}(D) - R_{i-2}(D)$ for $i \ge 2$.

Define

$$r_i(D) := R_{i+1}(D)/R_i(D)$$

and

$$r_{\infty}(D) := \lim_{i \to \infty} r_i(D),$$

which is easily seen to be

$$r_{\infty}(D) = \frac{3D + \sqrt{9D^2 - 4}}{2}.$$

We then have the following now well-studied example.

Definition 2.20. Let *D* be a positive integer. We define

$$\mathfrak{D}'_{\text{in}} := \left\{ \left(\mathbb{R}(1,0), (1+t_1 z^{(1,0)})^{3D} \right), \left(\mathbb{R}(0,1), (1+t_2 z^{(0,1)})^{3D} \right) \right\}.$$

Define

$$m'_{i,1} = (R_{i+1}(D), R_i(D)), \quad m'_{i,2} = (R_i(D), R_{i+1}(D)),$$

for $i \ge 1$, and define the ray

$$\mathfrak{d}'_{i,j} := \left(\mathbb{R}_{\leq 0} m'_{i,j}, (1 + t_1^{R_i(D)} t_2^{R_{i+1}(D)} z^{m'_{i,j}})^{3D} \right),$$

for $i \ge 1$, j = 1, 2.

Lemma 2.21. With notation as in Definition 2.20, we may write

$$\mathsf{S}(\mathfrak{D}') = \mathfrak{D}'_{\mathrm{in}} \cup \{\mathfrak{d}'_{i,j} \mid i \geq 1, j = 1, 2\} \cup \mathfrak{D}'_{\mathrm{dense}},$$

where \mathfrak{D}'_{dense} is a scattering diagram containing one non-trivial ray with support $\mathbb{R}_{\leq 0}(a,b)$ for a,b relatively prime precisely when a,b>0 and

$$(2.19) r_{\infty}(D)^{-1} < b/a < r_{\infty}(D).$$

None of the $\mathfrak{d}_{i,j}$ have slope in this range. Finally, if a,b are relatively prime and satisfy the inequality (2.19) then the function f attached to the ray $\mathbb{R}_{\leq 0}(a,b)$ in $\mathfrak{D}'_{\text{dense}}$ takes the form

$$f = \prod_{k=1}^{\infty} (1 + t_1^{ka} t_2^{kb} z^{(ka,kb)})^{c_{ka,kb}}$$

for $c_{ka,kb}$ strictly positive integers.

Proof. This follows from [20, Thm. 7, Lemmas 5.2, Lemma 5.3] and [26, Thm. 1.4]. \Box

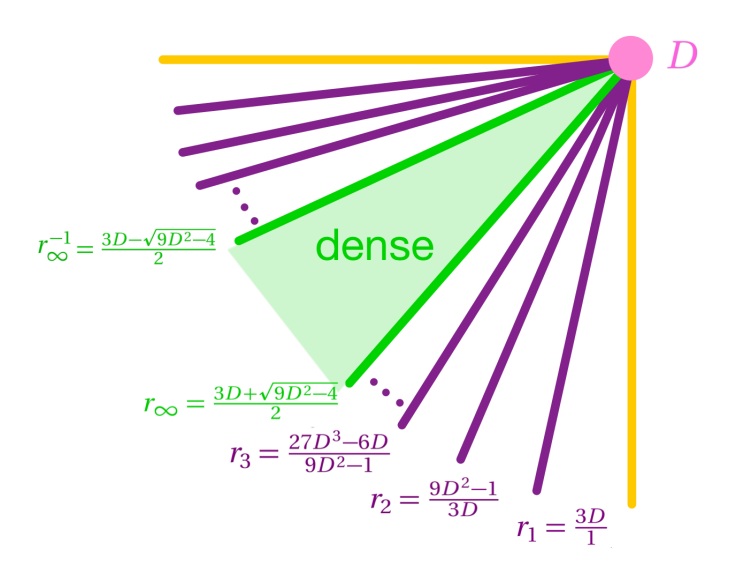


FIGURE 9. The scattering diagram of Lemma 2.21.

We may then use this to analyze the scattering which will happen in $\mathfrak{D}^{\text{stab}}$. Assume given a stability scattering diagram \mathfrak{D} consistent at a point $\sigma \in M_{\mathbb{R}}$, with local scattering diagram \mathfrak{D}_{σ} as in Definition 1.11. Let $m_1, m_2 \in M$ be primitive and linearly independent. Assume that there

are only two lines (as opposed to rays) in \mathfrak{D}_{σ} , with opposite vectors $m_1, m_2 \in M$, primitive and linearly independent. Further assume these lines are of the form $(\mathfrak{d}_i, H_i^{\sigma})$, where

$$\mathfrak{d}_i = \mathbb{R} m_i, \quad H_i = -\text{li}_2(-t^{\varphi_\sigma(m_i)}z^{m_i}).$$

Let $D = |m_1 \wedge m_2|$, and set for $i \ge 0$,

$$(a_{i,1}, b_{i,1}) = (R_{i+1}(D), R_i(D)), (a_{i,2}, b_{i,2}) = (R_i(D), R_{i+1}(D)),$$

and

$$(2.20) m_{i,j} = a_{i,j} m_1 + b_{i,j} m_2$$

for $i \ge 0$, j = 1, 2. By the definition of $R_i(D)$, it follows that

(2.21)
$$m_{0,1} = m_1, \quad m_{1,1} = 3D \, m_1 + m_2, \quad m_{i+1,1} = 3D \, m_{i,1} - m_{i-1,1}$$

$$m_{0,2} = m_2, \quad m_{1,2} = 3D \, m_2 + m_1, \quad m_{i+1,2} = 3D \, m_{i,2} - m_{i-1,2}$$

Define

$$\mathfrak{d}_{i,j} := \left(-\mathbb{R}_{\geq 0} m_{i,j}, -\operatorname{li}_2(-t^{\varphi_{\sigma}(m_{i,j})} z^{m_{i,j}})\right).$$

Lemma 2.22. In the above situation, we may write

$$\mathfrak{D}_{\sigma} = \{(\mathfrak{d}_1, H_1^{\sigma}), (\mathfrak{d}_2, H_2^{\sigma})\} \cup \{\mathfrak{d}_{i,j} \mid i \ge 1, j = 1, 2\} \cup \mathfrak{D}_{\sigma, \text{dense}},$$

where $\mathfrak{D}_{\sigma,\text{dense}}$ is a scattering diagram containing one non-trivial ray with support $-\mathbb{R}_{\geq 0}(a\,m_1+b\,m_2)$ for a,b relatively prime precisely when a,b>0 and

$$(2.23) r_{\infty}(D)^{-1} < b/a < r_{\infty}(D).$$

None of the $\mathfrak{d}_{i,j}$ have slope in this range.

Proof. This will follow from Lemma 2.21 via the *change of lattice trick*, see [19, Proposition C.13, Step IV] or [26, Section 2.3].

Let $\mathfrak{D}_{\mathrm{in}}=\{(\mathfrak{d}_1,H_1^{\sigma}),(\mathfrak{d}_2,H_2^{\sigma})\}$, recalling that $H_i^{\sigma}=-\mathrm{li}_2(-t^{\varphi_{\sigma}(m_i)}z^{m_i})$. Note that if we instead define $\mathfrak{D}'_{\mathrm{in}}=\{(\mathfrak{d}_1,H_1'),(\mathfrak{d}_2,H_2'))\}$ with $H_i'=-\mathrm{li}_2(-t_iz^{m_i})$, working in $\mathbb{Q}[M][[t_1,t_2]]$ rather than $\mathbb{Q}[M][t^{\mathbb{R}_{\geq 0}}]$, we may apply [28, Thm. 6] or [21, Thm. 1.4] to obtain a consistent diagram \mathfrak{D}'_{σ} from $\mathfrak{D}'_{\mathrm{in}}$. We may then obtain \mathfrak{D}_{σ} from \mathfrak{D}'_{σ} by applying the ring homomorphism $\mathbb{Q}[M][[t_1,t_2]] \to \mathbb{Q}[M][t^{\mathbb{R}_{\geq 0}}]$ given by $t_i \mapsto t^{\varphi_{\sigma}(m_i)}$.

We then further replace H_i^{σ} with the corresponding function f_i in (1.9), in order to convert \mathfrak{D}'_{in} into a scattering diagram of the sort used in Lemma 2.21. Note that $f_i = (1 + t_i z^{m_i})^3$, so that $\theta_{H_i'} = \bar{\theta}_{f_i}$ in the notation of the remark.

We now apply the change of lattice trick. We replace the lattice M with the sublattice M' generated by m_1 and m_2 . The index of this sublattice in M is D. The dual lattice N' of M' is a superlattice of N. Note that if $n_i \in N$ is a primitive vector with $\langle n_i, m_i \rangle = 0$, $\langle n_i, m_{i'} \rangle > 0$ for $\{i, i'\} = \{1, 2\}$, then one checks easily, e.g., by writing m_i , n_i in the standard basis for M and N, that $n_i = D n_i'$ for $n_i' \in N'$ primitive.

Consider for i=1,2 the line $\mathfrak{d}_i':=(\mathbb{R}m_i,(1+t_iz^{m_i})^{3D})$ viewed as a line in a scattering diagram in the lattice M'. Because $n_i=D\,n_i'$, in fact the wall-crossing automorphism of $\mathbb{Q}[M][[t_1,t_2]]$ associated to \mathfrak{d}_i agrees, after restriction to $\mathbb{Q}[M'][[t_1,t_2]]$, with the wall-crossing automorphism associated to \mathfrak{d}_i' .

We may now consider the initial scattering diagram \mathfrak{D}'_{in} consisting of the lines $\mathfrak{d}'_1, \mathfrak{d}'_2$, again with respect to the lattice M'. Let $\mathfrak{D}' = \mathsf{S}(\mathfrak{D}'_{in})$. This is the scattering diagram analyzed in

Lemma 2.21. We just need to check that the rays described in Lemma 2.21 for the lattice M' then correspond to the rays described in the current lemma.

Using the notation $m_{i,j}$ of the statement, we note that if we write an element of M' as vector using the basis m_1, m_2 , in fact $m_{i,j} \in M$ agrees with $m'_{i,j} \in M'$ of Lemma 2.21 under the inclusion $M' \subseteq M$. Thus the rays $\mathfrak{d}'_{i,j}$ and $\mathfrak{d}_{i,j}$ have the same support in $M'_{\mathbb{R}} = M_{\mathbb{R}}$.

We may then recover \mathfrak{D} from \mathfrak{D}' by modifying each function attached to a ray \mathfrak{d}' in \mathfrak{D}' to give a ray \mathfrak{d} so that the automorphism associated to \mathfrak{d}' is the restriction to $\mathbb{Q}[M'][[t_1,t_2]]$ of the automorphism associated to \mathfrak{d} , see [26, Prop. 2.16]. Thus it only remains to check that $\mathfrak{d}'_{i,j}$ induces the same automorphism of $\mathbb{Q}[M'][[t_1,t_2]]$ as $\mathfrak{d}_{i,j}$ does. For this, note that in N', a primitive vector annihilating $m_{i,j}$ is $n'_{i,j} = (-a_{i,j}n'_2 + b_{i,j}n'_1)/\gcd(a_{i,j},b_{i,j})$. However, say for j=1, we have

$$\gcd(a_{i,1},b_{i,1}) = \gcd(3Da_{i-1,1}-b_{i-1,1},a_{i-1,1}) = \gcd(a_{i-1,1},b_{i-1,1}) = \cdots = \gcd(a_{0,1},b_{0,1}) = 1.$$

Similarly by induction, note that for each i, either $3D|a_{i,j}$ and $\gcd(3D,b_{i,j})=1$, or $3D|b_{i,j}$ and $\gcd(3D,a_{i,j})=1$, with the two choices depending on the parity of i. Without loss of generality, assuming the former of the two choices, we see that $-a_{i,j}n_2'+b_{i,j}n_1'\equiv b_{i,j}n_1'\mod N$, and thus this normal vector represents an element of order D in N'/N. From this it follows that the primitive normal vector to $m_{i,j}$ in N must be $Dn'_{i,j}$. Hence indeed $\mathfrak{d}_{i,j}$ and $\mathfrak{d}'_{i,j}$ induce the same automorphism on $\mathbb{C}[M'][[t_1,t_2]]$.

By following a similar process for dense rays $(\mathfrak{d}', f_{\mathfrak{d}'}) \in \mathfrak{D}'_{\text{dense}}$ to obtain $(\mathfrak{d}, f_{\mathfrak{d}})$ inducing the same automorphism of $\mathbb{C}[M'][[t_1, t_2]]$, we obtain a scattering diagram $\mathfrak{D}_{\sigma, \text{dense}}$. We note that the relationship between $f_{\mathfrak{d}'}$ and $f_{\mathfrak{d}}$ may not be as simple as described above, but we do not need the precise form. This then defines a scattering diagram \mathfrak{D} as in (2.22) with the property that, for a loop γ around the origin, $\theta_{\gamma,\mathfrak{D}}$ and $\theta_{\gamma,\mathfrak{D}'}$ agree on $\mathbb{C}[M'][[t_1,t_2]]$, i.e., are both the identity. Since $\theta_{\gamma,\mathfrak{D}}$ is a ring automorphism, this implies that for $m \in M$, $\theta_{\gamma,\mathfrak{D}}(z^m) = \xi z^m$ for some root of unity $\xi \in \mathbb{C}$. Since $\theta_{\gamma,\mathfrak{D}}$ is the identity modulo \mathfrak{m} , we conclude $\xi = 1$ always. Thus $\theta_{\gamma,\mathfrak{D}}$ is the identity.

The following formula will be useful later:

Proposition 2.23 (Closed formula for $R_i(D)$). Let $m = \lfloor j/2 \rfloor$. Then

(2.24)
$$R_{j}(D) = \sum_{l=0}^{m} (-1)^{l} {j-l-1 \choose l} (3D)^{j-2l-1}.$$

Here we use the convention that $\binom{m-1}{m} = 0$.

Proof. We prove this by induction. For j=0 and 1, the formula obviously holds. Now, we assume that the formula holds for $j \le p-1$, and we want to show that it holds for j=p as well.

Let $m' := \lfloor (p-1)/2 \rfloor$ and $m'' = \lfloor (p-2)/2 \rfloor$. Then m'' = m-1 and either m = m' or m' = m'' depending on whether p is odd or even respectively. We get

$$\begin{split} R_p(D) &= (3D)R_{p-1}(D) - R_{p-2}(D) \\ &= \sum_{l=0}^{m'} (-1)^l \binom{p-l-2}{l} (3D)^{p-2l-1} - \sum_{l=0}^{m''} (-1)^l \binom{p-l-3}{l} (3D)^{p-2l-3} \\ &= \sum_{l=0}^{m'} (-1)^l \binom{p-l-2}{l} (3D)^{p-2l-1} - \sum_{l=1}^{m} (-1)^{l-1} \binom{p-l-2}{l-1} (3D)^{p-2l-1}, \end{split}$$

where in the last summation we have shifted the index of summation by 1. Using that $\binom{p-l-2}{l-1} = \binom{p-l-1}{l} - \binom{p-l-2}{l}$ in the last term, the above yields

$$(3D)^{p-1} + \sum_{l=1}^{m'} (-1)^l \binom{p-l-2}{l} (3D)^{p-2l-1} - \sum_{l=1}^{m} (-1)^{l-1} \binom{p-l-1}{l} (3D)^{p-2l-1} + \sum_{l=1}^{m} (-1)^{l-1} \binom{p-l-2}{l} (3D)^{p-2l-1}.$$

The first and third sums cancel, noting that in the case that m' = m - 1, the l = m contribution in the third term vanishes. Thus we obtain

$$(3D)^{p-1} + \sum_{l=1}^{m} (-1)^l \binom{p-l-1}{l} (3D)^{p-2l-1} = \sum_{l=0}^{m} (-1)^l \binom{p-l-1}{l} (3D)^{p-2l-1},$$

as claimed.

Corollary 2.24. For each j, we have

$$R_{i+1}(D) > R_i(D)$$
.

Theorem 2.25. Let $v \in M_{\mathbb{R}}$ be either an incoming vertex of a triangle Δ_w or any vertex of Δ_{w_0} . Then the local scattering diagram $\mathfrak{D}_v^{\mathrm{stab}}$ contains precisely two lines, (\mathfrak{d}_1, H_1) , (\mathfrak{d}_2, H_2) , corresponding to the two rays of $\mathfrak{D}_{\mathrm{in}}^{\mathrm{stab}} \cup \mathfrak{D}_{\mathrm{discrete}}$ containing the two edges of Δ_w containing v. It is equivalent to the scattering diagram \mathfrak{D}_σ described in Lemma 2.22 with $D = D_v$. Further, the rays of $\mathfrak{D}_v^{\mathrm{stab}}$ arising from elements of $\mathfrak{D}_{\mathrm{discrete}}$ are precisely the rays $\{\mathfrak{d}_{i,j} \mid i \geq 1, j = 1, 2\}$ of Lemma 2.22.

Proof. We first observe that the only lines in $\mathfrak{D}_v^{\text{stab}}$ have support as advertised. Note that if w_1, w_2 are the two children of w, then locally near v, $M_{\mathbb{R}} \setminus (\Delta_{w_1} \cup \Delta_{w_2} \cup \Delta_w)$ is a convex cone, see Figure 5. Thus any ray \mathfrak{d} containing v for which \mathfrak{d} is not an endpoint must intersect one of these three triangles. However, since there are no rays of $\mathfrak{D}^{\text{stab}}$ intersecting the interiors of these triangles by Theorem 2.7, the only choice is that \mathfrak{d} contains one of the two edges of Δ_w containing v.

If v is instead one of the hybrid vertices of Δ_{w_0} , then it is the point of intersection of \mathfrak{d}_{n-1}^+ and \mathfrak{d}_n^- for n=0 or n=1. The argument of the first paragraph also applies in this case, as the regions $\overline{U}_{0,L}^{\text{in}}, \overline{U}_{0,R}^{\text{in}}$ (see Figure 4) below these two rays is empty by [7, Lem. 4.10].

In either case, we know from Theorem 2.11 that the wall functions attached to these two lines are as given in Lemma 2.22. Given this, by uniqueness of the construction of scattering diagrams $\mathfrak{D}_{n}^{\text{stab}}$ must be equivalent to the scattering diagram given in Lemma 2.22.

The only thing remaining to check is that all the rays $\{\mathfrak{d}_{i,j} \mid i \geq 1, j = 1, 2\}$ are accounted for in $\mathfrak{D}_{\text{discrete}}$. This follows, however, from the construction of $\mathfrak{D}_{\text{discrete}}$. Assuming that v is an incoming vertex of Δ_w , we obtain all the discrete rays with endpoint v as follows. First one chooses one of the children w_1 of w in \mathcal{T} . One then repeatedly follows hybrid edges in \mathcal{T} to obtain an infinite chain of vertices w_2, w_3, \cdots . Then $\mathfrak{d}_{w_j} - v$ coincides with $\mathfrak{d}_{i,j}$ for some i = 1 or 2. Which we get depends on which child of w was chosen. This follows by comparing (2.4) and (2.21).

If instead v is one of the hybrid vertices of Δ_{w_0} , the situation is slightly more complicated. Without loss of generality, take v = (-1/2, 0). Then by first choosing the child w_1 of w_0 which corresponds to mutating at the vertex (1/2, 0) and then following a path of outgoing edges,

we obtain the rays $\mathfrak{d}_{i,j}$ for one choice of i. To get the other choice of i, we follow the same procedure at (1/2,0) instead of (-1/2,0) and then apply T^{-1} .

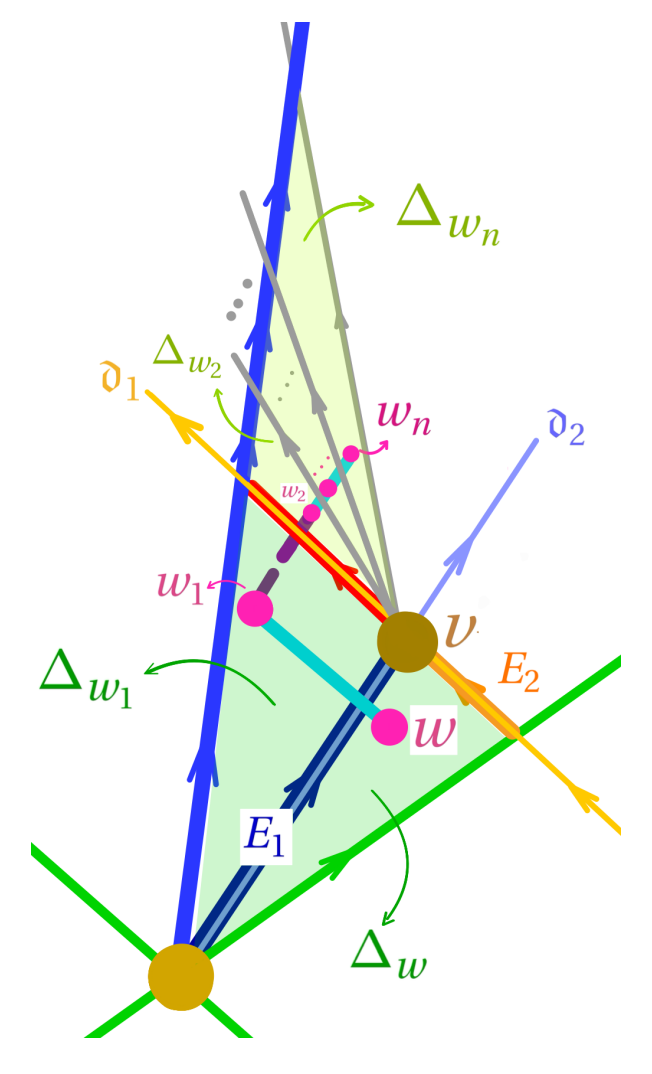


FIGURE 10. $\Delta_{w_1}, \dots, \Delta_{w_n}$ together with Δ_w with a common vertex v. Also, the corresponding part of \mathcal{T} is pictured here.

Definition 2.26 ($\mathfrak{D}_{\mathrm{dense}}$). We define $\mathfrak{D}_{\mathrm{dense}}$ to be the set of rays of $\mathfrak{D}^{\mathrm{stab}}$ which are not elements of $\mathfrak{D}^{\mathrm{stab}}_{\mathrm{in}} \cup \mathfrak{D}_{\mathrm{discrete}}$ but have endpoint a vertex of some triangle $T^k(\Delta_w)$.

It follows from Theorem 2.25 that the local scattering diagram $\mathfrak{D}_{\text{dense},\nu}$ agrees with the diagram $\mathfrak{D}_{\nu,\text{dense}}$ of Lemma 2.22.

3. DIAMONDS

In this brief section, we provide definitions related to the structure of diamonds.

Definition 3.1. Let w be a vertex of \mathcal{T} and v the incoming vertex of Δ_w . Then v is the intersection of two rays of $\{\mathfrak{d}_{-1}^+,\mathfrak{d}_1^-\}\cup\mathfrak{D}_{\text{discrete}}^0$, say $\mathfrak{d}_1,\mathfrak{d}_2$, with v lying in the interior of each, see

Theorem 2.25. If m_1 , m_2 are the opposite vectors of \mathfrak{d}_1 , \mathfrak{d}_2 , define the cone

$$C_{v} := \operatorname{closure} \left(\left\{ v - (a \, m_{1} + b \, m_{2}) \, \middle| \, a, b \in \mathbb{R}_{>0}, \quad \frac{3D_{v} - \sqrt{9D_{v}^{2} - 4}}{2} < \frac{b}{a} < \frac{3D_{v} + \sqrt{9D_{v}^{2} - 4}}{2} \right\} \right).$$

We can then define $C_{T^k(\nu)} = T^k(C_{\nu})$ for any $k \in \mathbb{Z}$.

If instead v is the intersection of \mathfrak{d}_n^+ and \mathfrak{d}_{n+1}^- for some n, then we may define

$$C_{v} := \operatorname{closure} \left(\left\{ a(1, -n) + b(-1, (n+1)) \,\middle|\, a, b \in \mathbb{R}_{>0}, \quad \frac{3 - \sqrt{5}}{2} < \frac{b}{a} < \frac{3 + \sqrt{5}}{2} \right\} \right).$$

We call such a vertex an initial vertex.

See Figure 11.

Remark 3.2. By Theorem 2.25 every ray of rational slope with endpoint v and contained in C_v is in fact a non-trivial ray of $\mathfrak{D}^{\text{stab}}$.

- **Lemma 3.3.** (1) Let v be an incoming vertex of a triangle Δ_w , with w_1 , w_2 the children of w in \mathcal{T} . Then $\mathfrak{d}_{w_1} \cap \mathfrak{d}_{w_2}$ is non-empty and lies in C_v . See Figure 11.
 - (2) If v is an initial vertex, the intersection of \mathfrak{d}_n^+ and \mathfrak{d}_{n+1}^- , then (1) is still true after replacing \mathfrak{d}_{w_1} , \mathfrak{d}_{w_2} with \mathfrak{d}_{n-1}^+ , \mathfrak{d}_{n+2}^- respectively.

Proof. For (1), let $(\mathcal{E}_0, \mathcal{E}_1, \mathcal{E}_2)$ be the strong exceptional triple associated to Δ_w . By (2.14),(2.15),(2.17), and (2.18), we have (see Figure 11), with suitable ordering of w_1, w_2 ,

$$\mathfrak{d}_{w_1} = V_{\mathcal{E}_2} - \mathbb{R}_{\geq 0} m_{\mathcal{E}_1}, \quad \mathfrak{d}_{w_2} = V_{\mathcal{E}_0} - \mathbb{R}_{\geq 0} m_{\mathcal{E}_1(-3)[1]}.$$

Since $m_{\mathcal{E}_1(-3)[1]} = -m_{\mathcal{E}_1(-3)} = (-r(\mathcal{E}_1(-3)), d(\mathcal{E}_1(-3)))$, we see that \mathfrak{d}_{w_1} heads to the left and \mathfrak{d}_{w_2} heads to the right, as depicted in Figure 11. This makes it clear that these two rays intersect. Suppose their intersection point does not lie in C_v . In this case, they must intersect at a point contained in the edge of some triangle $\Delta_{w'}$ with w' a descendent of w and with the property that one of \mathfrak{d}_{w_1} or \mathfrak{d}_{w_2} contains this edge. However, this is impossible by Theorem 2.7.

We can check (2) by hand, say for n=0, where C_{ν} is the cone based at $\nu=(1/2,0)$ generated by the two vectors $\left((-1+\sqrt{5})/2,(3-\sqrt{5})/2\right)$ and $\left((-1-\sqrt{5})/2,(3+\sqrt{5})/2\right)$. These have slope $\mu_1=(\sqrt{5}-1)/2>0$ and $\mu_2=-(\sqrt{5}+1)/2<0$ respectively. The intersection of the rays \mathfrak{d}_{-1}^+ and \mathfrak{d}_{-2}^- is (1/2,1), which lies vertically over ν , and hence clearly lies in C_{ν} .

Definition 3.4 (Dense diamond). If v is not an initial vertex, we define the *(dense) diamond based at v (or at v), \Diamond_v, to be, in the notation of Lemma 3.3, the closure of the connected component of C_v \setminus (\mathfrak{d}_{w_1} \cup \mathfrak{d}_{w_2}) containing the vertex v. If v is an initial vertex, the intersection of \mathfrak{d}_n^+ and \mathfrak{d}_{n+1}^-, we instead take \Diamond_v to be the closure of the connected component of C_v \setminus (\mathfrak{d}_{n-1}^+ \cup \mathfrak{d}_{n-2}^+).*

In other words, for any vertex v, we can define the dense diamond at v as a quadrilateral with sides as follows. The lower sides are the two limits of the discrete rays from the left side and right side at v; these have an irrational slope. The upper right and left sides, which we call the *roofs* of the diamond, are \mathfrak{d}_{w_1} and \mathfrak{d}_{w_2} in the notation above if v is not an initial vertex, and are \mathfrak{d}_{n-1}^+ and \mathfrak{d}_{n-2}^- if v is an initial vertex. We denote the diamond based at v by \diamond_v or \diamond (when there is no ambiguity about the vertex).

 $^{^{2}}$ We note that such a vertex is never an incoming vertex of a triangle.

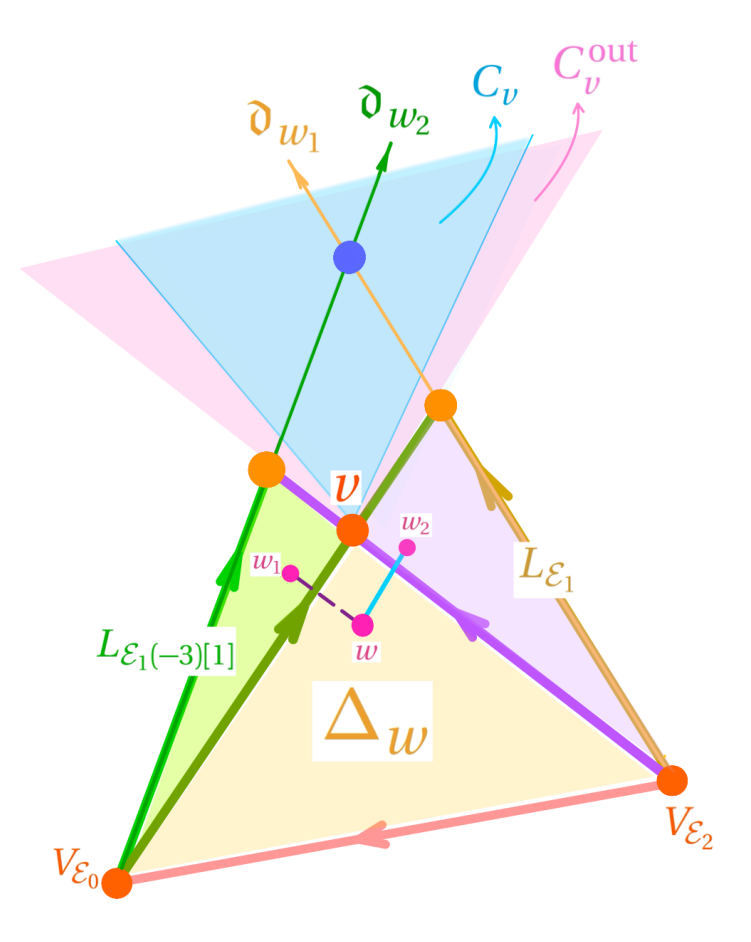


FIGURE 11

Definition 3.5 (Outer and initial diamond). Let ν be an incoming vertex of a triangle Δ_w . Define the cone

(3.1)
$$C_v^{\text{out}} := v - (\mathbb{R}_{\geq 0} m_1 + \mathbb{R}_{\geq 0} m_2),$$

where m_1, m_2 are tangent vectors to the edges of Δ_w containing v oriented away from w as usual. We define the *outer diamond based at* v (or at v), \Diamond_v^{out} , to be the closure of the connected component of $C_v^{\text{out}} \setminus (\mathfrak{d}_{w_1} \cup \mathfrak{d}_{w_2})$ containing the vertex v.

Similarly, if v is an initial vertex, the intersection of \mathfrak{d}_n^+ and \mathfrak{d}_{n+1}^- , take m_1, m_2 to be the opposite vectors of \mathfrak{d}_n^+ and \mathfrak{d}_{n+1}^- and define C_v^{out} as in (3.1). Then the *outer diamond based at v* in this case is the closure of the connected component of $C_v^{\text{out}} \setminus (\mathfrak{d}_{n-1}^+ \cup \mathfrak{d}_{n+2}^-)$ containing the vertex v. We call this diamond an *initial diamond* and denote it by \lozenge^{init} or \lozenge^{init}_v .

Alternatively, an initial diamond \lozenge^{init} is a quadrilateral bounded by the four lines $L_{\mathcal{O}(d)}$ for $d \in \{m-1, m, m+1, m+2\}$. This is an example of an outer diamond. See Figure 13.

For i=1,2, we call the rays \mathfrak{d}_i with direction vectors m_i , the left and right *generators* (or the left and right *generating rays*) of the outer diamond. The generators generate any other rays (dense or discrete) at the base vertex ν , i.e., any such ray has direction vector a positive linear combination of the direction vectors of \mathfrak{d}_1 and \mathfrak{d}_2 . See Figure 12.

An outer diamond at ν , $\Diamond_{\nu}^{\text{out}}$ or \Diamond^{out} can alternatively be defined as follows: it is bounded by the roofs of the dense diamond and the left and right generators (rather than the irrational

rays). Note that any outer diamond contains a unique dense diamond. The complement of the dense diamond in an outer diamond consists of *discrete triangles*. See Figure 12.

Definition 3.6 (Discrete and dense ray or object). A ray (or equivalently the object corresponding to the ray) is called a *dense ray or object* if the ray lies in \mathfrak{D}_{dense} . A ray (or equivalently an object corresponding to the ray) is called a *discrete ray or object* if the ray lies in $\mathfrak{D}_{in}^{stab} \cup \mathfrak{D}_{discrete}$. We note that the discrete objects are exceptional bundles \mathcal{E} and shifts of such $\mathcal{E}[1]$.

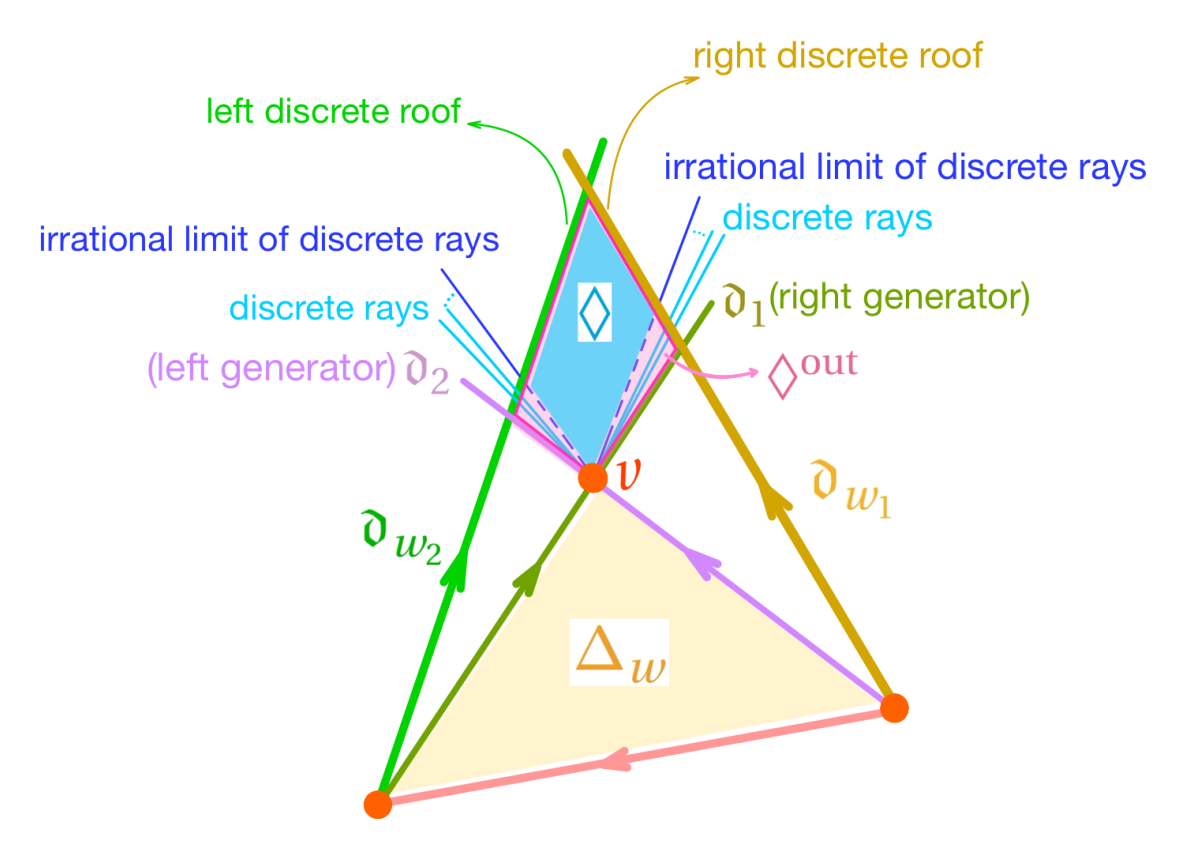


FIGURE 12. The dense diamond \Diamond at vertex v. It is *dense*, in the sense that it consists of all rays generated at v with the slope between the two irrational limits. The outer diamond at v, \Diamond^{out} , is given by the left and right generators $(\mathfrak{d}_2 \text{ and } \mathfrak{d}_1)$ together with the left and right roofs $(\mathfrak{d}_{w_1} \text{ and } \mathfrak{d}_{w_2})$. The triangle Δ_w is the base triangle for both \Diamond and \Diamond^{out} .

Definition 3.7 (R_{\Diamond} , R_{bdd} and R_{unbdd}). Let

$$R := \{(x, y) \in \mathbb{R}^2 | y \ge nx - 3n^2/2 \text{ for some } n \in \mathbb{Z}\}.$$

We define

$$R_{\Diamond} := \bigcup_{k \in \mathbb{Z}} T^k \left(\bigcup_{\nu} \Diamond_{\nu} \right),$$

where the union is over all incoming vertices v of triangles Δ_w and the initial vertex which is the intersection of \mathfrak{d}_0^+ and \mathfrak{d}_1^- . We write

$$R_{\mathrm{bdd}} := R_{\Delta} \cup R_{\Diamond} = \bigcup_{k \in \mathbb{Z}} T^k \left(\bigcup_{\nu} \Diamond_{\nu}^{\mathrm{out}} \right),$$

which we call the bounded region.

Finally, we denote by R_{unbdd} the complement of R_{bdd} in R, and call it the *unbounded region*.

Remark 3.8 (Uniqueness of diamond at each vertex). By definition, each vertex v uniquely determines the diamond at v.

Definition 3.9 (Initial triangle). We say that a triangle in the scattering diagram is *initial* if it is of the form $T^k(\Delta_{w_0})$ for some $k \in \mathbb{Z}$. In this case, all the sides are contained in unions of initial rays. We denote such a triangle by Δ^{init} . See Figure 13.

Definition 3.10 (Super-diamond). A *super-diamond*, \Diamond^{sup} , is a quadrilateral generated by the lines corresponding to $\mathcal{O}(m-1)$, $\mathcal{O}(m)$, $\mathcal{O}(m+2)$, $\mathcal{O}(m+3)$. See Figure 13.

Definition 3.11 (Base triangle). For non-initial (outer or dense) diamonds, the triangle Δ_w with its incoming vertex being the base of the diamond is called *base triangle* of the diamond. See Figure 12.

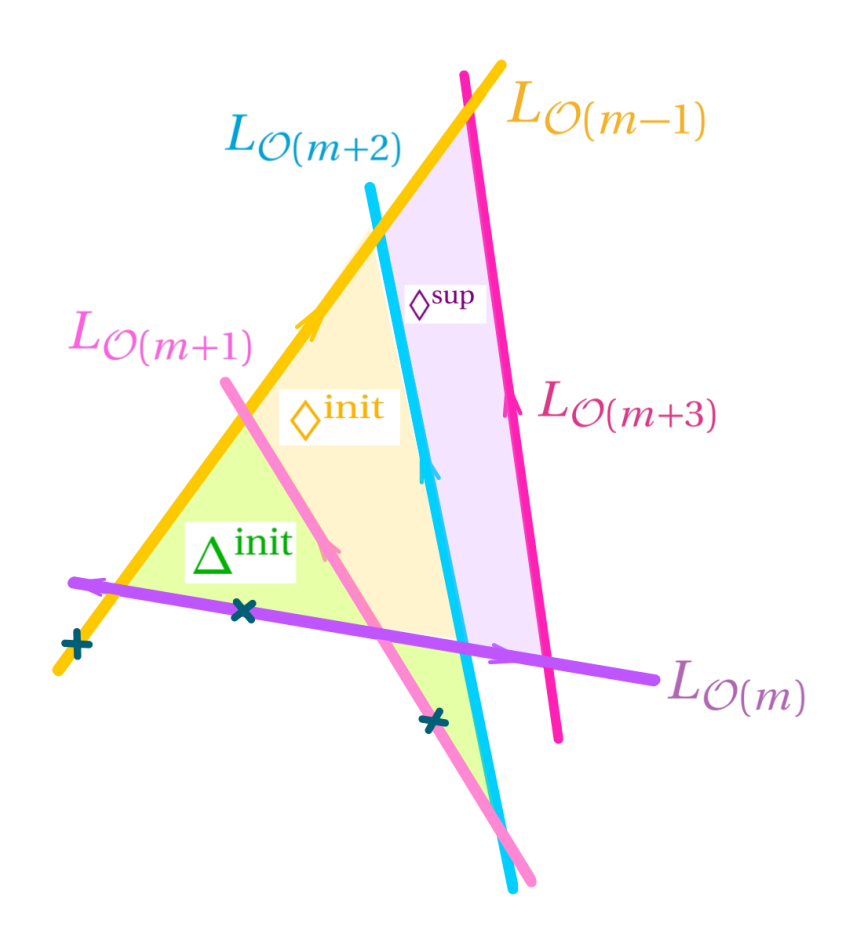


FIGURE 13. Super-diamond, \lozenge^{sup} , initial diamond, \lozenge^{init} , and initial triangle, Δ^{init} . All the non-initial (outer or dense) diamonds are contained in the super-diamond. \lozenge^{init} is an example of an outer diamond.

Definition 3.12 (Degenerate diamond). We define a *degenerate diamond* to be the intersection of a dense ray with endpoint v with the roof of \Diamond_v . We call the vertical line through a degenerate diamond the *vertical diagonal* of the degenerate diamond.

See Figure 14.

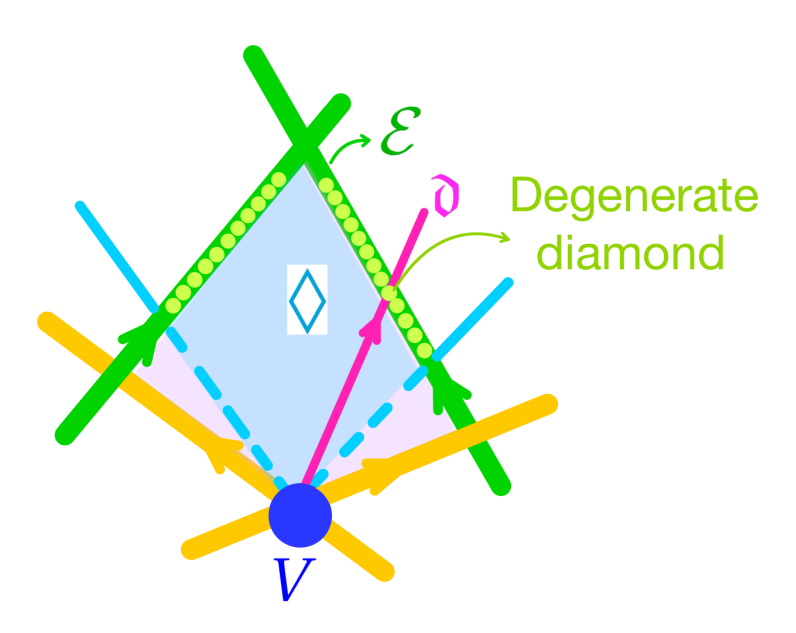


FIGURE 14. The intersection points of the roof \mathcal{E} with any rational dense ray \mathfrak{d} is a degenerate diamond.

Remark 3.13. Note that passing from a triangle contained in one outer diamond to an adjacent triangle contained in a neighbouring outer diamond corresponds to traversing a hybrid edge of \mathcal{T} . On the other hand, passing from a triangle contained in an outer diamond to an adjacent triangle contained in the same outer diamond corresponds to traversing an outgoing edge of \mathcal{T} . See Figure 10.

4. VERTICAL DIAGONALS AND VERTEX-FREENESS OF THE OUTER DIAMONDS

In this section, we prove the vertex-freeness for outer diamonds. This means that no two rays of $\mathfrak{D}^{\text{stab}}$ intersect in the interior of an outer diamond.

Theorem 4.1 (Vertical diagonals). For an (outer or dense) positive diamond, the diagonal joining the base v of the diamond to the vertex of the diamond which is the intersection of the two roofs is vertical.

Proof. Note that the twist operator T takes vertical line segments to vertical line segments. Thus for an initial diamond, we only need to check one such diamond. The proof of Lemma 3.3 shows that the two vertices in question for n = 0 are (1/2,0) and (1/2,1), thus giving a vertical diagonal. See Figure 15.

Further, following the first paragraph of the proof of Lemma 3.3, a diamond based at an incoming vertex $V_{\mathcal{E}_1}$ has a vertex at the intersection of the two roofs $\mathfrak{d}_{w_1} \cap \mathfrak{d}_{w_2}$ the intersection of the lines $L_{\mathcal{E}_1(-3)[1]}$ and $L_{\mathcal{E}_1}$. Writing $(r_1,d_1,e_1):=(r(\mathcal{E}_1),d(\mathcal{E}_1),e(\mathcal{E}_1))$, we have $(r(\mathcal{E}_1(-3)),d(\mathcal{E}_1(-3)),e(\mathcal{E}_1(-3)))=(r_1,d_1-3r_1,e_1-3d_1+9r_1/2)$. Thus the point of intersection is the solution (x,y) to the equations

$$r_1 y + d_1 x = e_1,$$

 $r_1 y + (d_1 - 3r_1)x = e_1 - 3d_1 + 9r_1/2,$

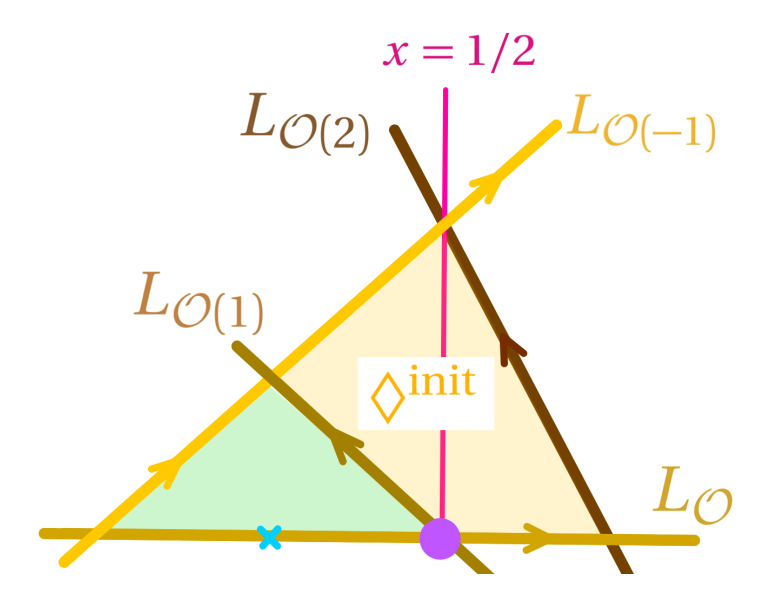


FIGURE 15. \Diamond^{init} has a vertical diagonal.

i.e.,

(4.1)
$$(x,y) = \left(\frac{d_1}{r_1} - \frac{3}{2}, \frac{e_1}{r_1} - \frac{d_1^2}{r_1^2} + \frac{3d_1}{2r_1}\right).$$

Note this has the same *x*-coordinate as $V_{\mathcal{E}_1}$, and thus this diagonal is vertical as promised.

Definition 4.2. Let v be the incoming vertex of a triangle Δ_w and \mathfrak{d} one of the two initial or discrete rays containing v in its interior. Let v' be the vertex of Δ_w not contained in \mathfrak{d} , and let \mathfrak{d}_1 be the ray containing the edge of Δ_w with endpoint v, v'. Let $\mathfrak{d}_2, \mathfrak{d}_3, \ldots$ be the sequence of discrete rays with endpoint v' encountered going clockwise (resp. counterclockwise) from \mathfrak{d}_1 around v' if v' is a right-most (resp. left-most) vertex of Δ_w . Let (a_i, b_i) , (c, d) be the direction vectors of \mathfrak{d}_i and \mathfrak{d} respectively. Let v_i be the intersection point of \mathfrak{d}_i with \mathfrak{d} .

- (1) By the j-th discrete ray \mathfrak{d}_i^j generated along \mathfrak{d} at v_i , we mean the ray with endpoint v_i with direction vector $R_{j+1}(D_i) \binom{c}{d} + R_j(D_i) \binom{a_i}{b_i}$, where D_i is the determinant of v_i . We write \mathfrak{d}_i^{∞} for the limit of the rays \mathfrak{d}_i^j as $j \to \infty$; this is a ray of irrational slope.
- (2) By the j-th opposite discrete ray $\mathfrak{d}_{i,\text{op}}^j$ generated along \mathfrak{d} at v_i , we mean the ray with endpoint v_i and direction vector $R_j(D_i) \binom{c}{d} + R_{j+1}(D_i) \binom{a_i}{b_i}$.

Note that \mathfrak{d}_i^0 and $\mathfrak{d}_{i,\mathrm{op}}^0$ are the rays with direction vectors (c,d) and (a_i,b_i) respectively.

Definition 4.3. Let \mathfrak{d} be a ray in $\mathfrak{D}^{\text{stab}}$. If its direction vector $-m_{\mathfrak{d}}$ has negative (resp. positive) x-coordinate, we call it a left-moving (resp. right-moving) ray.

Corollary 4.4 (Decreasing slopes). *Fix an initial or discrete ray* \mathfrak{d} .

(1) For a fixed i and every j, the slope of \mathfrak{d}_i^1 is greater than the slope of \mathfrak{d}_{i+1}^j , in the sense that the angle between \mathfrak{d} and \mathfrak{d}_i^1 is larger than the angle between \mathfrak{d} and \mathfrak{d}_{i+1}^j . In particular, the slope of \mathfrak{d}_i^1 is greater than the slope of $\mathfrak{d}_{i+1}^\infty$.

(2) For a fixed i and every j, $j' \ge 0$, along \mathfrak{d} , the slope of $\mathfrak{d}_{i,\text{op}}^j$ is greater than the slope of $\mathfrak{d}_{i+1,\text{op}}^{j'}$, in the sense that the angle between \mathfrak{d} and $\mathfrak{d}_{i,\text{op}}^j$ is larger than the angle between \mathfrak{d} and $\mathfrak{d}_{i+1,\text{op}}^{j'}$. In particular, the slope of $\mathfrak{d}_{i,\text{op}}^{\infty}$ is greater than the slope of $\mathfrak{d}_{i+1,\text{op}}^0$.

Proof. (1) Let \mathfrak{d} be an arbitrary (discrete or initial) ray along which we want to show the statement. Without loss of generality, we show the statement if \mathfrak{d} is moving to the right. Using the notation of Definition 4.2, we need thus need to show

notation of Definition 4.2, we need thus need to show the inequality $\frac{3D_id+b_i}{3D_ic+a_i} > \frac{R_{j+1}(D_{i+1})d+R_j(D_{i+1})b_{i+1}}{R_{j+1}(D_{i+1})c+R_j(D_{i+1})a_{i+1}}$. As in Figure 16(1) and without loss of generality, we can assume that $3D_ic+a_i>0$, $3D_id+b_i>0$, $R_{j+1}(D_{i+1})d+R_j(D_{i+1})b_{i+1}>0$ and $R_{j+1}(D_{i+1})c+R_j(D_{i+1})a_{i+1}>0$. With $\mathfrak d$ right-moving, (a_{i+1},b_{i+1}) , (a_i,b_i) form an oriented basis for $M_{\mathbb R}$, and hence $b_ia_{i+1}-a_ib_{i+1}>0$. The desired inequality then simplifies to

$$(4.2) (b_i a_{i+1} - a_i b_{i+1}) R_j(D_{i+1}) > D_i(3D_{i+1} R_j(D_{i+1}) - R_{j+1}(D_{i+1})) = D_i R_{j-1}(D_{i+1}),$$

the latter equality by Definition 2.19. By the same definition, we have $R_j(D_{i+1}) = 3D_{i+1}R_{j-1}(D_{i+1}) - R_{j-2}(D_{i+1})$. Hence, (4.2), becomes

$$(4.3) (b_i a_{i+1} - a_i b_{i+1}) (3D_{i+1} R_{i-1}(D_{i+1}) - R_{i-2}(D_{i+1})) > D_i R_{i-1}(D_{i+1}).$$

However, using $D_{i+1} > D_i$, $b_i a_{i+1} - a_i b_{i+1} \ge 1$, and Corollary 2.24, we have

$$0 < (b_i a_{i+1} - a_i b_{i+1})(D_{i+1} - D_i)R_{j-1}(D_{i+1}) + (b_i a_{i+1} - a_i b_{i+1})(2D_{i+1}R_{j-1}(D_{i+1}) - R_{j-2}(D_{i+1})),$$

yielding (4.3), proving the result.

Finally, since we have the statement for every j, taking the limit of $\{\mathfrak{d}_{i+1}^j\}$, when $j \to \infty$ we get the final statement.

Part (2) is similar as in Figure 16(2).

In this case we can show an even stronger statement: We will show that, along \mathfrak{d} , (a_{i+1}, b_{i+1}) (hence, each $\mathfrak{d}_{i+1,op}^j$) has a slope smaller than $\mathfrak{d}_{i,op}^j$. For this, we need to show

$$\frac{R_{j}(D_{i})d + R_{j+1}(D_{i})b_{i}}{R_{j}(D_{i})c + R_{j+1}(D_{i})a_{i}} > \frac{b_{i+1}}{a_{i+1}}.$$

Note the from Figure 16(2) and without loss of generality, we can assume $a_{i+1} < 0$ and $R_j(D_i)c + R_{j+1}(D_i)a_i < 0$; hence, (4.4) is equivalent to

$$(4.5) (a_{i+1}b_i - b_{i+1}a_i)R_{i+1}(D_i) > (b_{i+1}c - a_{i+1}d)R_i(D_i).$$

But as in Figure 16(2), we can assume $D = a_{i+1}b_i - b_{i+1}a_i > 0$ and $D_{i+1} = b_{i+1}c - a_{i+1}d > 0$. Hence, (4.5) is equivalent to $DR_{j+1}(D_i) - D_{i+1}R_j(D_i) > 0$. By definition, this is equivalent to the positivity of

$$(4.6) D(3D_iR_i(D_i) - R_{i-1}(D_i)) - D_{i+1}R_i(D_i) = (3DD_i - D_{i+1})R_i(D_i) - DR_{i-1}(D_i).$$

Note that since (D, D_i, D_{i+1}) and (D, D_{i-1}, D_i) are Markov triples related by mutation, we have $3DD_i = D_{i+1} + D_{i-1}$. Thus, (4.6) is equivalent to

$$D_{i-1}R_i(D_i) - DR_{i-1}(D_i),$$

which is positive since $D_{i-1} \ge D$ (by Proposition 2.18) and $R_i(D_i) > R_{i-1}(D_i)$ (Corollary 2.24).

The following statement is analogous to [34, Lem. 3.10].

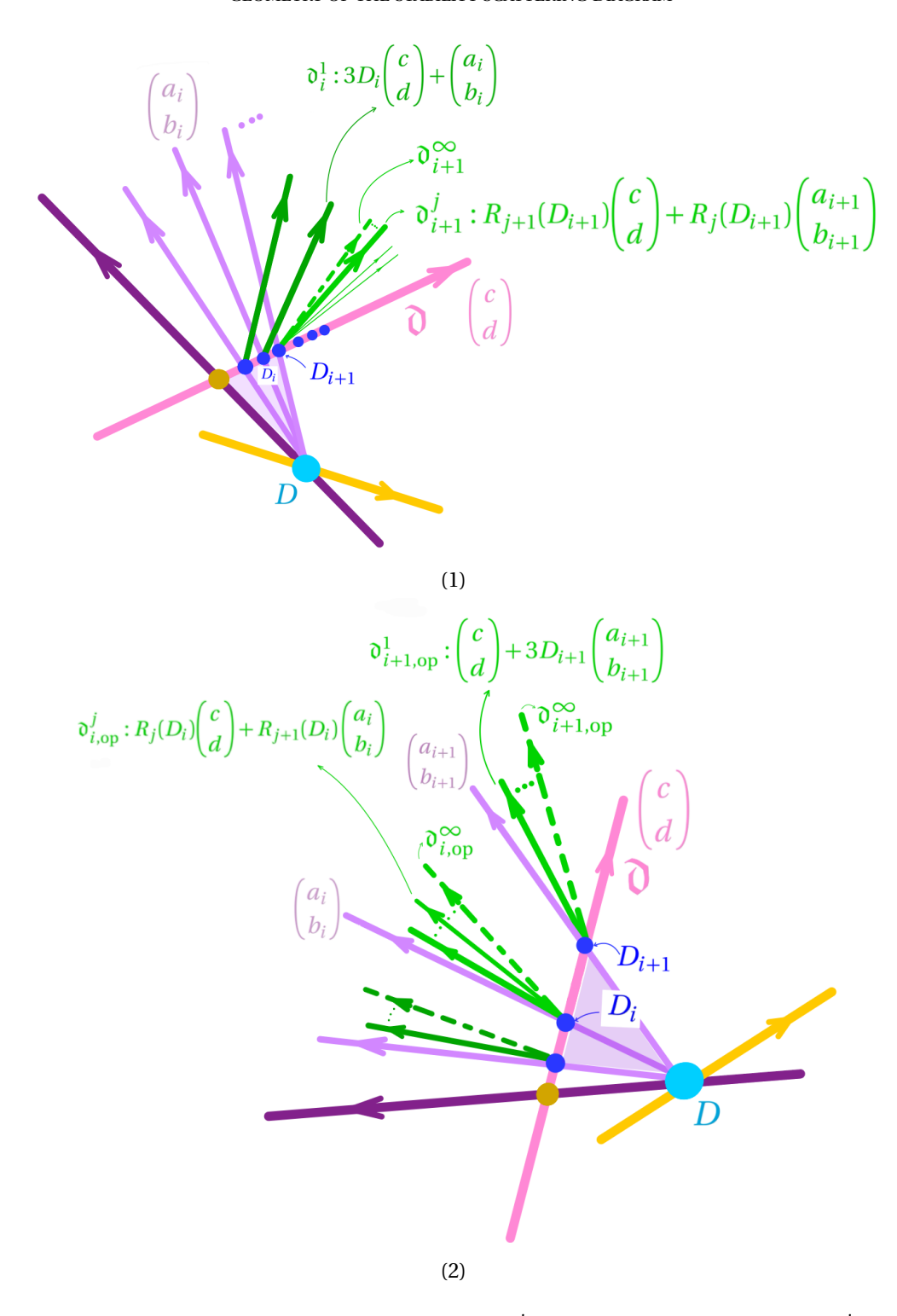


FIGURE 16. (1) Along \mathfrak{d} , $\mathfrak{d}_{i+1}^{\infty}$ (hence, each \mathfrak{d}_{i+1}^{j}) has a slope smaller than \mathfrak{d}_{i}^{j} . (2) Along \mathfrak{d} , (a_{i+1},b_{i+1}) (hence, each $\mathfrak{d}_{i+1,\mathrm{op}}^{j}$) has a slope smaller than $\mathfrak{d}_{i,\mathrm{op}}^{j}$. Here $D_i = b_i c - a_i d > 0$ and $D = a_{i+1} b_i - a_i b_{i+1} > 0$ are the corresponding determinants at the vertices.

Corollary 4.5. For w a vertex of the Markov tree \mathcal{T} , let v, v', v'' be the incoming, left-most and right-most vertices of the triangle Δ_w . Denote by \mathfrak{d}_v^- and \mathfrak{d}_v^+ the left-hand and right-hand rays

respectively generating the cone C_v . Let $\mathfrak{d}_{v'}^1$ be the first ray containing v' counter-clockwise from the edge of Δ_w joining v and v', and let $\mathfrak{d}_{v''}^1$ be the first ray containing v'' clockwise from the edge of Δ_w joining v and v''.

Then the slope of $\mathfrak{d}_{v'}^1$ is greater than the slope of \mathfrak{d}_v^+ and the slope of $\mathfrak{d}_{v''}^1$ is less than the slope of \mathfrak{d}_v^- . See Figure 17.

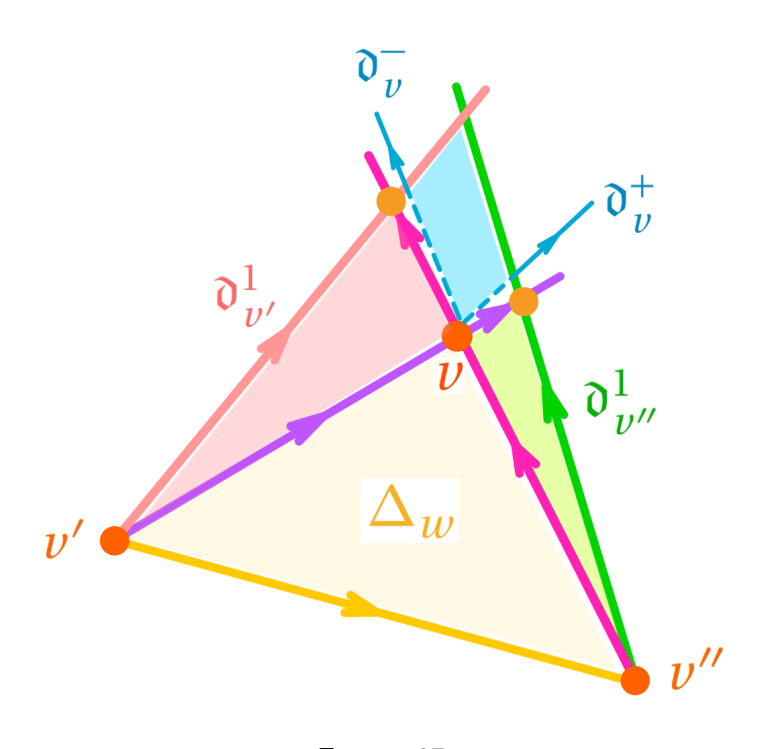


FIGURE 17

Proof. We consider the case of v', as the situation is symmetric. If Δ_w is the initial triangle, then one immediately checks this by hand, the slope of $\mathfrak{d}_{v'}^1$ being 3/2 and the slope of \mathfrak{d}_v^+ being $\sqrt{2}$.

Otherwise, the argument depends on whether v' is a hybrid or outgoing vertex. If it is hybrid, then Δ_w is as in Figure 16,(1), with vertices v, v', v'' having degrees D_{i+1}, D_i and D respectively. The claim then follows from Corollary 4.4,(1). On the other hand, if v' is an outgoing vertex, the picture is as in Figure 16,(2) (reflected about the y-axis), with Δ_w corresponding to the triangle with vertices v, v', v'' having degrees D_{i+1}, D and D_i respectively. The result in this case follows from Corollary 4.4,(ii).

We will need the following:

Theorem 4.6 (Inclusion in super-diamonds). (1) Let ∂ ∈ D⁰_{discrete}. If ∂ is right-moving the slope of ∂ is less than 2, while if ∂ is left-moving then the slope of ∂ is greater than −2.
(2) Every non-initial outer diamond is contained in a super-diamond.

Proof. By the analysis of §2.2, and in particular from Figure 7, every ray of $\mathfrak{D}^0_{\text{discrete}}$ is contained in $L_{\mathcal{E}(-3)[1]}$ for a right-moving ray or in $L_{\mathcal{E}}$ for a left-moving ray, for some exceptional bundle \mathcal{E} obtained via mutation from the strong exceptional triple $\mathcal{C} := (\mathcal{O}_{\mathbb{P}^2}(1), \mathcal{T}_{\mathbb{P}^2}, \mathcal{O}_{\mathbb{P}^2}(2))$. Since $\mu(\mathcal{O}_{\mathbb{P}^2}(1)) = 1$, $\mu(\mathcal{O}_{\mathbb{P}^2}(2)) = 2$, we have by Lemma 2.4,(2) that $\mu(\mathcal{E}) \in [1,2]$ (with $\mu(\mathcal{E}) = 1$ or 2

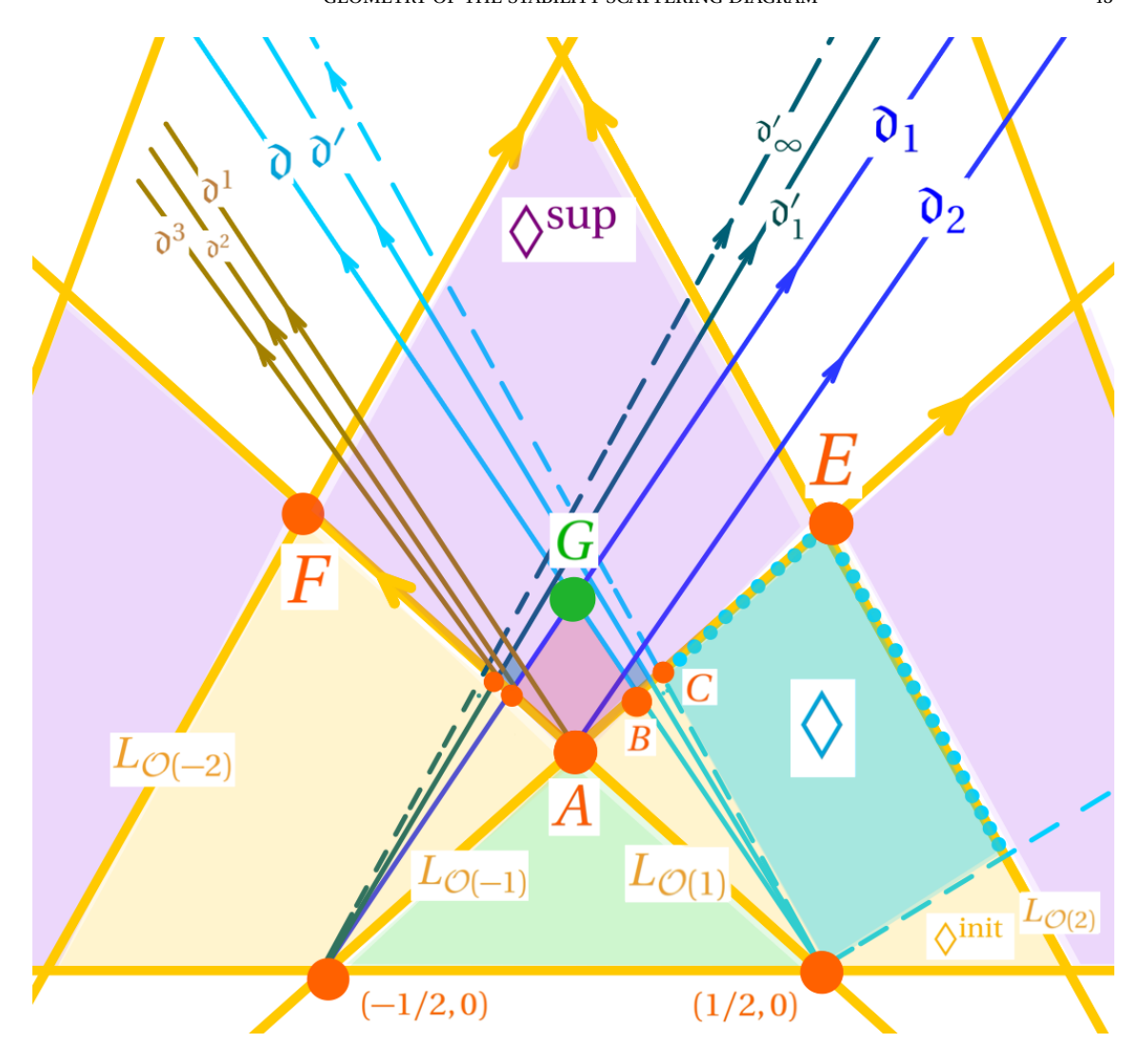


FIGURE 18. $L_{\mathcal{O}(-1)}$ bounds an initial diamond, \lozenge init (its big diamond) at (1/2,0) on the one side and infinitely many on the other.

if and only if $\mathcal{E}=\mathcal{O}_{\mathbb{P}^2}(1)$ or $\mathcal{O}_{\mathbb{P}^2}(2)$ respectively). The slope of the line $L_{\mathcal{E}(-3)[1]}$ is $-\mu(\mathcal{E}(-3))=-\mu(\mathcal{E})+3\in[1,2]$. The slope of the line $L_{\mathcal{E}}$ is $-\mu(\mathcal{E})\in[-2,-1]$. This shows (1). Note further this shows that if $\mathfrak{d},\mathfrak{d}'\in\{\mathfrak{d}_{-1}^+,\mathfrak{d}_1^-\}\cup\mathfrak{D}_{\mathrm{discrete}}^0$ are a right-moving and left-moving ray respectively, and the endpoints of these rays each lie below $L_{\mathcal{O}(2)}$ and $L_{\mathcal{O}(-2)}$, then the intersection $\mathfrak{d}\cap\mathfrak{d}'$, if non-empty, also lies below $L_{\mathcal{O}(2)}$ and $L_{\mathcal{O}(-2)}$.

For (2), first note that the projection of a super-diamond to the x-axis is [n-1/2, n+1/2] if the superdiamond is bounded by the lines $L_{\mathcal{O}(n-2)}, L_{\mathcal{O}(n-1)}, L_{\mathcal{O}(n+1)}, L_{\mathcal{O}(n+2)}$, see Figure 18. Focusing without loss of generality on the case n=0, it is thus enough to show the following. Let \mathcal{E} be an exceptional bundle of rank > 1 for which the x-coordinate of $V_{\mathcal{E}}$ lies in (-1/2, 1/2), i.e., $\mu(\mathcal{E}) \in (1,2)$. Then the outer diamond based at $V_{\mathcal{E}}$ is contained in the super-diamond \lozenge sup corresponding to n=0.

Denote by **Exc** the set of exceptional bundles on \mathbb{P}^2 obtained via mutation from \mathcal{C} (including the three elements of \mathcal{C} itself). For $\mathcal{E} \in \mathbf{Exc}$ not a line bundle, the vertex $V_{\mathcal{E}}$ is the intersection of a left-moving and right-moving ray in $\{\mathfrak{d}_{-1}^+,\mathfrak{d}_1^-\}\cup\mathfrak{D}_{\mathrm{discrete}}^0$, and hence $V_{\mathcal{E}}$ lies below $L_{\mathcal{O}(-2)}$ and

 $L_{\mathcal{O}(2)}$ respectively provided the endpoints of these two rays do. Thus, starting from $V_{\mathcal{E}}$ for \mathcal{E} in the strong exceptional triple \mathcal{C} , we see inductively that for all $\mathcal{E} \in \mathbf{Exc}$, $V_{\mathcal{E}}$ lies below $L_{\mathcal{O}(-2)}$ and $L_{\mathcal{O}(2)}$. Similarly, again consulting Figure 7, we see inductively that the roofs of the outer diamond based at $V_{\mathcal{E}}$ lie below $L_{\mathcal{O}(-2)}$ and $L_{\mathcal{O}(2)}$. Thus $\Diamond_{\mathcal{E}}^{\mathrm{out}}$ lies below these two lines.

On the other hand, provided that \mathcal{E} is rank > 1, then $V_{\mathcal{E}}$ lies on or above the lines $L_{\mathcal{O}(1)}$ and $L_{\mathcal{O}(-1)}$, as clearly $V_{\mathcal{E}}$ does not lie in the interior of the outer diamond based at (-1/2,0) or (1/2,0), see Figure 18. Thus we see that $\Diamond_{\mathcal{E}}^{\text{out}}$ lies in \Diamond^{sup} .

Lemma 4.7. Let \mathfrak{d} be an initial or discrete ray of $\mathfrak{D}^{\text{stab}}$. If \mathfrak{d} is right-moving (resp. left-moving), then there is no $\sigma \in \text{Int}(\mathfrak{d})$ and object $\mathcal{E} \in \mathcal{A}^{\sigma}$ which is semistable with respect to σ and has direction vector— $m_{\mathcal{E}}$ pointing to the right (resp. left) of \mathfrak{d} .

Proof. After twisting, we may assume that $\mathfrak{d} \in \{\mathfrak{d}_{-1}^+, \mathfrak{d}_0^\pm, \mathfrak{d}_1^-\} \cup \mathfrak{D}_{\text{discrete}}^0$. Now suppose that there exists $\sigma_0 \in \text{Int}(\mathfrak{d})$, $\mathcal{E} \in \mathcal{A}^\sigma$ which violates the statement of the lemma. We will first build a sequence of line segments or rays E_0, \ldots, E_n and $E_0', \ldots, E_{n'}'$ from this data.

Without loss of generality, let us focus on the right-moving case. Set $E_0 = \mathfrak{d}$. If \mathfrak{d} is an initial ray, we stop. Otherwise, we define the sequence E_1, \ldots, E_n inductively. The endpoint of \mathfrak{d} is an incoming vertex v_1 of some triangle Δ_1 . Take E_1 to be the left-hand edge of this triangle, with other endpoint v_2 . If E_1 contains one of the points of the form $(d, -d^2/2)$ from which initial rays emanate (so that E_1 is the edge of an initial triangle), then we replace E_1 with the subsegment of E_1 with endpoints $(d, -d^2/2)$ and v_1 . At this point we are done. Otherwise, we continue the process inductively. If we have chosen E_i with vertices v_i, v_{i+1} and E_i does not contain a point of the form $(d, -d^2/2)$, then v_{i+1} is an incoming vertex of a triangle Δ_{i+1} , and we take E_{i+1} to be the left-hand edge of Δ_{i+1} containing v_{i+1} . If E_{i+1} contains a point of the form $(d, -d^2/2)$, then we replace E_{i+1} with the line segment joining $(d, -d^2/2)$ and v_i and are done. Thus we have the data of a ray E_0 with endpoint E_0 , and line segments E_1, \ldots, E_n with E_n having endpoints E_1 , and E_1 and E_2 are the right-moving and in E_1 , and E_2 are the right-moving and in E_1 , and E_2 are the right-moving and in E_1 , and E_2 are the right-moving and in E_1 , and E_2 are the right-moving and in E_1 , and E_2 are the right-moving and in E_1 , and E_2 are the right-moving and in E_2 , and E_2 are the right-moving and in E_2 , and E_2 are the right-moving and in E_2 , and E_2 are the right-moving and in E_2 , and E_2 are the right-moving and in E_2 E_2 are the

We may similarly follow the procedure given in §1.3, starting with \mathcal{E} and obtaining a sequence of quotient objects $\mathcal{Q}_1, \ldots, \mathcal{Q}_{n'}$ and edges $E_0' = E(\mathcal{E}, \sigma_0), E_1', \ldots, E_{n'}'$. This sequence terminates at a point $(d', -(d')^2/2)$ for d' some integer. See Figure 19 for the first steps of this process.

For $E = E_i$ or E_i' , write $\mu(E)$ for the slope of the line segment E. Note that if $E \subseteq L_{\mathcal{E}}$ for some object \mathcal{E} , then $\mu(E) = -\mu(\mathcal{E})$. By construction $\mu(E_i) \ge \mu(E_{i+1})$ for all i. We will now show similarly that

(4.7)
$$\mu(E_i') > \mu(E_{i+1}')$$

for all i.

Indeed, this almost follows from the fact that at each step of the construction of the E_i' , \mathcal{Q}_i is chosen as a right generator, as in Figure 2. However, (4.7) would fail if $m_{\mathcal{Q}_i}$ points to the left but $m_{\mathcal{Q}_{i+1}}$ points to the right. To rule out this case, we proceed as follows. Extend E_0' in the direction $-m_{\mathcal{E}}$, i.e., replace E_0' with the ray $\sigma_1 - \mathbb{R}_{\geq 0} m_{\mathcal{E}}$. Since the sequence of edges terminates at a point on the parabola $y = -x^2/2$ and all edges E_i' (except the last one which has endpoint on this parabola) lie about this parabola, there is no choice but for this sequence of edges to cross itself, see Figure 20. Thus there exists some i, j with $j > i + 1 \geq 1$ for which $E_i' \cap E_j' \neq \emptyset$. After subdividing these two edges, we may assume they intersect in a vertex. Thus E_i' , E_{i+1}' , ... E_j' form a closed loop. Since this loop is compact, there is a point (x_0, y_0) on this

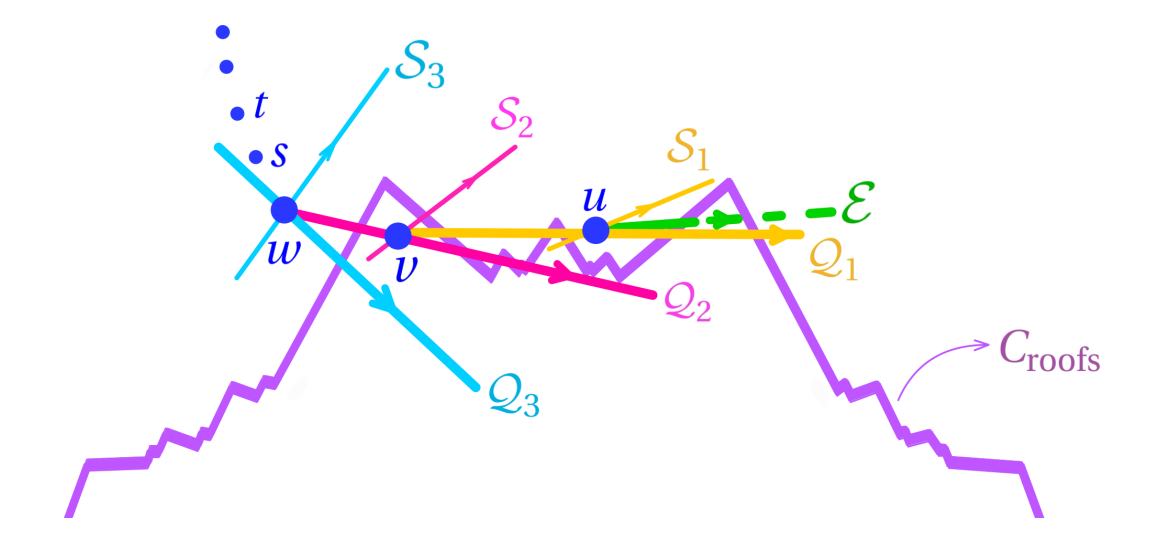


FIGURE 19

loop for which the function $h(x,y)=y+x^2/2$ achieves its maximum. This means that all E'_k with $i \leq k \leq j$ containing (x_0,y_0) must lie in the same half-plane with boundary the line $x_0(x-x_0)+(y-y_0)=0$. If (x_0,y_0) lies in the interior of an edge E'_k , then E'_k must lie in this line, contradicting (1.12), as then $\varphi_{(x_0,y_0)}(m_{\mathcal{Q}'_k})=0$. If this maximum occurs at the intersection of two adjacent edges E'_k , E'_{k+1} , then $\varphi_{(x_0,y_0)}(m_{\mathcal{Q}_k})$ and $\varphi_{(x_0,y_0)}(m_{\mathcal{Q}_{k+1}})$ have the opposite sign, again contradicting (1.12). The same contradiction occurs if (x_0,y_0) is the intersection point of E'_i and E'_j . This proves that (4.7) holds.

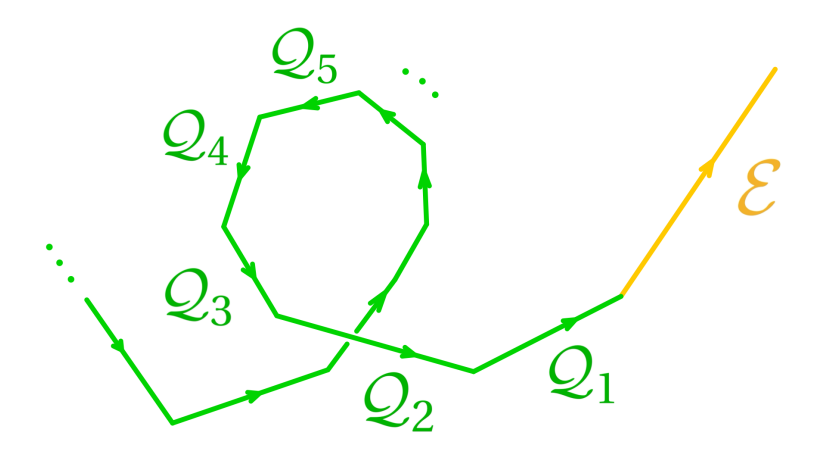


FIGURE 20

Now note that $d' \ge -1$. Indeed, if $d' \le -2$, then $\mu(E'_{n'}) \ge 2$. Using (4.7) repeatedly, we thus have $\mu(E'_1) \ge 2$. But by Theorem 4.6,(1), $\mu(\mathfrak{d}) < 2$. Thus $-m_{\mathcal{E}}$ cannot point to the right of \mathfrak{d} , contradicting our assumption.

It thus follows that $\cup_i E_i$ and $\cup_i E_i'$ must have an intersection point other than σ_0 . Thus, there is some i for which there exists a j with $E_i' \cap E_j \neq \emptyset$ and $\mu(E_i') > \mu(E_j)$. Take i as small as

possible, and given i, take j as small as possible. If j = 0, then by (4.7), $\mu(E_i') < \mu(E_1')$, but by assumption $\mu(E_1') < \mu(E_0)$ since E_1' crosses \mathfrak{d} from the left. This is a contradiction.

Otherwise, if j > 0, then E_j is a edge (or partial edge if $E_j = E_n$) of a triangle Δ_w for which v_j is an incoming vertex. If E_i' intersects E_j in its interior, then since E_j is the intersection of two triangles, E_i' intersects the interior of one of these two triangles. By Theorem 2.7, this is impossible. Thus E_i' must intersect E_j at a vertex. Since j was chosen to be as small as possible, this vertex is v_{j+1} . Thus E_i' must be a line segment contained in one of the rays through v_{j+1} in $\mathfrak{D}^{\text{stab}}$. Indeed, E_i' cannot lie between two adjacent discrete rays passing through v_{j+1} as this would violate Theorem 2.7. Hence, if E_i' is not contained in a discrete ray, it must be contained in the dense cone $C_{v_{j+1}}$, and hence in a dense ray of $\mathfrak{D}^{\text{stab}}$. It then follows from Corollary 4.5 that the slope of E_i' is greater than the slope of \mathfrak{d}_{v_j} . We may then use this corollary repeatedly to see that the slope of E_i' is greater than the slope of \mathfrak{d}_{v_j} again a contradiction.

Theorem 4.8 (Vertex-freeness). Let \Diamond_{v} be a dense diamond based at v.

- (1) For σ in the interior of \Diamond_v and γ a Chern character with $Z^{\sigma}(\gamma) \in i\mathbb{R}_{>0}$, then $\mathcal{M}^{\sigma}_{\gamma}$ is non-empty only if L_{γ} passes through v. Further, there are no actual walls in the interior of \Diamond_v on any ray passing through v.
- (2) The only rays meeting the roof of \Diamond_v are those passing through v.

Proof. Let \mathfrak{d} , \mathfrak{d}' be the discrete rays containing the left and right roofs of \lozenge_v respectively. For (1), suppose given $\sigma = \sigma_1$, γ as in the statement with $\mathcal{M}_{\gamma}^{\sigma_1}$ non-empty and L_{γ} not passing through v. Let \mathcal{E}_1 be an object in $\mathcal{M}_{\gamma}^{\sigma}$. We will construct a sequence of edges $E_1 = E(\mathcal{E}_1, \sigma_1), E_2, \ldots, E_n$. If the other endpoint of E_1 lies outside of \lozenge_v , we stop. Otherwise, let L_1 be the line through v and σ_2 . If $\mathcal{E}_2, \mathcal{E}_2'$ are the left and right generators of \mathcal{E}_1 in the language of §1.3, at least one of $m_{\mathcal{E}_2}, m_{\mathcal{E}_2'}$ is not tangent to L_1 since $m_{\mathcal{E}_1}$ is not tangent to L_1 and is a positive linear combination of $m_{\mathcal{E}_2}, m_{\mathcal{E}_2'}$. Interchanging \mathcal{E}_2 and \mathcal{E}_2' if necessary, we can assume $m_{\mathcal{E}_2}$ is not tangent to L_1 . We then take $E_2 = E(\mathcal{E}_2, \sigma_2)$. Repeating this process, we obtain E_1, \ldots, E_n where E_n has initial endpoint σ_n inside \lozenge_v and final endpoint σ_{n+1} outside of \lozenge_v . In particular, E_n must pass through one of the four edges of \lozenge_v . If it passes through the roof, i.e., through $\mathfrak{d} \cap \lozenge_v$ or $\mathfrak{d}' \cap \lozenge_v$, then this violates Lemma 4.7. If E_n passes through the interior of one of the lower edges, then it must enter the interior of a triangle, violating Theorem 2.7. We thus obtain a contradiction and the first statement of (1) holds. If an actual wall occured in the interior of \lozenge_v , then we would now have an object \mathcal{E} with $L_{\mathcal{E}}$ passing through v, with destabilizing subobject or quotient object \mathcal{F} having $L_{\mathcal{F}}$ not passing through v. This contradicts the first statement of (1).

For (2), after taking (1) into account, the only possibilities for $\mathfrak{d} \in \mathfrak{D}^{\text{stab}}$ meeting the roof of \Diamond_{ν} but not passing through ν is if \mathfrak{d} meets the apex of \Diamond_{ν} but does not enter the interior. However, this is also ruled out by Lemma 4.7.

The following gives a more refined picture of the diamonds.

Fix a (non-initial) discrete ray $\mathfrak{d} \in \mathfrak{D}_{\text{discrete}}$ with endpoint v. We let \mathfrak{d}° be the *previous ray*, which we define to be the first ray counterclockwise (resp. clockwise) from \mathfrak{d} through v if \mathfrak{d} is a left-moving (resp. right-moving) ray. Note that v may or may not be the endpoint of \mathfrak{d}° . We say a point $p \in \mathfrak{d}^{\circ}$ is past v if $p \in v - \mathbb{R}_{>0} m_{\mathfrak{d}^{\circ}}$. We have:

Proposition 4.9. Every outer diamond whose base lies on \mathfrak{d}° past v lies between \mathfrak{d}° and \mathfrak{d} .

Proof. By symmetry, we can assume \mathfrak{d} is a left-moving ray. Figure 18 shows one possible choice for \mathfrak{d} , with, in this case, \mathfrak{d}° being the left-moving ray contained in $L_{\mathcal{O}(1)}$.

Using Corollary 4.4 along \mathfrak{d}° , the angles of \mathfrak{d} , \mathfrak{d}^{1} , \mathfrak{d}^{2} , \mathfrak{d}^{3} ,... with \mathfrak{d}° are decreasing in the direction of \mathfrak{d}° . Here, \mathfrak{d}^{1} , \mathfrak{d}^{2} ,... denotes the first discrete rays generated along \mathfrak{d}° , i.e., \mathfrak{d}^{1}_{1} , \mathfrak{d}^{1}_{2} ,... in the notation of Definition 4.2. These rays are the right roofs of the diamonds with base on \mathfrak{d}° , and hence these right roofs all lie below \mathfrak{d} . Thus in particular all the diamonds with base past ν on \mathfrak{d}° lie between \mathfrak{d}° and \mathfrak{d} , as claimed.

Remark 4.10. We have the following picture of diamonds along any discrete ray \mathfrak{d} . Such a ray will always contain half the roof of some outer diamond \Diamond_v^{out} . This diamond will lie to the left (resp. right) of \mathfrak{d} if \mathfrak{d} is left-moving (resp. right-moving). On the other hand, before \mathfrak{d} reaches the dense diamond \Diamond_v based at v, there will be a sequence of outer diamonds based at points on \mathfrak{d} . These will all lie on the opposite side of \mathfrak{d} , i.e., on the right (resp. left) side of \mathfrak{d} if \mathfrak{d} is left-moving (resp. right-moving). See Figure 21. We use the following language.

Definition 4.11 (Effective interval, big diamond, and relatively big diamond). Let \mathfrak{d} be a discrete ray as above. We assign the following notions to \mathfrak{d} (for which we refer to the above discussion and Figure 21):

- (i) The outer diamond that \mathfrak{d} contains part of the roof of is called *big diamond* associated to \mathfrak{d} .
- (ii) The intersection of \mathfrak{d} with the big diamond is called the *effective interval* of \mathfrak{d} .
- (iii) The first and largest diamond on the side of $\mathfrak d$ opposite the big diamond is called *relatively big diamond* associated with $\mathfrak d$.

See Figure 21.

Note that each initial half-line bounds two initial diamonds, but only one of them (the one that has infinitely many diamonds on its other side along the half-line) is its big diamond. For example, in Figure 18, the big diamond associated to the half-line corresponding to $\mathcal{O}(-1)$ is the one based at (0,1/2). The diamond based at (-1/2,0) is another initial diamond bounded by this half-line, but it is not its associated big diamond (it is in fact the big diamond associated to the half-line corresponding to $\mathcal{O}(1)$).

Notation 4.12. We denote the curve given by the union of the roofs of the dense diamonds by C_{roofs} (see Figure 22).

Corollary 4.13 (Boundedness). The union of all outer diamonds is bounded above by the union of roofs of all super-diamonds. More precisely, the upper boundary of the union of all outer diamonds is C_{roofs} , which lies below the union of roofs of all super-diamonds.

Proof. All the initial diamonds lie below the union of roofs of the superdiamonds, and all other diamonds are contained in superdiamonds by Theorem 4.6, hence the first statement. The second statement is then clear.

Definition 4.14 (Bounded region). We define the *bounded region*, R_{bdd} , to be $R_{\Delta} \cup R_{\Diamond}$. Note this is the union of all outer diamonds, and that the upper boundary of this region is the union of the roofs of all the dense diamonds, C_{roofs} .

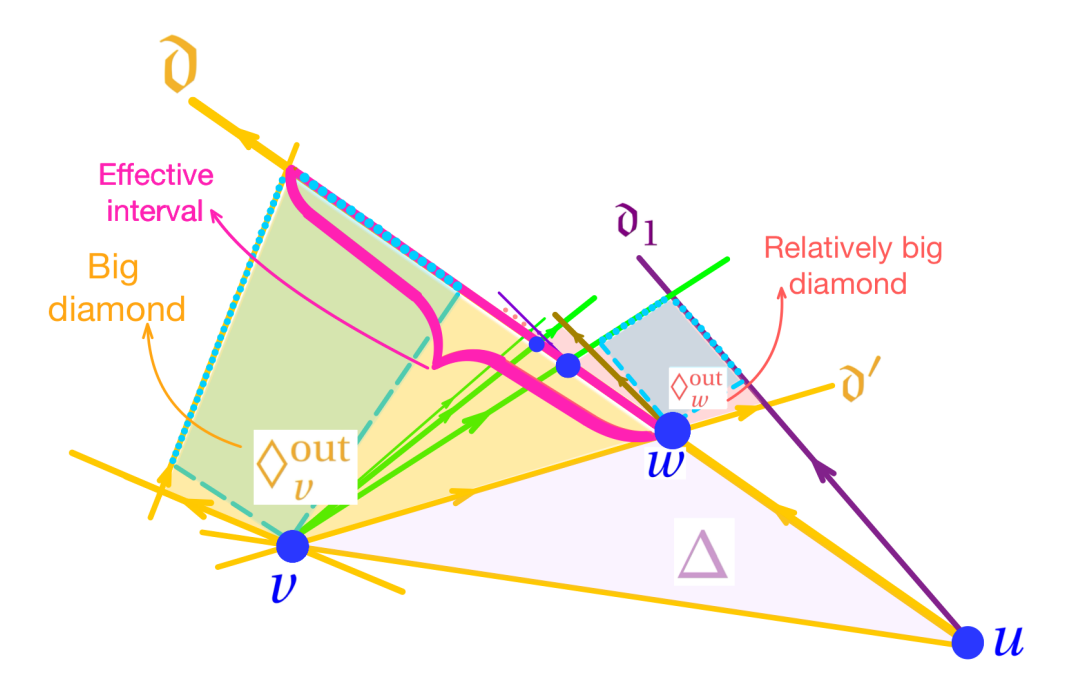


FIGURE 21. Effective interval, big diamond \lozenge_v^{out} , and relatively big diamond \lozenge_w^{out} .

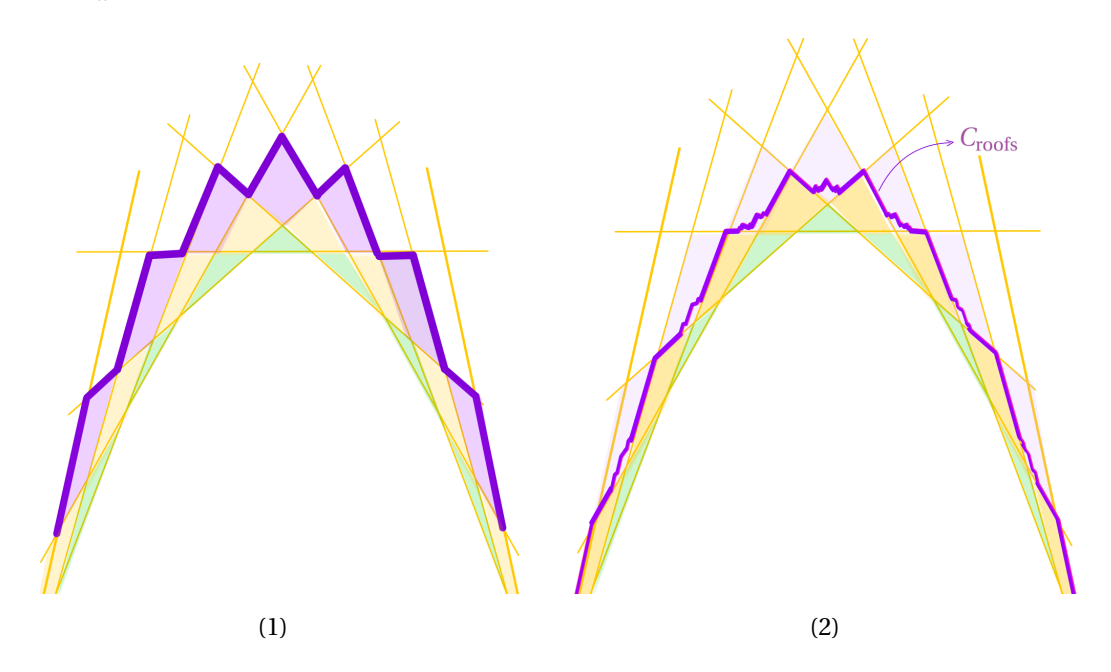


FIGURE 22. (1) The roofs of the super-diamonds provide an upper boundary for the space of all the outer diamonds. (2) A finer version fractal-like of the upper boundary, $C_{\rm roofs}$, is a curve consists of the roofs of all the dense diamonds.

Corollary 4.15. The scattering diagrams $\mathfrak{D}^{\text{stab}}$ and $\mathfrak{D}^{\text{stab}}_{\text{in}} \cup \mathfrak{D}_{\text{discrete}} \cup \mathfrak{D}_{\text{dense}}$ are equivalent in R_{bdd} .

Proof. This now follows from Theorem 4.8, which shows the initial, discrete and dense rays account for all rays in the bounded region. \Box

Theorem 4.16. Denote by $\operatorname{pr}_1: M_{\mathbb{Q}} \to \mathbb{Q}$ the projection to the x-axis. Then

$$\operatorname{pr}_1|_{C_{\operatorname{roofs}}\cap M_{\mathbb{Q}}}: C_{\operatorname{roofs}}\cap M_{\mathbb{Q}}\to \mathbb{Q}$$

is a bijection. In particular, any vertical line x = q for $q \in \mathbb{Q}$ intersects C_{roofs} at one point.

Proof. Denote by

$$S := \{\mu(\mathcal{E}) | \mathcal{E} \text{ is an exceptional bundle} \}$$

the set of slopes of exceptional bundles. [43, Thm. 3.1] states that S coincides with the set of Markov fractions. Also, the set of x-coordinates of the points $V_{\mathcal{E}}$ for \mathcal{E} ranging over exceptional bundles coincides with S-3/2, the shift of S to the left by 3/2.

For a given exceptional bundle \mathcal{E} , the left and right vertices of the dense diamond $\Diamond_{V_{\mathcal{E}}}$ are the intersection of a line ax + by = c with $a, b, c \in \mathbb{Q}$ and a line through $V_{\mathcal{E}} \in M_{\mathbb{Q}}$ of quadratic irational slope. Hence the left and right vertices have quadratic irrational x-coordinates.

For a given \mathcal{E} , let $I_{\mathcal{E}} \subseteq \mathbb{R}$ be the projection of the roof of the dense diamond $\Diamond_{V_{\mathcal{E}}}$, excluding the left and right vertices, so that this is an open interval with quadratic irrational endpoints. Note that $\operatorname{pr}_1(V_{\mathcal{E}})$ is a rational element of $I_{\mathcal{E}}$.

First we claim there is no exceptional bundle $\mathcal{E}' \neq \mathcal{E}$ such that $\mu(\mathcal{E}') - 3/2 \in I_{\mathcal{E}}$. Indeed, by Lemma 2.4,(8), $\mu(\mathcal{E}) \neq \mu(\mathcal{E}')$. However, if $V_{\mathcal{E}'}$ lies below the roof of $\Diamond_{V_{\mathcal{E}}}$, the vertical ray $\mathbf{R}_{\geq 0}(0,1) + V_{\mathcal{E}'}$ is a ray in $\mathfrak{D}_{\text{dense}}$ which intersects the interior of $\Diamond_{V_{\mathcal{E}}}$ but neither contains a roof nor has endpoint $V_{\mathcal{E}}$, violating Theorem 4.8. Similarly, if $V_{\mathcal{E}'}$ lies on or above the roof of $\Diamond_{V_{\mathcal{E}}}$, then $V_{\mathcal{E}'} \in C_{V_{\mathcal{E}}}$ and this again contradicts Theorem 4.8. Thus $I_{\mathcal{E}} \cap (S - 3/2) = \{ \operatorname{pr}_1(V_{\mathcal{E}}) \}$.

Second, from Remark 4.10, there is a sequence of diamonds \Diamond_{v_i} , $i \ge 1$ whose base lies on the discrete ray containing the left (resp. right) roof of $\Diamond_{V_{\mathcal{E}}}$ and whose bases approach the left (resp. right) vertex of \Diamond_v . Hence $I_{\mathcal{E}}$ is the largest open interval containing $\operatorname{pr}_1(V_{\mathcal{E}})$ and no other point of S-3/2. By [40, Lem. 4.16], we then have

$$I_{\mathcal{E}} = (\mu(\mathcal{E}) - \delta_{\mathcal{E}} - 3/2, \mu(\mathcal{E}) + \delta_{\mathcal{E}} - 3/2),$$

where

$$\delta_{\mathcal{E}} = \frac{3}{2} - \sqrt{\frac{9}{4} - \frac{1}{r(\mathcal{E})^2}}.$$

However, by [14], $\bigcup_{\mathcal{E}} I_{\mathcal{E}}$ contains all rational numbers, hence proving surjectivity. Since pr_1 is certainly injective on the roof of each diamond, and $I_{\mathcal{E}} \cap I_{\mathcal{E}'} = \emptyset$ whenever $\mathcal{E} \neq \mathcal{E}'$ by the above disussion, we obtain injectivity.

Remark 4.17. In Theorems 6.19 and 6.20, we recover the description of $I_{\mathcal{E}}$ via an explicit calculation rather than from using the general theory of Markov fractions. However, this theory is quite beautiful and it is worth drawing attention to it.

Also, we remark that [13] showed that the complement of $\bigcup_{\mathcal{E}} I_{\mathcal{E}}$ consists of the quadratic irrational endpoints of the intervals along with a set of transcendental numbers. So it is a quite subtle set.

5. Characterization of R_{unbdd} and moduli non-emptiness

In this section, we show that the behaviour in the unbounded region, $R_{\rm unbdd}$, is extremely chaotic. We do this by analyzing scattering at points of $C_{\rm roofs}$, showing that there are cones based at each such point in which every ray of rational slope appears as the support of a ray in

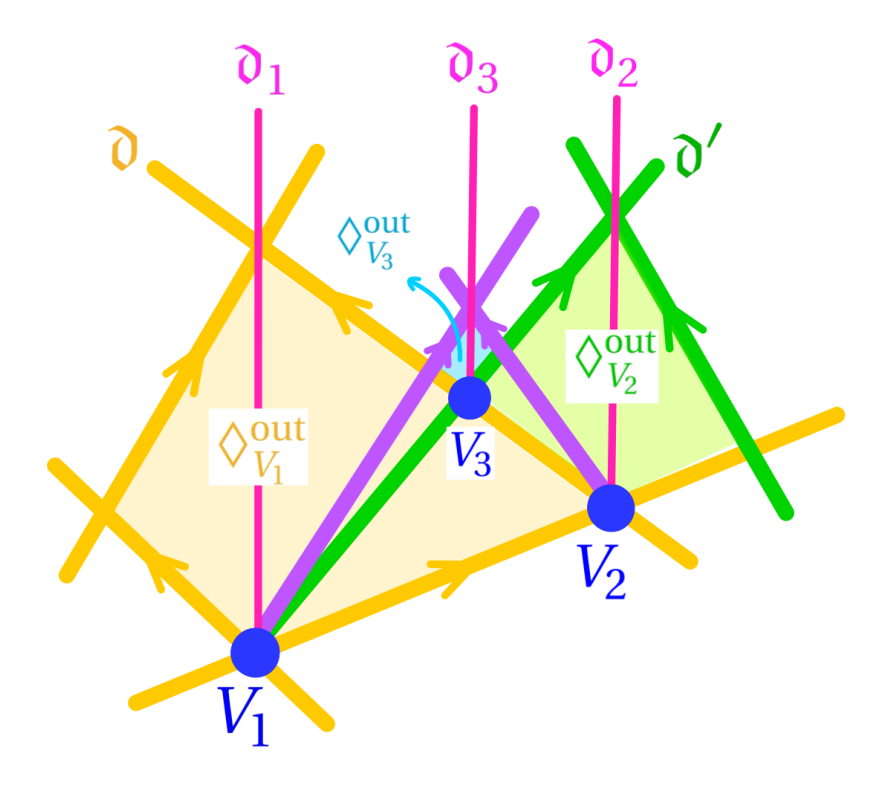


FIGURE 23. There is a diamond $\lozenge_{V_3}^{\text{out}}$ between any two outer diamonds $\lozenge_{V_1}^{\text{out}}$ and $\lozenge_{V_2}^{\text{out}}$.

 $\mathfrak{D}^{\text{stab}}$. We have two different behaviours, depending on whether the point is an *apex point*, i.e., the intersection of the left and right roofs of the diamond, or a degenerate diamond.

First, we prove several results about scattering in the setting of the scattering diagrams introduced at the beginning of §2.4.

Lemma 5.1. Let $m_1, m_2 \in M$ be linearly independent and primitive, and let

$$\mathfrak{D}_{\text{in}} = \{\mathfrak{d}_1 = (\mathbb{R}m_1, (1 + t_1 z^{-m_1})^3), \mathfrak{d}_2 = (\mathbb{R}m_2, \prod_{k=1}^{\infty} (1 + t_2^k z^{-km_2})^{a_k})\}$$

for a_k positive integers for all k. Then $S(\mathfrak{D}_{in})$ contains a non-trivial ray with support $\mathbb{R}_{\geq 0}(a\,m_1+b\,m_2)$ for all a,b>0 relatively prime with $a/b\leq 3|m_1\wedge m_2|$. Further, $S(\mathfrak{D}_{in})$ contains no rays with support $\mathbb{R}_{\geq 0}(a\,m_1+b\,m_2)$ with $a/b>3|m_1\wedge m_2|$.

Proof. We may first use the deformation trick as carried out in [26] by replacing the line $(\mathbb{R}m_2, \prod_{k=1}^{\infty} (1 + t_2^k z^{-km_2})^{a_k})$ with an infinite number of lines $\mathfrak{d}_2^k := (\mathbb{R}m_2, (1 + t_2^k z^{-km_2})^{a_k})$ for $k \ge 1$, and then perturbing these lines to be be parallel to each other, see Figure 24. We analyze the collision of \mathfrak{d}_1 with \mathfrak{d}_2^k . Set $\mathfrak{D}_{\text{in}}^k = \{\mathfrak{d}_1, \mathfrak{d}_2^k\}$. Now let $D = |m_1 \wedge m_2|$. We first show that for any $a/b < 3|m_1 \wedge m_2|$, there is some k such that $S(\mathfrak{D}_{\text{in}}^k)$ has a non-trivial ray with support $\mathfrak{d} = \mathbb{R}_{>0}(a\,m_1 + b\,m_2)$.

As in the proof of Lemma 2.22, we may pass to a sublattice M' spanned by $m_1' = m_1$ and $m_2' = km_2$, at the cost of replacing \mathfrak{d}_1 and \mathfrak{d}_2^k with $(\mathbb{R}m_1, (1+t_1z^{-m_1'})^{3kD})$ and $(\mathbb{R}m_2, (1+t_2^kz^{-m_2'})^{a_kkD})$ respectively. By [26, Thm. 1.4] $S(\mathfrak{D}_{in}^k)$ has non-trivial rays with support $\mathbb{R}_{\geq 0}(am_1 + bm_2) =$

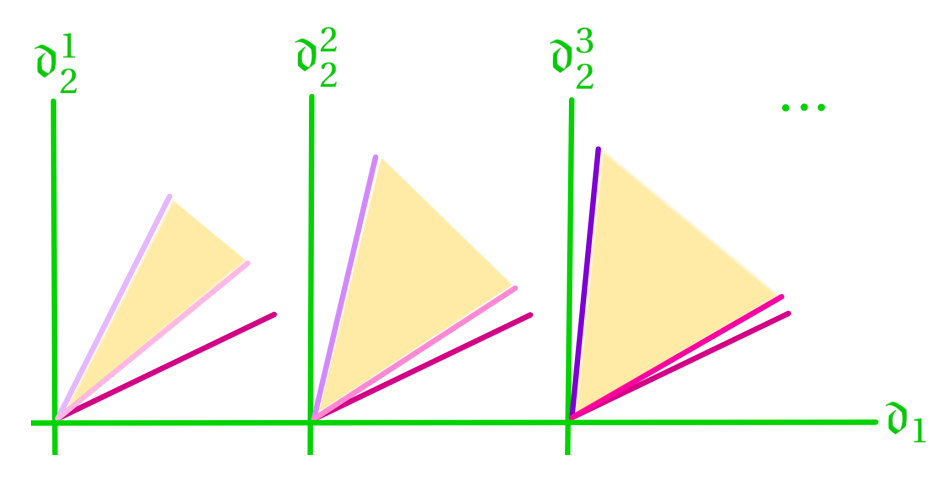


FIGURE 24

 $\mathbb{R}_{\geq 0}(a\,m_1' + (b/k)m_2')$ for

$$\frac{3k^2D^2a_k - \sqrt{3k^2D^2a_k(3k^2D^2a_k - 4)}}{6kD} < \frac{b}{ak} < \frac{3k^2D^2a_k + \sqrt{3k^2D^2a_k(3k^2D^2a_k - 4)}}{6kD}.$$

After multiplying all three quantities by k, we make take $k \to \infty$. The left-hand side converges to $(3D)^{-1}$ while the right hand side converges to ∞ . This shows the desired existence in the given range. These rays then necessarily contribute non-trivially to $S(\mathfrak{D}_{in})$ by positivity of the scattering process (see [19, Prop. C.13] as applied in [26, Prop. 2.9]). On one hand, by [26, Thm. 1.4], $S(\mathfrak{D}_{in}^k)$ contains a non-trivial ray with support $\mathbb{R}_{\geq 0}(3kD\,m_1'+m_2')=\mathbb{R}_{\geq 0}(3D\,m_1+m_2)$ for any k. Again, by positivity these rays contribute. On the other hand, [26, Prop. 3.13] states that this is the smallest slope of a ray appearing in $S(\mathfrak{D}_{in}^k)$, i.e., there is no ray with support $\mathbb{R}_{\geq 0}(a\,m_1+b\,m_2)$ with a/b>3D.

This implies that \mathfrak{D}_{in} can't contain any non-trivial rays with support $\mathbb{R}_{\geq 0}(a\,m_1+b\,m_2)$ with a/b>3D. Indeed, in the deformed scattering diagram, all collisions except the initial collisions of \mathfrak{d}_1 and \mathfrak{d}_2^k for various k must involve rays with support $\mathbb{R}_{\geq 0}(a\,m_1+b\,m_2)$ with $a/b\leq 3D$. Thus they cannot produce new rays with a/b>3D.

Lemma 5.2 (Denseness at degenerate diamonds of C_{roofs}). Let $\sigma \in M_{\mathbb{R}}$ coincide with a degenerate diamond. Then $\mathfrak{D}^{\text{stab}}$ contains precisely two rays $\mathfrak{d}_{\text{discrete}}$, $\mathfrak{d}_{\text{dense}}$ which contain σ in their interior. Here $\mathfrak{d}_{\text{discrete}} \in \mathfrak{D}_{\text{discrete}}$ and $\mathfrak{d}_{\text{dense}} \in \mathfrak{D}_{\text{dense}}$. Letting m_{discrete} and m_{dense} be the opposite vectors of these two rays and $D_{\sigma} = |m_{\text{discrete}} \wedge m_{\text{dense}}|$, we define the dense cone at σ to be the cone with vertex σ given by

$$C_{\sigma} := \{ \sigma - (a \, m_{\text{discrete}} + b \, m_{\text{dense}}) \, | \, a, b \in \mathbb{R}_{>0}, a/b \le 3D_{\sigma} \}.$$

Then there is a non-trivial ray $(\mathfrak{d}, H_{\mathfrak{d}}) \in \mathfrak{D}^{\text{stab}}$ with \mathfrak{d} having endpoint σ if and only if \mathfrak{d} lies in C_{σ} .

Proof. The description of the two rays of $\mathfrak{D}^{\text{stab}}$ follows immediately from the definition of degenerate diamond and Theorem 4.8. Given this, we look at the local scattering diagram $\mathfrak{D}_{\sigma}^{\text{stab}}$. By definition of degenerate diamond, σ is contained in the roof of a dense diamond \diamond_v contained in an outer diamond \diamond_v^{out} , with discrete generating rays $\mathfrak{d}_1, \mathfrak{d}_2$ with opposite vectors m_1, m_2 . Then we may write the opposite vector of $\mathfrak{d}_{\text{dense}}$ as $a_1 m_1 + a_2 m_2$ for some relatively prime positive integers a_1, a_2 .

If $H_{\mathrm{dense}}^{\sigma}$ is the function attached to the tangent line of $\mathfrak{d}_{\mathrm{dense}}$ in the local scattering diagram $\mathfrak{D}^{\mathrm{stab}}$, then the corresponding function f_{dense} as derived from $H_{\mathrm{dense}}^{\sigma}$ as in Remark 1.5 must take the form

$$f_{\text{dense}} = \prod_{k>1} (1 + t^{\alpha k} z^{a_1 k m_1 + a_2 k m_2})^{c_k}$$

for some positive integers c_k and some real number $\alpha > 0$. This form arises from the description of rays in $\mathfrak{D}'_{\mathrm{dense}}$ in Lemma 2.21 and the proof of Lemma 2.22. We note that the c_k may not agree with the c_{ka_1,ka_2} of Lemma 2.21 because the change of lattice trick might change these exponents. On the other hand,

$$f_{\text{discrete}} = (1 + t^{\beta} z^{m_{\text{discrete}}})^3$$

П

for some real number $\beta > 0$. The result now follows from Lemma 5.1.

Corollary 5.3 (Denseness at apex points of C_{roofs}). Let $\sigma \in M_{\mathbb{R}}$ be the apex of a diamond \Diamond . Then $\mathfrak{D}^{\text{stab}}$ contains precisely

three rays $\mathfrak{d}_{discrete}$, $\mathfrak{d}'_{discrete}$, \mathfrak{d}_{dense} which contain σ in their interior. Here $\mathfrak{d}_{discrete}$, $\mathfrak{d}'_{discrete} \in \mathfrak{D}_{discrete}$ are the discrete rays forming the left and right roofs of \Diamond , and \mathfrak{d}_{dense} is the vertical dense ray generated at the base of \Diamond . Letting m = (r, -d) and m' = (-r', d') be the direction vectors of $\mathfrak{d}_{discrete}$, with r, r' > 0, define the dense cone at σ to be the cone with vertex σ given by

$$C_{\sigma} := \{ \sigma + (am + (0,b)) \mid a,b \in \mathbb{R}_{>0}, a/b \le 3r \} \cup \{ \sigma + (am' + (0,b)) \mid a,b \in \mathbb{R}_{>0}, a/b \le 3r' \}.$$

Then there is a non-trivial ray $(\mathfrak{d}, H_{\mathfrak{d}}) \in \mathfrak{D}^{\text{stab}}$ with \mathfrak{d} having endpoint σ if and only if \mathfrak{d} lies in C_{σ} .

Proof. Let v be the base of \Diamond . Of course by definition, σ is the intersection of the two discrete rays forming the roof of \Diamond . Further, by Lemma 3.3, the vertical ray with endpoint v is contained in C_v , and hence supports a dense ray $\mathfrak{d}_{\text{dense}}$. By Definition 4.8, these are the only possible rays of $\mathfrak{D}^{\text{stab}}$ containing σ in their interior.

To analyze the scattering at σ , as in Lemma 5.2, we may pass to a scattering diagram of the sort considered in Lemma 5.1, this time with

$$\mathfrak{D}_{\text{in}} = \left\{ \left(\mathbb{R}m, (1 + t^{\alpha} z^{-m})^{3} \right), \left(\mathbb{R}m', (1 + t^{\beta} z^{-m'})^{3} \right), \left(\mathbb{R}(0, 1), \prod_{k \ge 1} (1 + t^{k\gamma} z^{(0, -k)})^{a_{k}} \right) \right\}$$

$$= \left\{ 0, 0', 0'' \right\}$$

We may then use the deformation trick to shift \mathfrak{d}'' as depicted in Figure 25. Note that this produces three initial collisions of these lines. By Lemma 5.1, the collision of \mathfrak{d} and \mathfrak{d}'' produces only rays with direction vector positively proportional to am + (0,1) for $a \le 3|m \land (0,1)| = 3r$.

Similarly, the collision of \mathfrak{d}' and \mathfrak{d}'' produces only rays with direction vector positively proportional to am' + (0,1) for $a \le 3|m' \wedge (0,1)| = 3r'$. On the other hand, using the change of lattice trick and applying [26, Prop. 3.13], we see that the collision of \mathfrak{d} and \mathfrak{d}' produces rays with support $\mathbb{R}_{>0}(am + bm')$ with $(3D_{\sigma})^{-1} \le a/b \le 3D_{\sigma}$, where $D_{\sigma} = |m \wedge m'|$.

We first show that any ray produced by the scattering of $\mathfrak{d},\mathfrak{d}'$ must be contained in C_{σ} . For this, it is sufficient to show that the rays $\sigma + \mathbb{R}_{\geq 0}(3D_{\sigma}m + m')$ and $\sigma + \mathbb{R}_{\geq 0}(m + 3D_{\sigma}m')$ are contained in the cone C_{σ} . By acting via some power of T, we can without loss of generality assume that the x-coordinate of σ lies in the interval [-1/2,1/2], and then d < 0, d' > 0. By symmetry, let us show that the former ray is contained in C_{σ} . We may write $D_{\sigma} = rd' - r'd > 0$ and $3D_{\sigma}m + m' = (3D_{\sigma}r - r', -3D_{\sigma}d + d')$. Noting that $3D_{\sigma}r - r' > 0$ by the assumption that

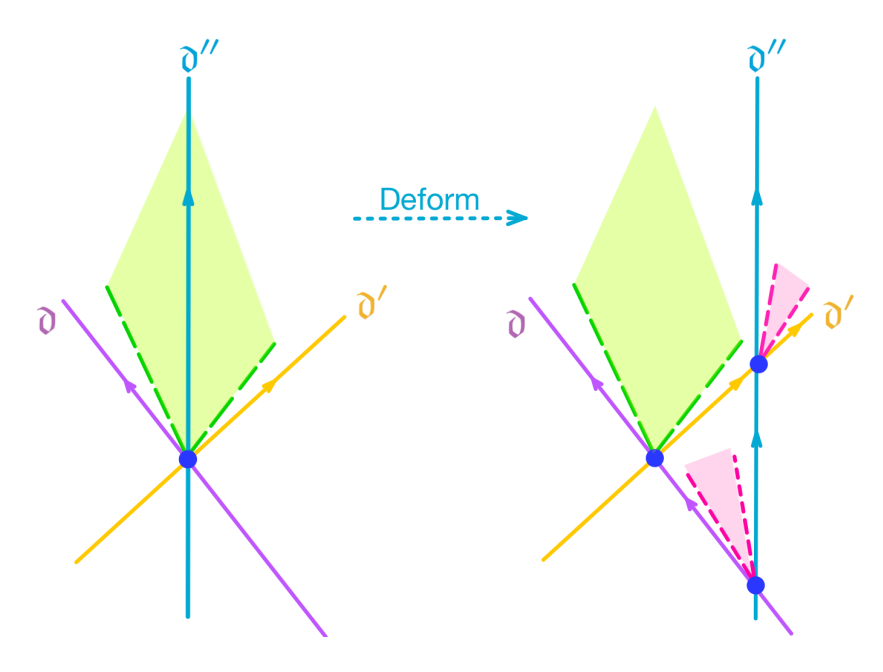


FIGURE 25

d < 0, d' > 0, we need to show the slope of this vector is larger than the slope of $3rm + (0, 1) = (3r^2, -3rd + 1)$, i.e.,

(5.1)
$$\frac{-3D_{\sigma}d + d'}{3D_{\sigma}r - r'} > \frac{-3rd + 1}{3r^2}.$$

Note both numerators and denominators are positive. We calculate

$$3r^2(-3D_{\sigma}d+d')-(3D_{\sigma}r-r')(-3rd+1)=(3d'r-3dr')r-3D_{\sigma}r+r'=r'>0,$$

hence (5.1).

It is now clear from the deformed scattering diagram Figure 25 that all further scattering only produces rays whose asymptotic direction lie in the asymptotic directions of the cone C_{σ} .

Corollary 5.4 (Unbounded region characterization). *Every rational point in* R_{unbdd} *is contained in the interior of a countable number of non-trivial rays of* \mathfrak{D}^{stab} . *See Figure 26.*

Proof. Let $\sigma = (x, y) \in R_{\text{unbdd}}$ be a point with rational coordinates. By Theorem 4.16, this point will lie above a unique dense diamond \Diamond_v , with base v, apex $v_A = (x_A, y_A)$ and left and right vertices $v_L = (x_L, y_L)$ and $v_R = (x_R, y_R)$. Without loss of generality, we can assume that $x_L < x \le x_A$. Note we have strict inequality on the left as x_L is necessarily irrational.

Let $\sigma' = (x', y')$ be a rational point in the left roof of \Diamond_v with $x < x' < x_A$ and such that σ lies to the right of the ray \mathfrak{d}' emanating from v through σ' . There will be an interval of points on the left roof with this property, hence a countable number of such possible σ' . Now for a given σ' , consider the cone $C_{\sigma'}$ of Lemma 5.2. We claim that $\sigma \in C_{\sigma'}$. Since σ lies to the left of σ' , it is enough to show that the cone $\sigma' + \mathbb{R}_{\geq 0} m' + \mathbb{R}_{\geq 0} (0,1)$ is contained in $C_{\sigma'}$, where m' is the direction vector of \mathfrak{d}' . Using the notation of Lemma 5.2 with $\mathfrak{d}_{\text{discrete}}$ being the left roof and $\mathfrak{d}_{\text{dense}}$ being \mathfrak{d}' , let (a_1, a_2) the the direction vector for $\mathfrak{d}_{\text{discrete}}$ and (b_1, b_2) be the direction vector for $\mathfrak{d}_{\text{dense}}$. Then $a_1 > 0$, $b_1 < 0$, and after twisting so that the base of the diamond has x-coordinate in [-1/2, 1/2], we can assume $a_2, b_2 > 0$. The right edge of $C_{\sigma'}$ has direction

vector

$$3(a_1b_2-a_2b_1)(a_1,a_2)+(b_1,b_2),$$

which then clearly has positive x-coordinate. Thus the ray $v + \mathbb{R}_{\geq 0}(0,1)$ is contained in $C_{\sigma'}$. As $v + \mathbb{R}_{\geq 0}m'$ is contained in $C_{\sigma'}$ by definition, we thus see that $\sigma' + \mathbb{R}_{\geq 0}m' + \mathbb{R}_{\geq 0}(0,1)$ is contained in $C_{\sigma'}$ as claimed.

We thus see that for every σ' as above, there is a ray in $\mathfrak{D}^{\text{stab}}$ with endpoint σ' and passing through σ . This proves the result.

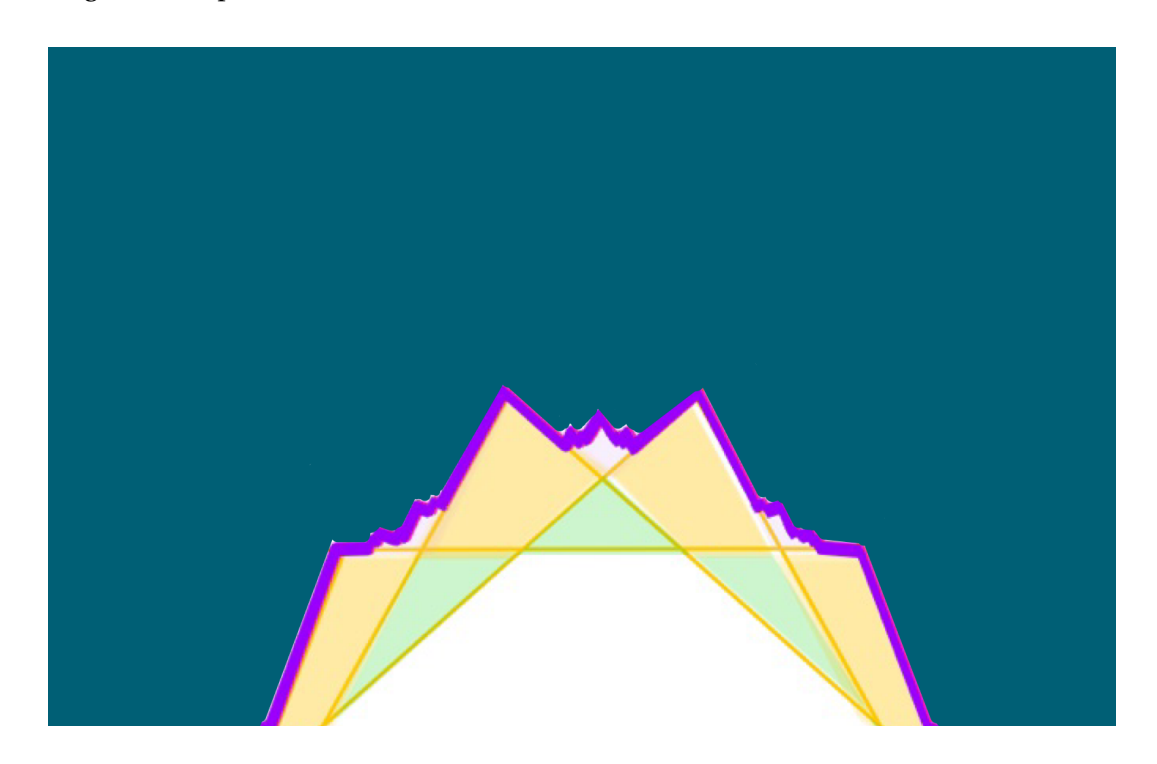


FIGURE 26. The rational points in the unbounded region are all vertices.

Corollary 5.5 (Classification of the rays generated in the unbounded region). Let $\gamma = (r, d, e)$ be the Chern character of an object in $D^b(\mathbb{P}^2)$, such that L_{γ} is not vertical and does not contain a discrete ray. Let $\sigma_0 \in L_{\gamma} \cap C_{\text{roofs}}$ be a point so that $\sigma_0 - \mathbb{R}_{>0} m_{\gamma} \subseteq R_{\text{unbdd}}$. Then the first generating point σ of γ lies in R_{unbdd} if and only if $\sigma_0 - \mathbb{R}_{>0} m_{\gamma}$ is not contained in the dense cone C_{σ_0} at σ_0 .

Proof. Let σ be the first generating point for γ , and let $(\mathfrak{d}, H_{\mathfrak{d}}) \in \mathfrak{D}^{\text{stab}}$ be a ray with endpoint σ . By assumption, \mathfrak{d} is not a discrete ray. By Theorem 4.8, we only have the three following possible cases (see Figure 27):

Case I. The intersection of L_{γ} with C_{roofs} is a point p such that $p - \mathbb{R}_{\geq 0} m_{\gamma}$ is contained in the dense cone C_p at p. In this case, from Lemma 5.2, $p = \sigma$ is in fact the first generating point of \mathfrak{d} . This also holds when p is an apex (for which we use Lemma 5.3).

Case II. The intersection of L_{γ} with C_{roofs} is a point p so that L_{γ} meets the base point v of the corresponding diamond (the dense diamond whose roof contains p). In this case v is in fact the first generating point of \mathfrak{d} .

Case III. If Cases I or II don't occur, then \mathfrak{d} is in fact generated at some point σ in R_{unbdd} .

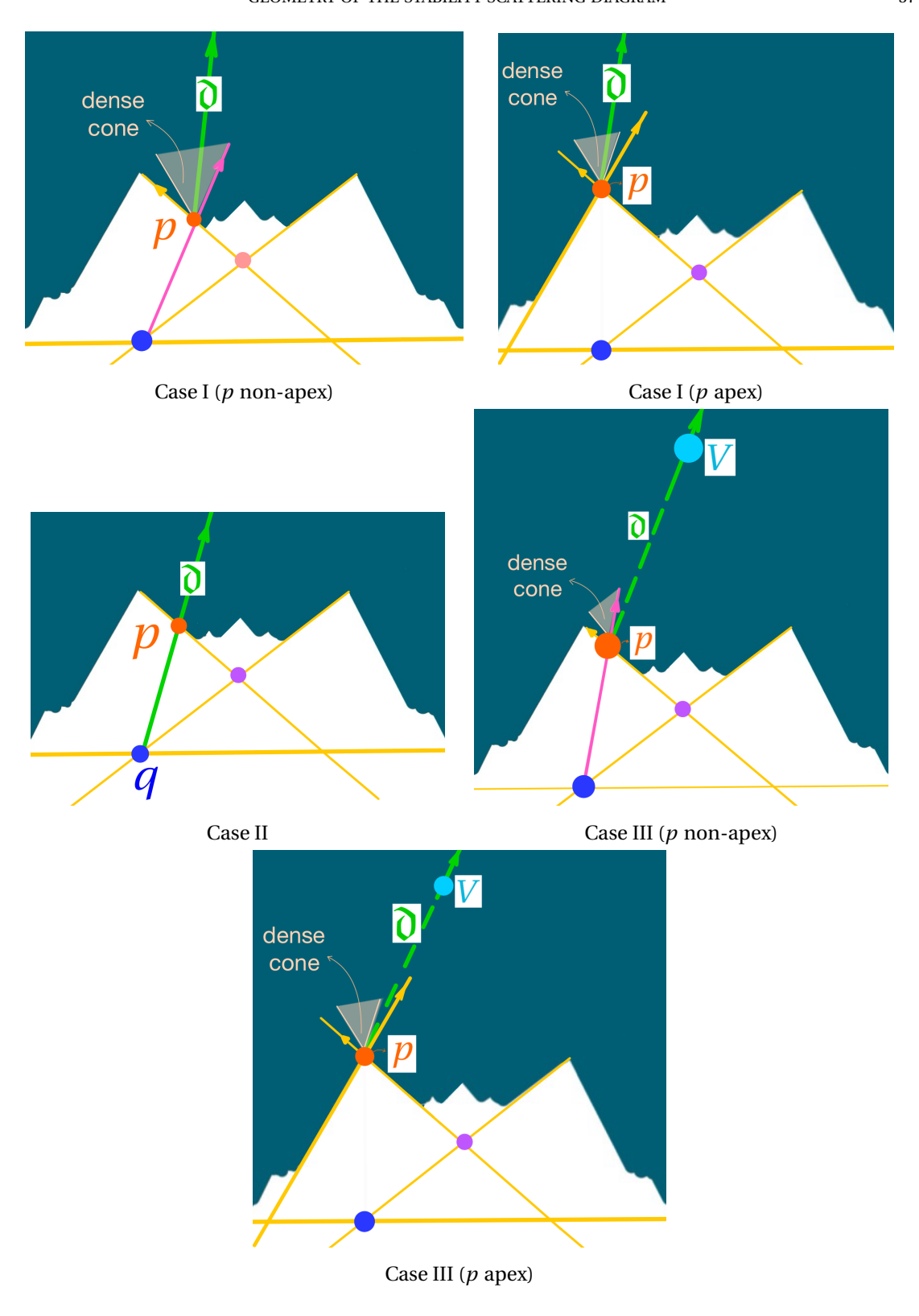


FIGURE 27. In Case I (p non-apex) or Case I (p apex), the first generating point of $\mathfrak d$ is p. In Case II, the first generating point of $\mathfrak d$ the base point q, and in Case III (p non-apex) or Case III (p apex), the first generating point of $\mathfrak d$ is a point V in the unbounded region.

Example 5.6. We give some explicit examples for the cases in the proof of Corollary 5.5 and Figure 27.

For Case I (p non-apex), we may take $\gamma = (5, -30, 10)$

For Case I (p apex), we may take $\gamma = (2, -7, 11/2)$. Note that the right boundary of the dense cone at p = (-1/2, 1) is given by 3y - 7x = 13/2. Hence, L_{γ} is contained in the dense cone.

For Case II, we may take $\gamma = (5, -20, 10)$.

For Case III (p non-apex), we may take $\gamma = (5, -12, 10)$.

For Case III (p apex), we may take $\gamma = (4, -9, 17/2)$. Again since the right boundary of the dense cone at p = (-1/2, 1) is given by 3y - 7x = 13/2, L_{γ} is not contained in the dense cone.

Remark 5.7. Note that if, in Corollary 5.5, the first generating point lies in $R_{\rm unbdd}$, it is still possible for a moduli space $\mathcal{M}^{\sigma}_{m\gamma}$ to be non-empty before the first generating point. This is because it is possible that the moduli space has zero Euler characteristic in intersection cohomology but nevertheless be non-empty. The analysis of the scattering at points of roofs of diamonds is purely numerical.

Conversely, once σ is past the first generating point, then $\mathcal{M}_{m\gamma}^{\sigma}$ is necessarily non-empty for some m.

6. An application: First wall-crossing for the moduli spaces of one-dimensional rank-zero objects

In this section, we will show how the scattering diagram allows us to easily determine the location of first (actual) walls for one-dimensional rank 0 objects. Recall the K-theory lattice Γ as in (1.1), which is identified via the Chern character with a sublattice of $\mathbb{Z} \times \mathbb{Z} \times \mathbb{Z}/2$ as in (1.3). In particular, the Chern characters of one-dimensional rank 0 objects are of the form (0, u, v) with either u even and v an integer, or u is odd and v is of the form (2k+1)/2. We will focus on primitive Chern characters. The reason for this is that we eventually want to get a correspondence between the rational vertical rays and the structure sheaves of schemes which are unions of $C \cup Z$ where C is a plane curve and Z is a finite length scheme, with C and Z having as small a degree as possible. We call an object with a primitive Chern character a *primitive object*.

Lemma 6.1 (Diamonds/one-dimensional rank 0 objects correspondence). The one-dimensional rank-zero objects of $D^b(\mathbb{P}^2)$ correspond to vertical lines. In particular, there is a one-to-one correspondence between (outer or degenerate diamonds) diamonds and primitive Chern characters of one-dimensional rank-zero objects.

Proof. The first sentence is evident as a one-dimensional rank-zero object with Chern character (0, u, v), for $u \neq 0$, corresponds to the line x = -v/u. For the second statement, by Theorem 4.16, the line x = -v/u intersects C_{roofs} at one point. If this point is the apex of an outer diamond, we associate this rank-zero object with this outer diamond. Otherwise the intersection is a degenerate diamond in the sense of Definition 3.12. This gives the desired correspondence.

Remark 6.2. It is worth noting that rank 0 objects play a special role here. For example, at a vertex $V_{\mathcal{E}}$ for \mathcal{E} an exceptional bundle, one may check that for any fixed $r \in \mathbb{Z}^+$, there are infinitely many rays with endpoint $V_{\mathcal{E}}$ in $\mathfrak{D}_{\text{dense}}$ corresponding to rank r objects.

Definition 6.3 (Discrete and dense rational number/line). We call a rational number q, a discrete rational number, if x = q contains the vertical diagonal of an outer diamond. If x = q contains a degenerate diamond, then we call q a dense rational number. Alternatively, we call x = q a dense rational line.

First, we need some lemmas, beginning with:

Lemma 6.4 (A necessary condition for being generators of an outer diamond). Let \mathfrak{d}_1 and \mathfrak{d}_2 be respectively the left and right generators of an outer diamond \Diamond with respective primitive Chern characters (r_1, d_1, e_1) and (r_2, d_2, e_2) with $r_1, r_2 > 0$. Then

(6.1)
$$D = \frac{2}{3}(r_1r_2 - d_1d_2 + r_1e_2 + r_2e_1),$$

where $D = r_2 d_1 - r_1 d_2 > 0$ is the determinant at $\mathfrak{d}_1 \cap \mathfrak{d}_2$.

Proof. First note that indeed D is positive: the direction vectors for \mathfrak{d}_2 and \mathfrak{d}_1 are $(r_2, -d_2)$ and $(-r_1, d_1)$ respectively, and these form an oriented basis, as is visible in Figure 28. Let Δ_w be the triangle whose incoming vertex is the base of \Diamond , corresponding to an strong exceptional triple $(\mathcal{E}_0, \mathcal{E}_1, \mathcal{E}_2)$. Then recall from Remark 2.8 and Figure 7 that \mathfrak{d}_1 corresponds to \mathcal{E}_0 and \mathfrak{d}_2 corresponds to $\mathcal{E}_2(-3)[1] = \mathcal{S}_2$. Let χ_1, χ_2 be the Euler characteristics of \mathcal{E}_0 , $\mathcal{E}_2(-3)$ respectively. Then by (2.8), $0 = \chi(\mathcal{E}_0, \mathcal{E}_2) = \chi(\mathcal{E}_0, \mathcal{E}_2(-3)[1]) = -\chi(\mathcal{E}_0, \mathcal{E}_2(-3))$, so the pairing (1.4) must vanish:

$$0 = ((r_1, d_1, \chi_1), (r_2, d_2, \chi_2)) = -3d_1r_2 - r_1r_2 - d_1d_2 + r_1\chi_2 + \chi_1r_2$$

$$= -3d_1r_2 - r_1r_2 - d_1d_2 + r_1(e_2 + r_2 + \frac{3}{2}d_2) + r_2(e_1 + r_1 + \frac{3}{2}d_1)$$

$$= -\frac{3}{2}d_1r_2 - d_1d_2 + r_1e_2 + \frac{3}{2}r_1d_2 + r_2e_1 + r_1r_2.$$

Multiplying this by $\frac{2}{3}$ gives the result.

Lemma 6.5 (Characterization of the Chern character of the vertical diagonals of outer/dense diamonds). Let $\gamma = (0, u, v)$ or (0, -u, -v), for $u \in \mathbb{Z}^{>0}$, $v \in \frac{\mathbb{Z}}{2}$, be primitive in Γ . Then L_{γ} contains the vertical diagonal of an outer/dense diamond if and only if

(6.2)
$$\begin{cases} r = u, \\ d = v + \frac{3}{2}u, \\ e = \frac{4+5u^2+4v^2+12uv}{8u} = \frac{1+v^2}{2u} + \frac{5}{8}u + \frac{3}{2}v, \end{cases}$$

where $(r, d, e) \in \Gamma$ is the Chern character of the exceptional bundle \mathcal{E} such that $V_{\mathcal{E}}$ is the base of the diamond.

Proof. First suppose (6.2) holds. Then as L_{γ} is the line $x = \frac{v}{u}$, and $\frac{v}{u} = \frac{d}{r} - \frac{3}{2}$ by (6.2), we see L_{γ} passes through $V_{\mathcal{E}}$ by (2.6) and hence contains the vertical diagonal of the diamond based at $V_{\mathcal{E}}$.

For the opposite direction, first, we show that r=u. Since $\chi=v+\frac{3}{2}u$, we can write $\gamma=(0,u,\chi-\frac{3}{2}u)$. Therefore, we obtain

$$\frac{d}{r} = \frac{\chi}{u}.$$

Now, the primitivity of $\gamma = (0, u, v)$ in Γ implies the primitivity of $(0, u, \chi)$, which in turn implies that $\gcd(u, \chi) = 1$. On the other hand, $\gcd(d, r) = 1$ by Lemma 2.4,(6). Hence, from (6.3), we must have r = u and $d = \chi$. Also, the latter immediately implies $d = v + \frac{3}{2}u$.

Finally, for $e = \frac{4+5u^2+4v^2+12uv}{8u}$, it is enough to use Lemma 2.4(6) and substitute d, r:

$$e = \frac{d^2 - r^2 + 1}{2r} = \frac{v^2 + 3vu + \frac{9u^2}{4} - u^2 + 1}{2u} = \frac{4v^2 + 12uv + 5u^2 + 4}{8u}.$$

Next, we have a useful statement on the length of the vertical diagonals of diamonds.

Lemma 6.6 (Length of the vertical diagonal). The vertical diagonal corresponding to the primitive Chern character (0, u, v) of a diamond based at a vertex $V_0 = (x_0, y_0)$ dual to a ray (in the sense of Definition 2.10) \mathfrak{d} of Chern character (r, d, e) has length $\frac{1}{r^2}$, which by Lemma 2.16 and and (6.2), is the same as $\frac{1}{D^2}$ and $\frac{1}{u^2}$, where D is the determinant at the base, and u is the first (primitive) Chern character associated to the vertical diagonal.

Proof. Let V'=(x',y') be the intersection of $x=x_0$ and \mathfrak{d} . Hence, we have $x'=x_0$ and $y'=\frac{e-d\,x_0}{r}=\frac{e-d\,\frac{y}{u}}{r}$. Then, using (2.6) and (6.2), we get

$$y'-y_0=2\frac{e}{r}-\frac{d}{r}\frac{v}{u}-\frac{3}{2}\frac{d}{r}+1=2\frac{e}{r}-\left(\frac{d}{r}\right)^2+1=\frac{1}{r^2}.$$

The last equality comes from Lemma 2.4(6). Therefore, we have the result. See Figure 28.

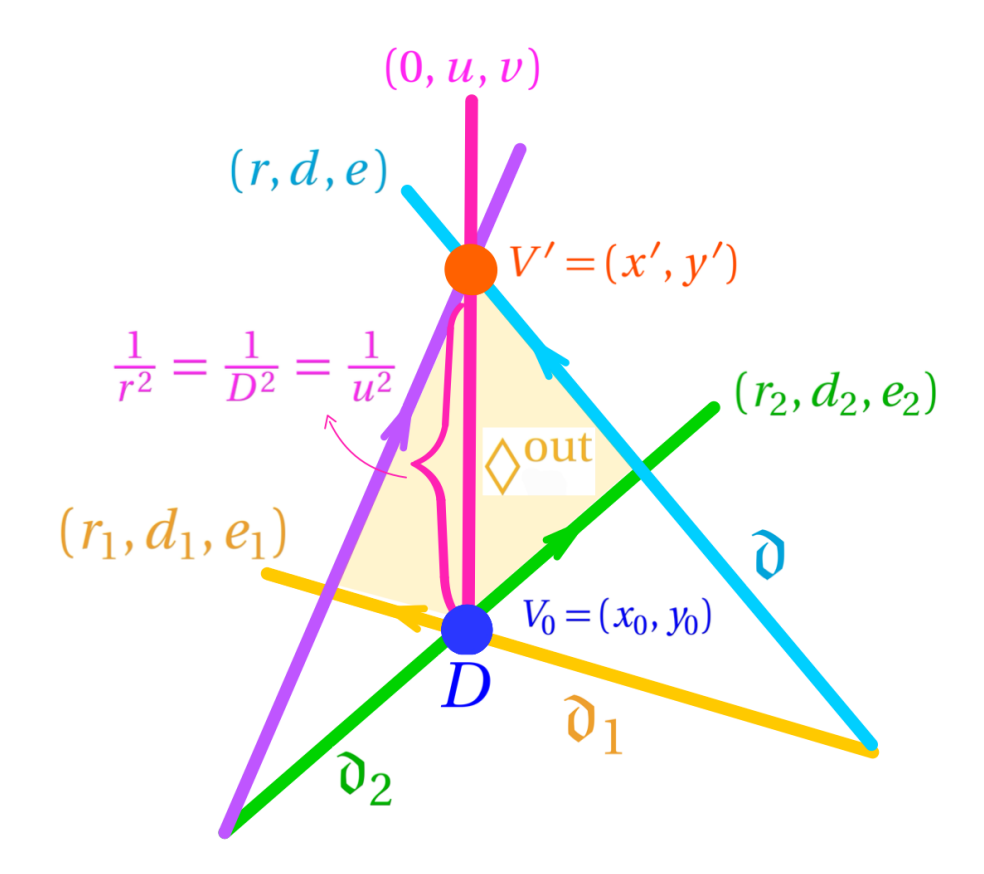


FIGURE 28. The length of the vertical diagonal of the diamond \lozenge^{out} based at the vertex V_0 dual to the ray \mathfrak{d} of rank r is $1/r^2 = 1/D^2 = 1/u^2$, where D is the determinant at the base, and u is the first (primitive) Chern character associated to the vertical diagonal.

Now, we can prove one of the main results of this section. First, we need some definitions.

Definition 6.7 (Equivalent objects). We call objects \mathcal{E} , \mathcal{F} in $D^b(\mathbb{P}^2)$ with the same Chern character *equivalent objects* and will be denoted by $\mathcal{E} \sim \mathcal{F}$.

Definition 6.8 (Dual objects). Let \mathcal{E} be an object in the derived category of Chern character (r,d,e). The object $\mathcal{E}^{\vee} = \mathbf{R}\operatorname{Hom}(\mathcal{E},\mathcal{O}_{\mathbb{P}^2})$ with Chern character (r,-d,e) is called the *dual object* of \mathcal{E} .

Definition 6.9. We use the notation $\mathcal{O}_{C_d \cup n}$ for the equivalence class of objects containing the structure sheaf of a degree d curve in \mathbb{P}^2 union n points. We use the convention that $\mathcal{O}_{C_d \cup n}$ does not exist if n < 0.

Lemma 6.10. The Chern character of $\mathcal{O}_{C_d \cup n}$ is $(0, d, n - d^2/2)$.

Proof. A straightforward argument (either using a corresponding short exact sequence, or using the definition of arithmetic genus) implies the claim.

Theorem 6.11 (First actual wall for moduli spaces of discrete one-dimensional rank-zero objects). Let $\gamma = (0, u, v)$ or (0, -u, -v), for $u \in \mathbb{Z}^{>0}$, $v \in \frac{\mathbb{Z}}{2}$, be primitive, such that L_{γ} contains the vertical diagonal of an outer/dense diamond. Then the associated primitive object to γ is $\mathcal{O}_{C_u \cup (u^2/2+v)}$ or $\mathcal{O}_{C_u \cup (u^2/2-v)}^{\vee}$ in the two cases for γ . Also, the first actual wall for the moduli space of one-dimensional rank-zero objects in $D^b(\mathbb{P}^2)$ of Chern character (at least a multiple of)

 γ is given by the vertex $(\frac{v}{u}, \frac{5}{8} - \frac{1+v^2}{2u^2})$.

Proof. By Lemma 6.10, the Chern character of $\mathcal{O}_{C_u \cup (u^2/2+v)}$ is (0, u, v). Similarly, the Chern character of $\mathcal{O}_{C_u \cup (u^2/2-v)}$ is (0, u, -v), and hence the Chern character of the dual object is (0, -u, -v).

From (2.6) and (6.2), if the base of the diamond is $V_{\mathcal{E}}$ for \mathcal{E} an exceptional bundle with Chern character (r, d, e), the coordinates (x_0, y_0) of the first generating point are given by

$$\begin{cases} x_0 = \frac{d}{r} - \frac{3}{2} = \frac{v}{u}, \\ y_0 = \frac{3d}{2r} - \frac{e}{r} - 1 = \frac{3}{2}(\frac{3}{2} + \frac{v}{u}) - 1 - \frac{3}{2}\frac{v}{u} - \frac{5}{8} - \frac{1}{2u^2} - \frac{v^2}{2u^2} = \frac{5}{8} - \frac{1+v^2}{2u^2}, \end{cases}$$

as claimed. The non-emptiness of the moduli space comes from Lemma 5.2. \Box

We have the following corollaries for special cases.

Corollary 6.12 (Rank-zero moduli spaces generated at the initial diamonds). *Let i be an odd integer.*

- (1) The upward vertical ray contained in the line x = i/2 with endpoint $(\frac{i}{2}, \frac{1-i^2}{8})$, corresponds to an initial diamond and the primitive object $\mathcal{O}_{L \cup \frac{i+1}{2}} \sim \mathcal{O}_L(\frac{i+1}{2})$, where L is a line in the plane.
- (2) For $\mathcal{O}_{L\cup\frac{1+i}{2}}\sim\mathcal{O}_L((i+1)/2)$, the left generator is $\mathcal{O}(\frac{i+1}{2})$ and the right generator is $\mathcal{O}(\frac{i-1}{2})[1]$.

Proof. The generators of the initial diamonds are given by the lines corresponding to $\mathcal{O}(\frac{i-1}{2})$ and $\mathcal{O}(\frac{i+1}{2})$:

$$\begin{cases} y + \frac{i-1}{2}x = \frac{(\frac{i-1}{2})^2}{2}, \\ y + \frac{i+1}{2}x = \frac{(\frac{i+1}{2})^2}{2}, \end{cases}$$

which gives $x = \frac{i}{2}$ and $y = \frac{-i^2 + 1}{8}$.

Twisting $\mathcal{O}(-1) \to \mathcal{O} \to \mathcal{O}_L$ by $\frac{i+1}{2}$, we obtain the triangle:

$$\mathcal{O}\!\left(\frac{i-1}{2}\right)\!\rightarrow\!\mathcal{O}\!\left(\frac{i+1}{2}\right)\!\rightarrow\!\mathcal{O}_L\!\left(\frac{i+1}{2}\right),$$

which concludes the statement about the primitive Chern character $(0,1,\frac{i}{2})$ for $\mathcal{O}_L(\frac{i+1}{2})$, and the statement about the left and right generators.

Corollary 6.13 (Rank-zero moduli spaces generated at the center of super-diamonds). *Let* $i \in \mathbb{Z}^{\geq 0}$.

- (1) Consider the diamond \Diamond_v based at $v=(i,\frac{1-i^2}{2})$. The upward vertical ray contained in the line x=i generated at v has corresponding primitive object $\mathcal{O}_{C_2\cup 2(1+i)}\sim \mathcal{O}_{C_2}(i+1)$ or $\mathcal{O}_{C_2\cup 2(1-i)}^{\vee}$. The latter only makes sense when i=0,1.
- (2) Consider the diamond \Diamond_v based at $v=(-i,\frac{1-i^2}{2})$. The upward vertical ray contained in the line x=-i generated at v has corresponding primitive object $\mathcal{O}_{C_2\cup 2(1+i)}^\vee$ or $\mathcal{O}_{C_2\cup 2(1-i)}$. Again, the latter only makes sense when i=0,1.
- (3) For $\mathcal{O}_{C_2\cup 2(1+i)}\sim \mathcal{O}_{C_2}(i+1)$, the left generator is $\mathcal{O}(i+1)$ and the right generator is $\mathcal{O}(i-1)[1]$. For $\mathcal{O}_{C_2\cup 2(1-i)}^{\vee}$, the left generator is $\mathcal{O}(-i+1)[-1]$ and the right generator is $\mathcal{O}(-i-1)$.

Proof. We prove (1); then, (2) is similar.

The lower edges of the central diamonds in the super-diamonds are given by the lines corresponding to O(i-1) and O(i+1):

$$\begin{cases} y + (i-1)x = \frac{(i-1)^2}{2}, \\ y + (i+1)x = \frac{(i+1)^2}{2}, \end{cases}$$

which gives x = i and $y = \frac{1-i^2}{2}$.

For (3) and the second part of (1) and (2), we note that from

$$\mathcal{I}_{C_2}(i+1) \rightarrow \mathcal{O}(i+1) \rightarrow \mathcal{O}_{C_2}(i+1),$$

we have the exact triangle

$$\mathcal{O}(i+1) \to \mathcal{O}_{C_2}(i+1) \to \mathcal{O}(i-1)[1].$$

Dualizing this, we get

$$\mathcal{O}(-i-1) \leftarrow \mathcal{O}_{C_2}^{\vee}(-i-1) \leftarrow \mathcal{O}(-i+1)[-1].$$

Hence, (1) and (2) and the statement about the left and right generators in (3).

Lemma 6.14 (Ranks of the lower sides of outer diamonds are coprime). Let (r', d', e') and (r'', d'', e'') be the primitive Chern characters corresponding the rays \mathfrak{d}' and \mathfrak{d}'' that generate a diamond \lozenge out with r', r'' > 0. Then we have

(6.4)
$$\gcd(r', r'') = 1.$$

Proof. From Lemma 2.16 and Figure 7, we have r' = D' and r'' = D'', where $D^{(i)}$ for i = 1, 2 is the determinant at the vertex dual to the ray corresponding to the object with Chern character $(r^{(i)}, d^{(i)}, e^{(i)})$. But D', D'' are part of a Markov triple, and by [45, Theorem B] or [16], we know that the elements of any Markov triple are pairwise coprime. Hence, r' = D' and r'' = D'' are coprime, as claimed.

Starting from two generating rays of an arbitrary outer diamond, we can determine the one-dimensional rank-zero object.

Theorem 6.15. Let $\gamma' = (r', d', e')$ and $\gamma'' = (r'', d'', e'')$ be the Chern characters of the exceptional bundles corresponding to the rays \mathfrak{d}' and \mathfrak{d}'' that generate a diamond \lozenge^{out} , with r', r'' > 0. If D = r''d' - r'd'' > 0 is the determinant at $\mathfrak{d}' \cap \mathfrak{d}''$, then the vertical diagonal of \lozenge out $corresponds \ to \ \mathcal{O}_{C_D \cup \left(\frac{D^2}{2} + r''e' - r'e''\right)} \ or \ \mathcal{O}^{\vee}_{C_D \cup \left(\frac{D^2}{2} - r''e' + r'e''\right)}.$

Proof. From Lemma 6.14, we have gcd(r', r'') = 1. We calculate

$$r''\gamma' - r'\gamma'' = (0, r''d' - r'd'', r''e' - r'e'') = (0, D, r''e' - r'e''),$$

which is the Chern character of $\mathcal{O}_{C_D \cup \left(\frac{D^2}{2} + r''e' - r'e''\right)}$ by Lemma 6.10. Similarly, if we consider $r'\gamma'' - r''\gamma'$ instead, we end up with (0, -D, -r''e' + r'e''), which is the Chern character for $\mathcal{O}_{C_D \cup \left(\frac{D^2}{2} - r''e' + r'e''\right)}^{\vee}$.

This implies the result in both cas

Theorem 6.16 (Discrete rational numbers determine outer diamonds). The reduced rational numbers associated to discrete vertical rays (or the discrete reduced rational numbers) determine the Chern characters of exceptional bundles associated to the generating rays of the corresponding outer diamond. More precisely, let (0, u, v) be the primitive Chern character corresponding to a vertical line x = q for q a discrete rational number, $q \notin \mathbb{Z}/2$. Then the Chern characters (r', d', e') and (r'', d'', e'') of the exceptional bundles associated to the generators of the corresponding diamond are given by

(6.5)
$$\begin{cases} r' = D', \\ r'' = D'', \\ d' = (\frac{v}{u} + \frac{3}{2})D' - \frac{D''}{u}, \\ d'' = \frac{D'}{u} + (\frac{v}{u} - \frac{3}{2})D'', \\ e' = D'(\frac{5u^2 + 12uv + 4v^2 - 4}{8u^2}) - D''\frac{v}{u^2}, \\ e'' = D''(\frac{5u^2 - 12uv + 4v^2 - 4}{8u^2}) + D'\frac{v}{u^2}, \end{cases}$$

where D is the determinant at the base of the diamond, and (D', D'', D) is the Markov triple of determinants of vertices of the base triangle of the diamond, ordered $D > D'' \ge D'$, (see Figure *29*).

П

Proof. Let (0, u, v) be the associated Chern character of the vertical ray, which has the first generating point at $(\frac{v}{u}, \frac{5}{8} - \frac{1+v^2}{2u^2})$ (see Theorem 6.11). Also, if $V_{\mathcal{E}}$ is the base of the diamond, let (r, d, e) be the Chern character of \mathcal{E} . Via Figure 7, we see that $L_{\mathcal{E}}$ is the right roof of the diamond, and $L_{\mathcal{E}(-3)}$ is the left roof of the diamond. Using (6.2), one sees the Chern character of $\mathcal{E}(-3)$ is (r, d-3u, e-3v).

Let (D', D'', D) be the Markov triple corresponding to the base triangle Δ of \Diamond^{out} , ordered so that $D > D'' \ge D'$. In particular, if Δ is not an initial triangle, then by Proposition 2.18, D is the determinant of the incoming vertex of Δ , the hybrid vertex of Δ has determinant D'', the outgoing vertex has determinant D', and D'' > D'.

If, on the other hand, Δ is an initial triangle, obviously D' = D'' = 1 and D = 2 is still the determinant of the incoming vertex.

Without loss of generality, we assume that the vertex with determinant D'' is to the right of $V_{\mathcal{E}}$, and the vertex with determinant D' is to the left of it, as depicted in Figure 29. Let $(r^{(i)}, d^{(i)}, e^{(i)})$ be the primitive Chern characters of the generators of the diamond with r', r'' > 0.

Recall from Lemma 2.16 that the determinant of a vertex can be computed in any triangle containing it. Hence, in Figure 29, we can calculate D',D'' as follows. First, we have D'=rd''-dr''+3rr'' and D''=r'd-rd'. From Lemma 2.16, we have $D^{(i)}=r^{(i)}$ for $0 \le i \le 2$. Hence, we obtain

(6.6)
$$d'' = \frac{D'}{r} + \frac{d}{r}D'' - 3D'',$$

(6.7)
$$d' = \frac{d}{r}D' - \frac{D''}{r}.$$

On the other hand, since for i=1,2, the rays corresponding to the objects with Chern characters $(r^{(i)},d^{(i)},e^{(i)})$ intersect at $V_0=(x_0,y_0)=(\frac{v}{u},\frac{5}{8}-\frac{1+v^2}{2u^2})$ from Theorem 6.11, and using (6.7) and (6.6), we have

(6.8)
$$e' = D' \left(\frac{5u^2 + 12uv + 4v^2 - 4}{8u^2} \right) - D'' \frac{v}{u^2},$$

(6.9)
$$e'' = D'' \left(\frac{5u^2 - 12uv + 4v^2 - 4}{8u^2} \right) + D' \frac{v}{u^2}.$$

Then, combining (6.7),(6.6),(6.8), (6.9) with Lemma 2.16 and (6.2), we obtain the result.

Remark 6.17. The Frobenius unicity conjecture [16] states that the Markov triple (D', D'', D) is determined by its largest element. Thus in Theorem 6.16, one expects that the only input needed is u and v as D = u.

We assume the notation in the proof of Theorem 6.16 and Figure 29, and obtain the following important corollary, which describes the left and right generators at the first generating point of discrete vertical rays.

Corollary 6.18 (Explicit left/right generators for discrete vertical rays). Let $\gamma = (0, u, v)$ be a primitive Chern character of a one-dimensional rank-zero object such that L_{γ} contains the vertical diagonal of a outer/dense diamond. Then the Chern character of the left and right generators at the first generating point for the moduli space of objects with Chern character

(0, u, v) are

$$\left(D', (\frac{v}{u} + \frac{3}{2})D' - \frac{D''}{u}, D' \left(\frac{5u^2 + 12uv + 4v^2 - 4}{8u^2}\right) - D'' \frac{v}{u^2}\right),$$

$$\left(D'', \frac{D'}{u} + (\frac{v}{u} - \frac{3}{2})D'', D'' \left(\frac{5u^2 - 12uv + 4v^2 - 4}{8u^2}\right) + D' \frac{v}{u^2}\right),$$

where D', D'' are as in the statement of Theorem 6.16.

Proof. This comes from (6.5) and Figure 29.

Theorem 6.19 (The first generating point for dense one-dimensional rank-zero moduli spaces (non-initial base triangle)). Let \lozenge^{out} be an outer diamond based at a non-initial triangle with base $V_{\mathcal{E}}$ for an exceptional bundle \mathcal{E} with Chern character (r,d,e), so that $L_{\mathcal{E}}$ contains the right roof of \lozenge^{out} . Let the primitive Chern character of the vertical diagonal of \lozenge^{out} be (0,u,v), where u=r and $v=d-\frac{3}{2}r$ as in (6.2). Also, we fix the notation for determinants as above. Then, the x-coordinates q of the degenerate diamonds contained in the right roof of \lozenge^{out} are in the range

(6.10)
$$\frac{v}{u} < q < \frac{v}{u} + \left(\frac{3}{2} - \frac{\sqrt{9r^2 - 4}}{2r}\right).$$

In particular, the first generating point for the Chern character $\gamma = (0, u', v')$ with q = v'/u' in this range is a degenerate diamond on the right roof of \Diamond ^{out} and the object with Chern character (r, d, e) corresponding to δ is the left generator at this point.

Proof. From Lemma 6.5, we have u = r. Also from Definition 2.5, we get $v = d - \frac{3}{2}r$.

Recall from Definition 3.1 that $r_{\infty}(D)^{-1} = \frac{3D - \sqrt{9D^2 - 4}}{2}$ is the slope of the right boundary of the dense diamond \lozenge based at a vertex of determinant D, with respect to the basis m_1, m_2 of Definition 3.1. For short-hand, we omit the D and write r_{∞}^{-1} . Also, recall that the left and the right lower sides of \lozenge correspond to objects of Chern characters (r', d', e') and (r'', d'', e''), respectively. See Figure 29. Without loss of generality, we consider the ray $\mathfrak d$ corresponding to the right roof of a diamond, the direction vector of the right boundary of the dense diamond is given by

$$r_{\infty}^{-1} \binom{-r'}{d'} + \binom{r''}{-d''} = \binom{-r_{\infty}^{-1}D' + D''}{r_{\infty}^{-1}(\frac{dD' - D''}{r}) - \frac{D'}{r} - (\frac{d}{r} - 3)D'')},$$

using (6.6), (6.7). Therefore, the ray is given by

$$\begin{split} \left(r_{\infty}^{-1}D' - D''\right)y + \left(r_{\infty}^{-1}\left(\frac{dD' - D''}{r}\right) - \frac{D'}{r} - \left(\frac{d}{r} - 3\right)D''\right)x \\ &= \left(r_{\infty}^{-1}D' - D''\right)\left(\frac{3d}{2r} - 1 - \frac{e}{r}\right) + \left(r_{\infty}^{-1}\left(\frac{dD' - D''}{r}\right) - \frac{D'}{r} - \left(\frac{d}{r} - 3\right)D''\right)\left(\frac{d}{r} - \frac{3}{2}\right). \end{split}$$

Intersecting this with the equation of \mathfrak{d} , ry + dx = e, applying Lemma 2.4(6), and then using u = r, $v = d - \frac{3}{2}r$, and Lemma 2.4(6), we get the following x-coordinate

$$x = \frac{-r_{\infty}^{-1}(vD'' + D') - vD' + (1 + 3uv)D''}{-r_{\infty}^{-1}uD'' - uD' + 3u^2D''},$$

which determines all the dense rational rays on \mathfrak{d} , i.e., any rational vertical ray x = q, with

$$\frac{v}{u} < q < \frac{-r_{\infty}^{-1}(vD'' + D') - vD' + (1 + 3uv)D''}{-r_{\infty}^{-1}uD'' - uD' + 3u^2D''}$$

$$= \frac{v}{u} + \frac{-r_{\infty}(D)^{-1}D' + D''}{D(-r_{\infty}(D)^{-1}D'' + 3DD'' - D')}$$

has its first generating point on the right roof of the dense diamond \Diamond .

Claim. We have
$$\frac{-r_{\infty}(D)^{-1}D'+D''}{D\left(-r_{\infty}(D)^{-1}D''+3DD''-D'\right)} = \frac{3}{2} - \frac{\sqrt{9r^2-4}}{2r}.$$

Proof. We use the notation $R:=r_{\infty}(D)^{-1}=\frac{3D-\sqrt{9D^2-4}}{2}$. Then, we have

$$R^{2} = \left(\frac{3D - \sqrt{9D^{2} - 4}}{2}\right)^{2} = \frac{9D^{2} - 2 - 3D\sqrt{9D^{2} - 4}}{2} = 3DR - 1.$$

From this, it follows that

$$-R^2D'' + 3RDD'' - RD' = -RD' + D''.$$

However, this is equivalent to

$$\frac{R}{D} = \frac{-RD' + D''}{D(-RD'' + 3DD'' - D')}$$

In turn, this is equivalent to

$$\frac{-r_{\infty}(D)^{-1}D'+D''}{D(-r_{\infty}(D)^{-1}D''+3DD''-D')} = \frac{3}{2} - \frac{\sqrt{9r^2-4}}{2r},$$

which is the claim.

The last statement about the left generator is also a straightforward implication of this. The fact that this degenerate diamond is a first generating point comes from Lemma 5.2.

By a direct calculation, we can obtain the following results for diamonds at the center of super-diamonds and the initial diamonds, respectively (see Figure 30):

Theorem 6.20 (The first generating point for dense one-dimensional rank-zero moduli spaces (initial base triangle)). Let \lozenge out be an outer diamond based at an initial triangle with base $(m, \frac{1-m^2}{2})$, the intersection point of $L_{\mathcal{O}(m+1)}$ and $L_{\mathcal{O}(m-1)}$. Then, the x-coordinates q of the degenerate diamonds contained in the right roof of \lozenge are in the following range

(6.11)
$$m < q < m + \frac{3 - 2\sqrt{2}}{2}.$$

Theorem 6.21 (The first generating point for dense one-dimensional rank-zero moduli spaces (initial diamonds)). Let \lozenge initial diamond with base $(m+\frac{1}{2},\frac{-m-m^2}{2})$, the intersection point of $L_{\mathcal{O}(m)}$ and $L_{\mathcal{O}(m+1)}$. Then, the x-coordinates q of the degenerate diamonds contained in the right roof of \lozenge init are in the following range

(6.12)
$$m + \frac{1}{2} < q < m + \frac{1}{2} + \frac{3 - \sqrt{5}}{2}.$$

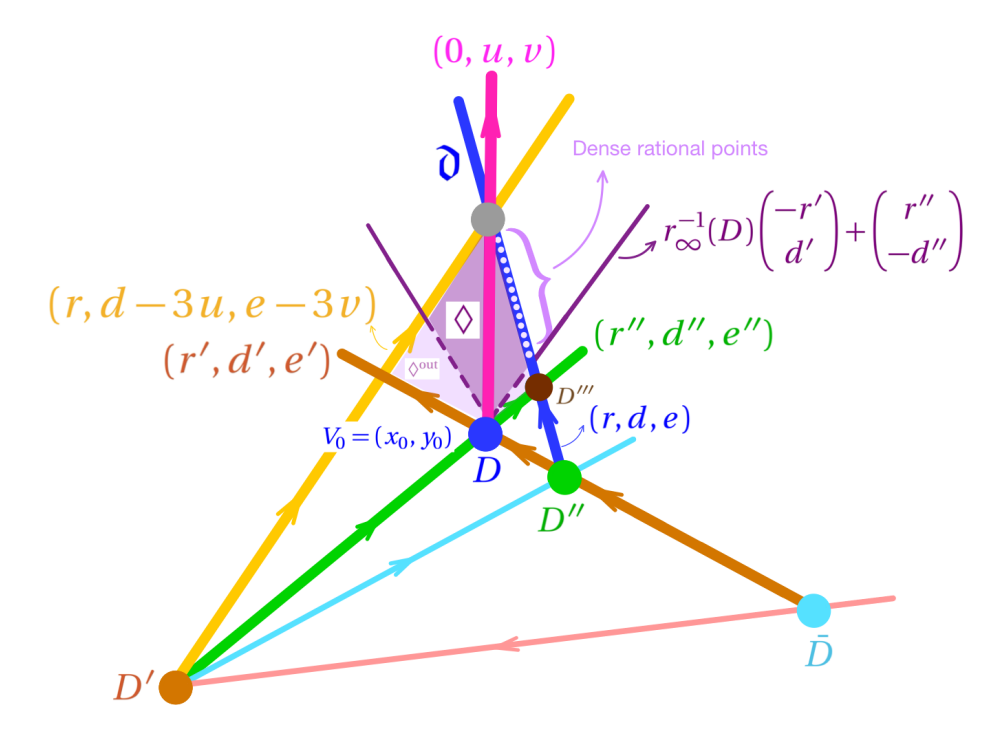
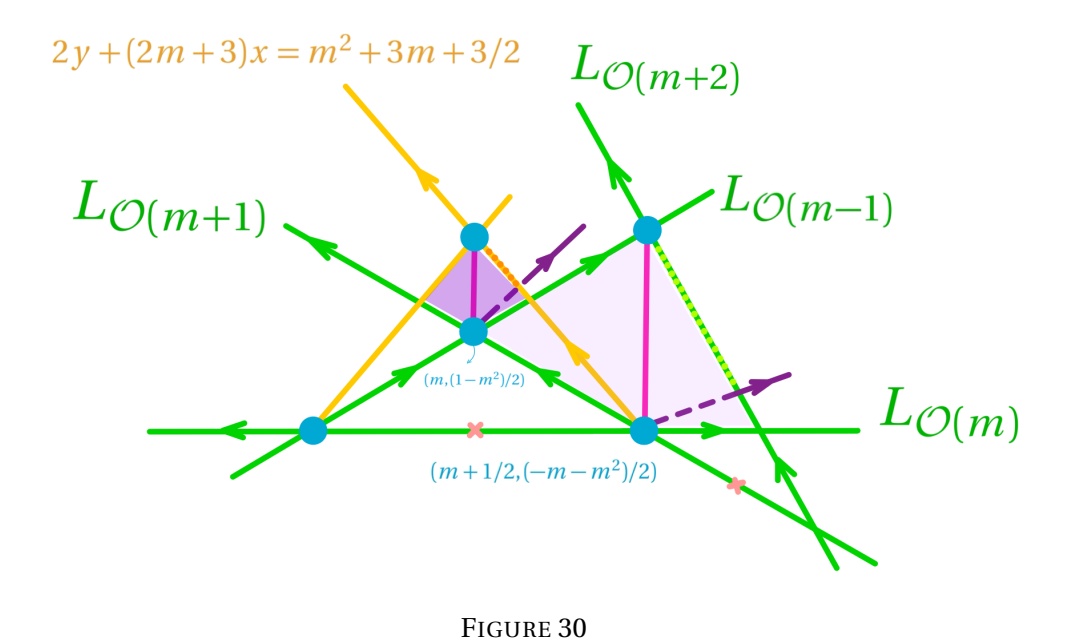


FIGURE 29. The Chern character of the objects corresponding to lower rays can be determined in terms of $u, v, D^{(i)}$ (see (6.5)). Moreover, we can determining all the rational dense points on a given ray \mathfrak{d} (Theorem 6.19).



Example 6.22. Considering the rays generated by $L_{\mathcal{O}(1)}$ and $L_{\mathcal{O}(2)}$ at the vertex (3/2,-1), we can show that vertical diagonals of the outer diamonds in the super-diamond, \lozenge^{\sup} along the line corresponding to \mathcal{O} , are explicitly given by $x=\frac{3}{2}-\frac{F_{2k+1}}{F_{2k+3}}$. The primitive Chern character for the vertical diagonal $x=\frac{3}{2}-\frac{F_{2k+1}}{F_{2k+3}}$, is $(0,F_{2k+3},\frac{3}{2}F_{2k+3}-F_{2k+1})$. One can show that the primitive object for this is $\mathcal{O}_{C_{F_{2k+3}}\cup\#}(m)$, a one-dimensional rank-zero object, where $C_{F_{2k+3}}\cup\#$ is a curve of degree F_{2k+3} , together with $\#=\frac{F_{2k+3}(F_{2k+3}+3)}{2}-F_{2k+1}$ number of points.

Corollary 6.23. Let \mathcal{E} be an exceptional bundle of rank r and first Chern class d, u = r, $v = d - \frac{3}{2}r$. Let \Diamond be the (dense) diamond based at $V_{\mathcal{E}}$. Then the image of the union of the left and right roofs of \Diamond under the projection to the x-axis is

$$\left[\frac{u}{v} - \left(\frac{3}{2} - \frac{\sqrt{9r^2 - 4}}{2r}\right), \frac{u}{v} + \left(\frac{3}{2} - \frac{\sqrt{9r^2 - 4}}{2r}\right)\right].$$

Proof. The right half is an immediate corollary of Theorem 6.19, and the left half is obtained by symmetry.

7. AN APPLICATION: CONNECTION TO [29] AND THE LE POTIER CURVE

[29] considers the geography of coherent sheaves on \mathbb{P}^2 by using what the author calls the $\{1,\frac{ch_1}{ch_0},\frac{ch_2}{ch_0}\}$ -plane. Omitting the 1, we identify this plane with \mathbb{R}^2 , with coordinates

$$X = \frac{\operatorname{ch}_1}{\operatorname{ch}_0}, \quad Y = \frac{\operatorname{ch}_2}{\operatorname{ch}_0}.$$

Any coherent sheaf $\mathcal E$ of non-zero rank gives a point

$$V_{\mathcal{E}}^{\text{Li}} := (\cosh_1(\mathcal{E})/\cosh_0(\mathcal{E}), \cosh_2(\mathcal{E})/\cosh_0(\mathcal{E}))$$

in this plane.

Via (2.6), there is a clear relationship between the plane $M_{\mathbb{R}}$ (with coordinates x, y) and the $\{1, \frac{\operatorname{ch}_1}{\operatorname{ch}_0}, \frac{\operatorname{ch}_2}{\operatorname{ch}_0}\}$ -plane. We define an affine linear transformation

$$\Upsilon: \mathbb{R}^2 \to M_{\mathbb{R}},$$

$$(X, Y) \mapsto (X - 3/2, 3X/2 - Y - 1).$$

Using $\chi = ch_2 + \frac{3}{2}ch_1 + ch_0$ and (2.6), we see that

$$\Upsilon(V_{\mathcal{E}}^{\mathrm{Li}}) = V_{\mathcal{E}}.$$

The inverse map is

$$\Upsilon^{-1}(x, y) = (x + 3/2, -y + 3x/2 + 5/4).$$

[29] introduces the parabolas

$$\overline{\Delta}_a = \left\{ (X, Y) \left| \frac{1}{2} X^2 - Y = a \right. \right\}.$$

Note that if $V_{\mathcal{E}}^{\text{Li}} \in \overline{\Delta}_0$, then the Bogomolov-Gieseker inequality is an equality for \mathcal{E} . If \mathcal{E} is stable, then $V_{\mathcal{E}}^{\text{Li}}$ lies on or below $\overline{\Delta}_0$.

One calculates that

$$\Upsilon(\overline{\Delta}_a) = \partial_b := \{(x, y) \in M_{\mathbb{R}} \mid y = -x^2/2 + b\}$$

with b = a + 1/8.

In particular, $\Upsilon(\overline{\Delta}_0)$ is the upward translation of the boundary of the closure of U by 1/8. For any $\mathcal E$ stable of non-zero rank, the Bogomolov-Gieseker inequality now implies that $V_{\mathcal E}$ lies on or above $\partial_{1/8}$. Further, this curve contains $V_{\mathcal O(n)}=(n-3/2,-(n-1)(n-2)/2)$ for all $n\in\mathbb Z$, being the hybrid vertices of the initial triangles. On the other hand, $V_{\mathcal E}$ for $\mathcal E$ an exceptional bundle of rank greater than one lies above the curve $\partial_{1/8}$, as follows easily from Lemma 2.4,(6). In particular, $\partial_{1/8}$ lies below all diamonds and contains the bases of the initial diamonds, and hence $\partial_{1/8}$ provides the best lower bound for the outer diamonds among all parabolas ∂_b .

Similarly, translating the boundary of the closure of U by 9/8 to obtain $\partial_{9/8} = \Upsilon(\overline{\Delta}_1)$, we obtain a parabola which meets each initial diamond in its apex. Further, the apex of every other diamond lies strictly below $\partial_{9/8}$. Indeed, if the base of a diamond \Diamond_v is $V_{\mathcal{E}}$ for some exceptional bundle \mathcal{E} , then the apex has coordinates $(d/r-3/2,(3d-\chi)/r+1/r^2)$ by Lemma 6.6. Plugging this into the inequality $y \le -x^2/2 + 9/8$, writing χ in terms of the second Chern class e and simplifying, we obtain the inequality $-d^2 + 2er + 2r^2 - 2 \ge 0$. Using Lemma 2.4(6), this reduces to $r^2 \ge 1$. Thus the inequality always holds and is an equality only when $V_{\mathcal{E}}$ is the base of an initial diamond. See Figure 31.

[29, Def. 1.6] defines the Le Potier curve in the $\{1, \frac{ch_1}{ch_0}, \frac{ch_2}{ch_0}\}$ -plane, which we paraphrase as follows. For an exceptional bundle \mathcal{E} , set

$$V_{\mathcal{E}}^{+} := V_{\mathcal{E}}^{\text{Li}} - (0, 1/\cosh_0(\mathcal{E})^2).$$

If $(\mathcal{E}_0,\mathcal{E}_1,\mathcal{E}_2)$ is a strong exceptional triple, define $V_{\mathcal{E}_1}^l$ (resp. $V_{\mathcal{E}_1}^r$) to be the intersection of the line segment with endpoints $V_{\mathcal{E}_0}^{\text{Li}}$, $V_{\mathcal{E}_1}^+$ (resp. $V_{\mathcal{E}_2}^{\text{Li}}$, $V_{\mathcal{E}_1}^+$) with the parabola $\overline{\Delta}_{1/2}$. The Le Potier curve C_{LP} is then the union of all line segments $[V_{\mathcal{E}_1}^l,V_{\mathcal{E}_1}^+]$ joining $V_{\mathcal{E}_1}^l$ to $V_{\mathcal{E}_1}^+$ and $[V_{\mathcal{E}_1}^r,V_{\mathcal{E}_1}^+]$ joining $V_{\mathcal{E}_1}^r$ to $V_{\mathcal{E}_1}^+$, running over all strong exceptional triples. By construction, this curve lies between $\overline{\Delta}_{1/2}$ and $\overline{\Delta}_1$. As shown in [15], it has the fundamental property that if $\gamma = (r,d,e) \in \Gamma$ satisfies (d/r,e/r) lying on or below C_{LP} , then there is a slope semistable coherent sheaf of Chern character γ . Conversely, a slope semistable coherent sheaf \mathcal{E} of positive rank is either exceptional, or $V_{\mathcal{E}}^{\text{Li}}$ lies below C_{LP} .

Proposition 7.1. C_{LP} corresponds to C_{roofs} , i.e.,

$$\Upsilon(C_{LP}) = C_{\text{roofs}}$$
.

Proof. Let $(\mathcal{E}_0, \mathcal{E}_1, \mathcal{E}_2)$ be a strong exceptional triple, and let \Diamond be the dense diamond with base $V_{\mathcal{E}_1}$. Let v be the apex of this diamond. By Lemma 6.6, $v = V_{\mathcal{E}_1} + (0, 1/r_1^2)$, where r_1 is the rank of \mathcal{E}_1 . Let L, R be the line segments which are the left and right roofs of \Diamond . By the definition of C_{roofs} , it is sufficient to show that

$$\Upsilon([V_{\mathcal{E}_1}^l, V_{\mathcal{E}_1}^+]) = L, \quad \Upsilon([V_{\mathcal{E}_1}^r, V_{\mathcal{E}_1}^+]) = R.$$

To show this, first note that

$$\Upsilon(V_{\mathcal{E}_1}^+) = \Upsilon(V_{\mathcal{E}_1}^{\text{Li}} - (0, 1/r_1^2)) = V_{\mathcal{E}_1} + (0, 1/r_1^2) = v.$$

Second, we will show that $\Upsilon(V_{\mathcal{E}_1}^r)$ is the right-hand vertex of \Diamond . From Figure 7, we see that the line through v and $V_{\mathcal{E}_2}$ is $L_{\mathcal{E}_1}$, and hence this is the image of the line through $V_{\mathcal{E}_1}^+$ and $V_{\mathcal{E}_2}^{\text{Li}}$ under Υ . Thus we need to check that the intersection point of $\partial_{5/8}$ with $L_{\mathcal{E}_1}$ is the right vertex of \Diamond .

The x-coordinate of this vertex is $\frac{d_1}{r_1} - \frac{\sqrt{9r_1^2-4}}{2r_1}$ by Corollary 6.23. So it is sufficient to compare this with the x-coordinate of $L_{\mathcal{E}_1} \cap \partial_{5/8}$. Solving the equations $r_1y + d_1x = e_1$, $y = -x^2/2 + 5/8$ and using Lemma 2.4, we get

(7.1)
$$x = \frac{d_1}{r_1} \pm \frac{\sqrt{9r_1^2 - 4}}{2r_1},$$

and indeed there are two intersection points. However, one checks that

$$1 < \frac{\sqrt{5}}{2} \le \frac{\sqrt{9r_1^2 - 4}}{2r_1} < \frac{3}{2}.$$

Since the difference in x-coordinates of $V_{\mathcal{E}_1}$ and $V_{\mathcal{E}_2}$ is less than 1 by Lemma 2.4,(3), the intersection point with the larger value of x in fact lies to the right of $V_{\mathcal{E}_2}$. Hence the desired intersection point has x-coordinate given by the minus sign in (7.1). This is the desired value.

The argument for the left-hand intersection point is similar.

To summarize, to go from the $\{1,\frac{\mathrm{ch}_1}{\mathrm{ch}_0},\frac{\mathrm{ch}_2}{\mathrm{ch}_0}\}$ -plane to the stability scattering diagram, we decompose Υ as follows: We first flip the $\{1,\frac{\mathrm{ch}_1}{\mathrm{ch}_0},\frac{\mathrm{ch}_2}{\mathrm{ch}_0}\}$ -plane about the X-axis, and then shift everything up by 1/8. At this stage $\overline{\Delta}_0$ goes to $\partial_{1/8}$ and $\overline{\Delta}_1$ goes to $\partial_{9/8}$. Then, using the following transformation only on the Le Potier curve,

(7.2)
$$(\alpha, \beta) \mapsto (\alpha - 3/2, 3/2\alpha + \beta - 9/8),$$

the Le Potier curve C_{LP} will go to the boundary of the bounded region of the scattering diagram, C_{roofs} . Also, each exceptional bundle \mathcal{E} in the $\{1,\frac{\text{ch}_1}{\text{ch}_0},\frac{\text{ch}_2}{\text{ch}_0}\}$ -plane goes to the dual object of the corresponding line/ray to \mathcal{E} in the scattering diagram.

See Figure 31.

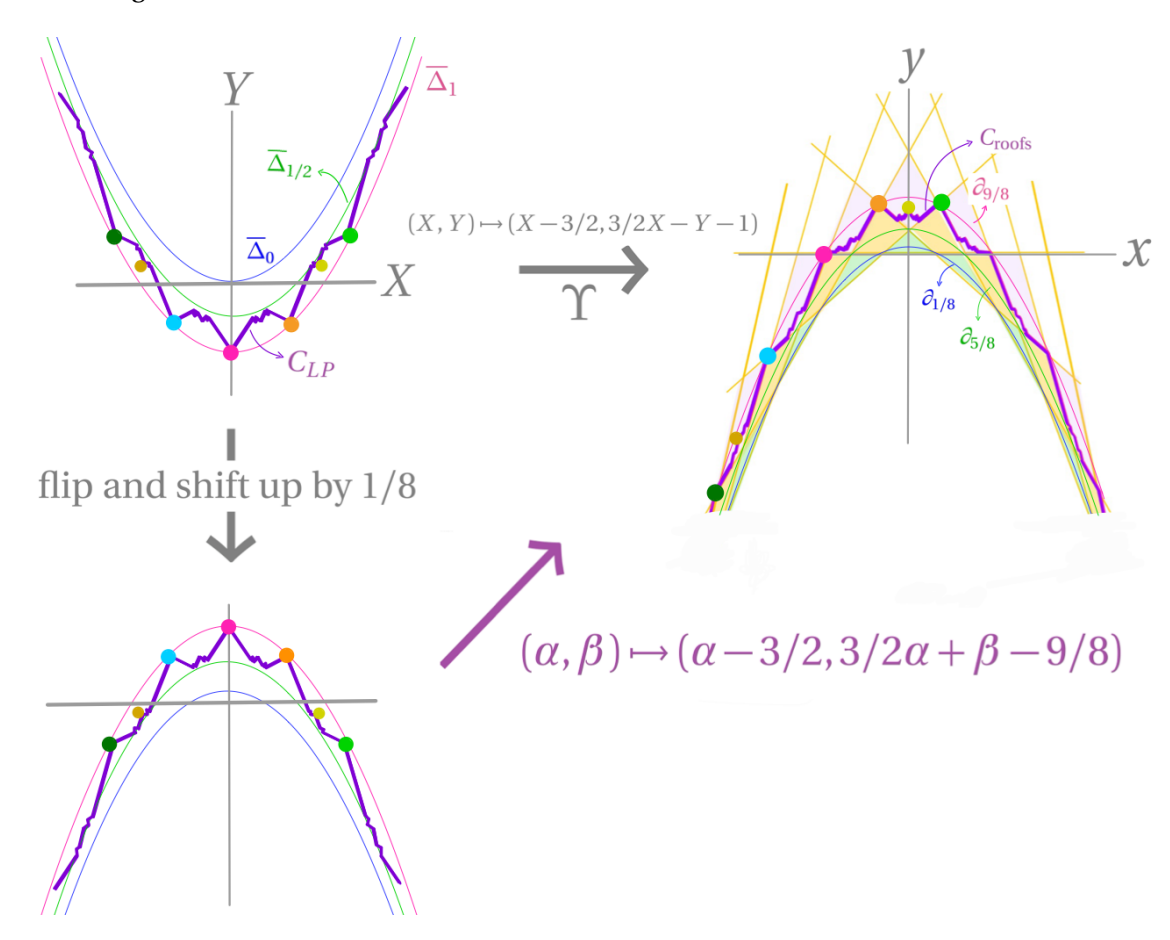


FIGURE 31. From the $\{1,\frac{\mathrm{ch}_1}{\mathrm{ch}_0},\frac{\mathrm{ch}_2}{\mathrm{ch}_0}\}$ -plane to the stability scattering diagram: Under this transformation, the fractal Le Potier curve, C_{LP} , goes to the fractal upper boundary of the bounded region in the scattering diagram, C_{roofs} . Also, $\overline{\Delta}_0$ goes to $\partial_{1/8}$, $\overline{\Delta}_{1/2}$ goes to $\partial_{5/8}$, and $\overline{\Delta}_1$ goes to $\partial_{9/8}$. Further, the points in the $\{1,\frac{\mathrm{ch}_1}{\mathrm{ch}_0},\frac{\mathrm{ch}_2}{\mathrm{ch}_0}\}$ -plane transform to the dual vertices in the scattering diagram: e.g., in this picture, $\mathcal{T}_{\mathbb{P}^2}$ corresponding to the point (3/2,3/4) in the (X,Y) coordinate transforms to $V_{\mathcal{T}_{\mathbb{P}^2}}$ corresponding to the point (0,1/2) in the (x,y) coordinate.

Corollary 7.2. Let $(x_0, y_0) \in U$ be a point with rational coordinates. Then (x_0, y_0) is the intersection of two non-trivial rays of $\mathfrak{D}^{\text{stab}}$ with distinct tangent lines if and only if $(x_0, y_0) = \left(\frac{\text{ch}_1(\mathcal{E})}{\text{ch}_0(\mathcal{E})} - \frac{3}{2}, \frac{3d - \chi(\mathcal{E})}{\text{ch}_0(\mathcal{E})}\right)$ for some slope-stable coherent sheaf of positive rank \mathcal{E} .

Proof. We have seen from Theorem 2.7 and Theorem 4.8 that the points of $R_{\rm bdd}$ below $C_{\rm roofs}$ which are intersections of two rays are precise points of the form $V_{\mathcal{E}}$ for \mathcal{E} an exceptional bundle. Further, every rational point on $C_{\rm roofs}$ or above is the intersection of two rays by Corollary 5.4. On the other hand, by [15, §4.4] (see [31, Thm. 1.8] for the statement as needed here), a rational point σ of U satisfies $\sigma = V_{\mathcal{E}}$ for a slope-stable coherent sheaf \mathcal{E} if and only if $\sigma = V_{\mathcal{E}}$ for \mathcal{E} an exceptional bundle or σ lies on $C_{\rm roofs}$ or above. This proves the result.

REFERENCES

- 1. D. Arcara, A. Bertram, I. Coskun, and J. Huizenga, *The minimal model program for the Hilbert scheme of points on* \mathbb{P}^2 *and Bridgeland stability*, Adv. Math. **235** (2013), no. 3, 580–626.
- 2. A. Bayer and E. Macrì, *The space of stability conditions on the local projective plane*, Duke Mathematical Journal **160** (2011), no. 2, 263–322.
- 3. A. Bayer, E. Macrì, and Y. Toda, *Bridgeland stability conditions on threefolds I: Bogomolov-Gieseker type inequalities*, J. Algebraic Geom. **23** (2014), no. 1, 117–163.
- 4. A. Bertram and I. Coskun, *The birational geometry of the Hilbert scheme of points on surfaces. birational geometry, rational curves, and arithmetic, Springer, New York* **173** (2013), 15–55.
- 5. A. Bertram, C. Martinez, and J. Wang, *The birational geometry of moduli spaces of sheaves on the projective plane*, Geom. Dedicata **173** (2014), 37–64.
- 6. B. Bolognese, J. Huizenga, Y. Lin, E. Riedl, B. Schmidt, M. Woolf, and X. Zhao, *Nef cones of Hilbert schemes of points on surfaces*, Algebra Number Theory **10** (2016), no. 4, 907–930.
- 7. P. Bousseau, *Scattering diagrams, stability conditions, and coherent sheaves on* \mathbb{P}^2 , Journal of Algebraic Geometry **31** (2022), 593–686.
- 8. P. Bousseau, A proof of N. Takahashi's conjecture for (\mathbb{P}^2, E) and a refined sheaves/Gromov–Witten correspondence, Duke Math. J. **172** (2023), no. 15, 2895–2955.
- 9. P. Bousseau, P. Descombes, B. Le Floch, and B. Pioline, *BPS dendroscopy on local* ℙ², Commun. Math. Phys. **405** (2024), no. 108.
- 10. T. Bridgeland, Stability conditions on triangulated categories, Ann. of Math. (2) 166 (2007), no. 2, 317–345.
- 11. M. Carl, M. Pumperla, and B. Siebert, *A tropical view on Landau-Ginzburg models*, Acta Math. Sin. (Engl. Ser.) **40** (2024), no. 1, 329–382.
- 12. I. Coskun and J. Huizenga, *The ample cone of moduli spaces of sheaves on the plane*, Algebr. Geom. **3** (2016), no. 1, 106–136.
- 13. I. Coskun, J. Huizenga, and M. Woolf, *The effective cone of the moduli space of sheaves on the plane*, J. Eur. Math. Soc. (JEMS) **19** (2017), no. 5, 1421–1467.
- 14. J.-M. Drezet, *Fibrés exceptionnels et variétés de modules de faisceaux semi-stables sur* **P**₂(**C**), J. Reine Angew. Math. **380** (1987), 14–58.
- 15. J-M. Drezet and J. Le Potier, *Fibrés stables et fibrés exceptionnels sur* **P**₂, Ann. Sci. École Norm. Sup. (4) **18** (1985), no. 2, 193–243.
- 16. G. Frobenius, Über die Markoffschen Zahlen, Königliche Akademie der Wissenschaften (1913), 458-487.
- 17. P. Gallardo, César L. Huerta, and B. Schmidt, *On the Hilbert scheme of elliptic quartics.*, Michigan Math. J. **67** (2018), no. 4, 787–813.
- 18. A. L. Gorodentsev and A. N. Rudakov, *Exceptional vector bundles on projective spaces*, Duke Math. J. **54** (1987), no. 1, 115–130.
- 19. M. Gross, P. Hacking, S. Keel, and M. Kontsevich, *Canonical bases for cluster algebras*, Journal of the American Mathematical Society **31** (2018), no. 2, 497–608.
- 20. M. Gross and R. Pandharipande, *Quivers, curves, and the tropical vertex*, Portugal. Math. (N.S.) Portugaliae Mathematica **67** (2010), no. 6, 211–259.
- 21. M. Gross, R. Pandharipande, and B. Siebert, The tropical vertex, Duke Math. J. 153 (2010), no. 2, 297-362.

- 22. M. Gross and F. Rezaee, *Bridgeland wall-crossing for* $Hilb^n(\mathbb{P}^2)$ *from scattering diagram*, in preparation (2025).
- 23. M. Gross and B. Siebert, *From real affine geometry to complex geometry*, Ann. of Math. **174** (2011), no. 3, 1301–1428.
- 24. T. Gräfnitz, *Tropical correspondence for smooth del pezzo log Calabi-Yau pairs*, J. Alg. Geom. **31** (2022), no. 4, 687–749.
- 25. T. Gräfnitz, *Theta functions, broken lines and 2-marked log Gromov-Witten invariants*, manuscripta math. **176** (2025), no. 41.
- 26. T. Gräfnitz and P. Luo, *The dense region in scattering diagrams*, Bulletin of the Australian Mathematical Society (2025), 1–13.
- 27. T. Gräfnitz, H. Ruddat, and E. Zaslow, *The proper Landau-Ginzburg potential is the open mirror map*, Adv. Math. **447** (2024).
- 28. M. Kontsevich and Y. Soibelman, *Affine structures and non-Archimedean analytic spaces*, Progr. Math. **244** (2006), 321–385.
- 29. C. Li, The space of stability conditions on the projective plane, Selecta Mathematica 23 (2017), 2927–2945.
- 30. C. Li and X. Zhao, *The MMP for deformations of Hilbert schemes of points on the projective plane*, Algebraic Geometry **5** (2018), no. 3, 328–358.
- 31. C. Li and X. Zhao, *Birational models of moduli spaces of coherent sheaves on the projective plane*, Geometry and Topology **23** (2019), 347–426.
- 32. A. Maciocia, Computing the walls associated to Bridgeland stability conditions on projective surfaces, Asian J. Math. 18 (2014), no. 2, 263–279.
- 33. E. Macrì, Stability conditions on curves, Math. Res. Lett. 14 (2007), 657-672.
- 34. T. Prince, *The tropical superpotential for* \mathbb{P}^2 , Algebr. Geom. **7** (2020), no. 1, 30–58.
- 35. F. Rezaee, Geometry of canonical genus four curves, Proc. LMS 128 (2024), no. 1.
- 36. F. Rezaee, *An interesting wall-crossing: Failure of the wall-crossing/MMP correspondence*, Selecta Mathematica, New Series **30** (2024), no. 102.
- 37. A. N. Rudakov, *The Markov numbers and exceptional bundles on* \mathbb{P}^2 , Mathematics of the USSR-Izvestiya **32** (1989), no. 1, 99–112.
- 38. B. Schmidt, *A generalized Bogomolov–Gieseker inequality for the smooth quadric threefold*, Bull. Lond. Math. Soc. **46** (2014), no. 5, 915–923.
- 39. B. Schmidt, Bridgeland stability on threefolds—First wall crossings, J. Algebraic Geom. 29 (2020), no. 2, 247-283.
- 40. B. Springborn, The worst approximable rational numbers, J. Number Theory 263 (2024), 153–205.
- 41. Y. Toda, Stability conditions and extremal contractions, Math. Ann. 357 (2013), 631-685.
- 42. Y. Toda, Stability conditions and birational geometry of projective surfaces, Compos. Math. 150 (2014), 1755–1788
- 43. A. P. Veselov, Markov fractions and the slopes of the exceptional bundles on \mathbb{P}^2 , 2025.
- 44. B. Xia, *Hilbert scheme of twisted cubics as a simple wall-crossing*, Trans. Amer. Soc. Math. **370** (2018), no. 8, 5535–5559.
- 45. Y. Zhang, Congruence and uniqueness of certain Markoff numbers, Acta Arithmetica 128 (2007), no. 3, 295–301.

CENTRE FOR MATHEMATICAL SCIENCES, UNIVERSITY OF CAMBRIDGE, WILBERFORCE ROAD, CB3 0WA, CAMBRIDGE, UNITED KINGDOM

 $\textit{Email address} : \verb|mgross@dpmms.cam.ac.uk| \\$

Email address: fr414@cam.ac.uk